Plant Stem Cell Homeostasis: Phylogenies and Expression Patterns of Different Components

Inaugural-Dissertation

zur

Erlangung des Doktorgrades

der Mathematisch-Naturwissenschaftlichen Fakultät

der Universität zu Köln

vorgelegt von

Diego Durantini

aus Mailand (Italien)

Köln 2009

Berichterstatter: Prof. Dr. Wolfgang WERR

Prof. Dr. Martin HÜLSKAMP

Tag der mündliche Prüfung: 16/10/2009

a me, per noi

“I dare do all that may become a man; Who dares do more is none.”
Macbeth

SUMMARY

In *Arabidopsis*, the shoot apical meristem (SAM) homeostasis is finely regulated by the *WUSCHEL*-*CLAVATA* antagonism. *WUSCHEL* (*WUS)* encodes for a homeodomain protein essential for the SAM maintenance and its expression marks the organizing center (OC). On the other hand, the interaction between the three *CLAVATA* (*CLV*) proteins, which all together code for a heterodimeric transmembrane leucin-rich repeat (LRR) receptor like kinase (*CLV1-2*) and its specific ligand (*CLV3*), correctly restricts the *WUS* expression to the OC. In contrast to *Arabidopsis*, in maize two different *WUS* orthologs and a single *CLV1* ortholog, *Thick tassel Dwarf1* (*TD1*), have been so far characterized. Like in *Arabidopsis*, the *TD1* and *ZmWUS2* expression domains overlap but, unlike *Arabidopsis,* their expression is detected in cells recruited for leaf primordia. Conversely, *ZmWUS1* is expressed within the SAM dome, not in a OC-type manner but rather in a dynamic fashion that always correlates to phytomer establishment. The expression of the single *CLV1* ortholog *TD1* does not overlap with *ZmWUS1* expression domain, leaving an open question over the putative regulator of *ZmWUS1* function. To answer this question, the closest *TD1* paralogs were identified and their expression pattern elucidated. Unfortunately, none of the three maize candidate genes identified has shown the potential to regulate *ZmWUS1* activity, indicating that none of the closest *CLV1* relatives in maize are able to regulate *ZmWUS1* activity.

WUSCHEL is the founding member of a large gene family, the *WUSCHEL*-related homeobox (*WOX*) genes, which appear to be involved in several aspects of plant development, from defining the organizers of the shoot and root apical meristems, to conferring distinct cell fates as early as the 2-cell stage during *Arabidopsis* embryogenesis. The *WOX* gene family is present throughout the plant kingdom, from the most basal algae and land plants to the most evolved angiosperms. As the members of this gene family take part in key plant developmental aspects, it is intriguing to study the evolution of the *WOX* gene family. In this respect, the lycophyte scenario is described in this work, in which both *Selaginella kraussiana* and *S.moellendorffii* has been the object of study. As for moss *Physcomitrella patens*, also the *Selaginella WOX* genes belong to the *WOX13*-like clade. *S.moellendorffii* genome has nine putative *WOX* homeodomains, six of them grouping together in a *S.moellendorffii* specific *WOX13* sister group, whereas only three *WOX*-like gene were identified by degenerate primer PCR in *S.kraussiana*, all belonging to the *WOX13*-like clade. Despite the expression analysis of the three *S.kraussiana WOX13*-like genes and their *S.moellendorffii* closer orthologs demonstrate their subfunctionalization and their high conservation through the Selaginellaceae evolution, the phylogenetic reconstruction is in favor of the presence of only a single ancestor *WOX13*-like gene before the separation of the lycophyte and euphyllophyte lineage, which was probably present from the dawn of the plant kingdom.

ZUSAMMENFASSUNG

In *Arabidopsis* wird die Homöostase des Sproßapikalmeristems (SAM) durch den *WUSCHEL*-*CLAVATA*-Antagonismus reguliert. *WUSCHEL* (*WUS*) kodiert für ein Homöodomänenprotein das essentiell für den Erhalt des SAM ist, und dessen Expression das Organisierende Zentrum (OC) markiert. Die Interaktion zwischen den drei *CLAVATA*-Proteinen (*CLV*), die zusammen für eine heterodimere *Leucine-Rich-Repeat* (LRR) rezeptorähnliche Kinase (*CLV1-2*) und deren spezifischen Liganden (*CLV3*) kodieren, beschränken die Expression von *WUS* auf das OC. Im Gegensatz zu *Arabidopsis* wurden in Mais zwei *WUS*-Orthologe und ein einzelnes *CLV1*-Ortholog, *thick tassel dwarf1* (*TD1*) charakterisiert. Wie in *Arabidopsis* überlappen die Expressionsdomänen von *ZmWUS2* und *TD1*, aber im Gegensatz zu *Arabidopsis* werden beide Gene in Zellen exprimiert, die in Blattprimordien rekrutiert wurden. *ZmWUS1* wird ebenfalls nicht in einer OC-ähnlichen Domäne exprimiert sondern hat im SAM ein hochdynamisches Expressionsmuster, das mit der Etablierung neuer Phytomere korreliert. Die Expression von *ZmWUS1* überlappt nicht mit der des einzigen *CLV1*-Orthologs *TD1*, was die Frage nach einem Regulator der *ZmWUS1*-Expression aufwirft. Um diese Frage zu beantworten, wurden die am nächstverwandten Paraloge von *TD1* identifiziert und ihre Expressionsmuster untersucht. Leider konnte keines der drei Kandidatengene als potentieller Regulator von *ZmWUS1* identifiziert werden, was auf einen Mechanismus der *WUS*-Regulation hinweist, der unabhängig von den nächsten Verwandten von *CLV1* ist.

WUSCHEL ist das Gründungsmitglied einer großen Genfamilie, den *Wuschel*-verwandten Homöobox-Genem (*WOX*), die an einer Vielzahl von pflanzlichen Entwicklungsprozessen, von der Organisation der Sproß- und Wurzelmeristeme bis zur Determination von Zelltypen bereits ab dem 2-Zell-Stadium des *Arabidopsis*-Embryos, beteiligt sind. Die *WOX*-Genfamilie ist im ganzen Pflanzenreich verbreitet, von basalen einzelligen Algen bis zu hochentwickelten Angiospermen. Da die Mitglieder der Familie zu wichtigen Aspekten der Pflanzenentwicklung beitragen, ist es von Interesse, die Evolution dieser Familie zu untersuchen. In dieser Arbeit wurde der Stand der Entwicklung der *WOX-Gene* in Lycophyten untersucht; hierbei wurden sowohl *Selaginella moellendorffii* als auch *Selaginella kraussiana* untersucht. Wie im Moos *Physcomitrella patens* gehören die *WOX*-Gene aus Selaginella zur Gruppe der *WOX13*-Gene. Das Genom von *S.moellendorffii* enthält 9 *WOX*-Homöodomänen von denen 6 eine für *S.moellendorffii* spezifische Schwestergruppe zu *WOX13*-Genen bilden; in *S.kraussiana* dagegen konnten mittels PCR mit degenerierten Primern nur drei Homöodomänen identifiziert werden, die wie die übrigen Gene aus *S.moellendorffii*, eindeutig in die *WOX13*-Gruppe gehören. Phylogenie und Expressionsanalysen deuten darauf hin, dass Entstehung und Subfunktionalisierung dieser *WOX13*-Gene vor der Trennung der Linien beider *Selaginella*-Spezies stattgefunden haben, jedoch zum Zeitpunkt der Trennung der Lycophyten und Euphyllophyten nur ein gemeinsamen *WOX13*-Vorläufer vorhanden war, der wahrscheinlich schon bei der Entstehung des Pflanzenreichs existierte.

Table of Contents

INTRODUCTION

Plants grow and form new organs throughout their life cycle, while integrating developmental and environmental signals. All postembryonically formed organs and tissues are derived from pluripotent stem cell populations that lie in the growing tips of the plant, the shoot and root meristems. The cells located in the center of the meristem maintain an undifferentiated state, whereas any daughter cell that is displaced from the niche is compelled to go through a differentiation program and is subsequently recruited for the formation of lateral organs.

Meristems are already established during embryogenesis. In the model plant *Arabidopsis thaliana*, the fertilized egg cell firstly elongates and then divides asymmetrically to form two daughter cells of different size and cytoplasmic densities. The apical daughter cell gives rise to the embryo proper, whereas the descendants of the basal daughter cell divide transversely to form the suspensor and its uppermost cell, the hypophysis (Mansfield *et al.*, 1991).

Already at the eight-cell stage, four regions with different developmental fates can be recognized in the *Arabidopsis* embryo: (1) the apical embryo domain, made up of the four uppermost cells, will generate the shoot meristem and most of the cotyledons, (2) the central embryo domain, consisting of the cell tier just below, will form the hypocotyl and root, and will partially contribute to cotyledons and the root meristem, (3) the hypophysis, which will give rise to the distal portion of the root meristem, the quiescent center (QC) and the central root cap stem cells, and (4) the suspensor, which provides a connection to the mother tissue and nutrient supply during early embryogenesis (Mansfield *et al.*, 1991; Mansfield and Briarty, 1991; also reviewed by Laux *et al*., 2004). The first indication of embryonic shoot meristem initiation is the onset of

WUSCHEL (*WUS*) expression in the four subepidermal apical cells of the 16-cell embryo (Mayer *et al*., 1998). Subsequently, these cells divide asymmetrically several times, establishing the *WUS* expression domain at its correct position within the developing shoot meristem. Thus, in *Arabidopsis* the fate of the uppermost tier and the hypophysis are determined already at the 8-cells stage and the shoot stem cell niche is established immediately after.

In contrast to *Arabidopsis*, where apical/basal polarity and radial organization are established by a stereotypic pattern of cell division planes in early embryogenesis, in the monocotyledonous model plant *Zea mays* only the plane of the first division is predictable in the zygote (Randolph, 1936), and it is oriented perpendicularly to the micropylar/chalazal axis, resulting in a small apical and a large basal cell. As in *Arabidopsis*, the latter will form the suspensor and the first will develop into the embryo proper by a sequence of irregular cell divisions, making impossible to trace future organs back to a defined cell or group of cells (Randolph, 1936). Later, at the end of the pro-embryo stage, the maize embryo acquires a club-shaped form with little differentiation, mainly large vacuolated cells in the suspensor and cells that remain small and with high cytoplasmic density in the upper embryo proper (Randolph, 1936; van Lammeren, 1986). Histologically, the shoot apical meristem (SAM) is first apparent as a group of densely packed cells located laterally on the adaxial side of transition stage embryo (Randolph, 1936), recognizable by the scutellum that protrudes on the opposite abaxial and thereby breaks radial symmetry. Slightly later a clearly distinguishable second group of meristematic cells is detectable in the basal part of the embryo proper, just above the suspensor (Randolph, 1936; van Lammeren, 1986), and begins to differentiate into the root apical meristem (RAM). The SAM develops protruding from slightly below the apical tip. A notch on top of the SAM is the first sign of the coleoptile, which forms a ring of tissue enveloping the meristem, and later borders and protects the plumule during germination (Randolph, 1936; Abbe and Stein, 1954). In contrast to *Arabidopsis*, where only the two cotyledons are established during embryogenesis, the maize embryo initiates its single cotyledon (the coleoptile) and up to six true leaves prior to seed dormancy. Newly formed leaf primordia will develop as the coleoptile, but on the opposite flank compared to the previously established primordia, already displaying the distichous phyllotaxy typical of the adult plant. Also in maize, as

in *Arabidopsis*, the stem cell niches fate is establòished early during embryo formation although the cell division pattern is poorly defined. In contrast to *Arabidopsis*, during monocot embryogenesis the SAM is established laterally and not in a central position, emphasizing a first difference between mono- and dicotyledonous shoot apical meristem development.

Another key difference between monocots and dicots involves the SAM architecture. Some peculiar characteristics mark the distinct evolution of dicot and monocot meristems. In dicot species, the SAM appears to have three layers, with a tunica comprising two clonal layers (L1 + L2) and the corpus commonly designated as the L3 layer (Szymkowiak and Sussex 1996; Evans and Barton 1997). In contrast, monocots such as maize have a single histologically apparent tunica layer and the inner corpus (Abbe *et al*. 1951; Steffensen 1968). Moreover, *Arabidopsis* leaves originate from few founder cells specified in the meristem peripheral zone (Irish and Sussex 1992), whereas each maize leaf may be traced back to approximately 200 leaf founder cells recruited from the whole circumference of the shoot apex (Poethig, 1984). Despite the existing differences between mono- and dicotyledons, there is evidence that the SAM homeostasis regulatory system is conserved throughout angiosperms. Maize and rice ortholog of *Arabidopsis* genes act in the *WUS-CLV* pathway, such as the *CLV1* orthologs *THICK TASSEL DWARF1* (*TD1*; Bommert *et al.*, 2005) and *FLORAL ORGAN NUMBER1* (*FON1*; Suzaki *et al.*, 2004) , or the *CLV2* ortholog *FASCIETED EAR2* in maize (*FEA2*; Taguchi-Shiobara *et al*., 2001). Conserved *WUS* orthologs expression patterns have also been described in rice and maize (Nardmann and Werr, 2006). These studies suggest possible evolutionary conservation of the *WUS-CLV* feedback loop, but also highlight major differences between monocots and dicots in terms of domain patterning of genes involved in SAM maintenance.

The existing differences between monocots and dicots in embryogenesis and adult SAM development may be related to different expression of key genes involved in these crucial events. In this respect, both the *WUSCHEL*-related homeobox genes and the *CLAVATA* orthologs might be important actors, accounting for the major patterning differences that have led to such great divergence between the two angiosperm classes over evolutionary time.

1.1 Stem cells homeostasis in the shoot apical meristem

In *Arabidopsis*, expression of the homeodomain transcription factor *WUSCHEL* (*WUS*) is required to maintain a functional shoot apical meristem, as emphasized by the loss-of-function mutation at the WUSCHEL locus that causes the premature termination of the shoot apical meristem after the production of few leaves due to the consumption of the stem cell population (Laux *et al.*, 1996). *WUS* expression is detected in the organizing center (OC), a small group of cells situated just beneath the stem cells, and it is required to maintain the latter in an undifferentiated state, indicating the existence of a signaling pathway from the OC toward stem cells (Mayer *et al*., 1998). In addition, the stem cells respond by expressing the secreted peptide *CLAVATA3* (*CLV3*) (Rojo *et al.*, 2002), which probably interacts with *CLAVATA1* (CLV1) and *CLAVATA2* (*CLV2*). *CLV1* is a transmembrane receptor-like kinase composed of an extracellular leucine-rich repeat (LRR) domain, with putative receptor activity, linked via a single transmembrane domain to a cytoplasmatic Ser/Thr kinase domain (Clark *et al.*, 1997). Although structurally similar to *CLV1*, with a LRR extracellular and a transmembrane domain, the *CLV2* protein lacks the intracellular kinase domain, and therefore is unable to transmit the signal by itself (Jeong *et al.*, 1999). *CLV1* is expressed in the shoot meristem in a region comprising a subset of the central stem cell niche and the inner portion of the OC (Clark *et al.*, 1997), surrounding the *WUS* expression domain. Mutations involving the three *CLAVATA* loci result in an opposite phenotype compared to *wus* mutants, with enlarged meristems and supernumerary floral organs (Clark *et al.*, 1993; Clark *et al.*, 1995; Kayes and Clark, 1998). Moreover, the *WUS* expression domain expands in the *clv* mutant (Schoof *et al.*, 2000), suggesting a direct repression by *CLV* genes. The recent characterization of *CORYNE* (*CRN*) adds a possible new player in the *CLV/WUS* negative feedback loop and in SAM homeostasis. Müller and co-authors (2008) reported that the *crn-1* mutation can suppress the *CLV3* overexpression phenotype and behaves similarly to *clv2* mutants, but not to *clv1* mutant. This suggests the possibility of parallel pathways involving *CLV1* and, independently, *CLV2/CRN* complexes to trigger the *CLV3* signal. Overall, the interaction between the three *CLV* genes and

CRN is able to restrict *WUS* expression to the OC region, within the *CLV1* expression domain (Schoof *et al.*, 2000; Brand *et al*., 2000), establishing a negative feedback loop between the OC and the surrounding stem cell population and providing a mechanism by which stem cell homeostasis could be finely regulated.

Ultimately, SAM homeostasis depends on the correct and buffered balance between stem cell growth rate, which tends to increase cell number, and cells recruited into the formation of lateral organs, which in turn reduces the cell number. The *KNOTTED1*-like homeobox (*KNOX*) genes, such as *SHOOT MERISTEMLESS* (*STM*) and *KNOTTED1* (*KN1*) from *Arabidopsis* and maize, respectively, are transcribed throughout the entire SAM dome (Long *et al.*, 1996; Endrizzi *et al.*, 1996), and their expression is downregulated in cells recruited to become the future primordia by the activity of the ARP genes (*ASYMMETRIC LEAVES1*, *ROUGH SHEATH2*, *PHANTASTICA,* orthologous genes from *Arabidopsis*, maize and *Anthirrinum*, respectively; Waites *et al*., 1998; Timmermans *et al*., 1999; Tsiantis *et al*., 1999; Byrne *et al*., 2000). *RS2* and *AS1* interact with the chromatin-remodeling factor *HIRA* (Phelps-Durr *et al.*, 2005) and with the LOB (Lateral Organ Boundaries) domain protein *AS2* (Xu *et al.*, 2003; Phelps-Durr *et al.*, 2005). Both *RS2*/*AS1* and *AS2* are able to bind *KNOX* promoter sequences (Guo *et al.*, 2008) and may recruit *HIRA* to establish a repressive chromatin state that is stably inherited throughout organ development. Therefore, in plants the correct balance between stem cell population growth and recruitment of cells to form lateral organs is finely regulated and it involves different pathways which interact to maintain the correct SAM homeostasis.

In monocotyledons, the cloning and characterization of genes orthologous to the main actors in *WUS*/*CLV* and *KNOX*/*ARP* antagonisms lead to the idea that these regulatory pathways are conserved among angiosperms. In maize, *thick tassel dwarf1 (td1)* and *fasciated ear2 (fea2)* mutants display enlarged inflorescence and floral meristems, and their causal genes are orthologs to *CLV1* and *CLV2,* respectively (Taguchi-Shiobara *et al.*, 2001; Bommert *et al.*, 2005). In rice, loss-of-function mutants of *FLORAL ORGAN NUMBER1 (FON1)* and *FON2* (Suzaki *et al.*, 2004; Suzaki *et al.*, 2006) showed an increased number of floral organs due to enlarged floral meristems and to abnormal meristem determinacy similar to that seen in *Arabidopsis clv* mutants. Molecular cloning of *FON1* revealed that it encodes a leucine-rich repeat receptor-like kinase that is orthologous to

CLV1 (Suzaki *et al.*,2004). These results indicate that components of the CLAVATA signaling pathway is conserved between grasses and *Arabidopsis.* However, differences between monocot and dicot *CLV1* orthologs were also reported. The most significant is the expression pattern of *TD1* and *FON1*. During the vegetative phase, *TD1* is expressed in leaf primordia and leaves but excluded from the SAM dome whereas *CLV1* is expressed deeper inside the SAM, never in touch with lateral organ primordia. Moreover, *TD1* and *FON1* are expressed in all layers of the floral meristem, whereas *CLV1* is expressed in most cells of just the inner layer of the *Arabidopsis* floral meristems from stage 2 on (Clark *et al.*, 1997; Suzaki *et al.*, 2004; Bommert *et al.*, 2005). Moreover, *clv* mutants show defects in shoot, inflorescence, and floral meristem, whereas the vegetative SAMs in *fon1* and *td1* mutants are apparently normal. These facts suggest that other redundant factors regulating SAM activity might function during vegetative development in grasses.

Phylogenetic reconstructions unequivocally identified two potential *WUS* orthologs in maize, *ZmWUS1* and *ZmWUS2*, and a single ortholog in rice, *OsWUS* (Nardmann and Werr, 2006). Comparative expression analysis uncovered striking similarities between the two grasses but major differences to *Arabidopsis*. During the reproductive phase, the grass *WUS* orthologs exhibit meristem-specific expression patterns, though their transcripts are detected more broadly and are predominantly not restricted to an OC-type domain in different types of reproductive meristems. By contrast, during the vegetative phase, the expression patterns diverged strongly from those in *Arabidopsis* and expression of *WUS* orthologs correlates with the specification of new leaf primordia. *ZmWUS1* expression appears close to the tip of the shoot in the center of the SAM at the height of the new leaf primordium (P_0) and shifts basally until the new leaflet (P_1) appears histologically, whereas *ZmWUS2* is primarily expressed in cells recruited for leaf primordia and is maximally expressed basal lateral leaf margins. In parallel, *OsWUS* expression oscillates between apical and deeper layers in the center of the SAM but is constant in leaf primordia founder cells, indicating that the expression pattern of the single rice ortholog in the SAM center and periphery has been split between the two maize paralogs. Consistently, however, the expression of *WUS* and *CLV1* orthologs has been recruited for the anlage of new leaf phytomers in the course of maize and rice evolution.

Interestingly, *TD1* expression overlaps the expression domain of *ZmWUS2,* as its *Arabidopsis* ortholog *CLV1* surrounds the OC *WUS* expressing cells, but it does not overlap *ZmWUS1* expression in the SAM center. This apparent lack of regulation raises the question as to which is, if it does exist, the putative gene able to regulate of *ZmWUS1* activity in maize. This work will try to answer this scientific question.

1.2 The *WOX* gene family

WUSCHEL is the founding member of a large family of homeodomain-related genes that are present from the most basal land plants, bryophytes, through the most evolved angiosperms (Nardmann and Werr, 2007). *WUSCHEL* is known to play a major role in the establishment and maintenance of stem cell homeostasis in the shoot (Laux *et al*., 1996; Mayer *et al*., 1998) as do the *Antirrhinum* homolog *ROSULATA* (Kieffer *et al.*, 2006) and the *Petunia* homolog *TERMINATOR* (Stuurman *et al.*, 2002), which suggests that its function could be conserved.

Like their most famous and studied relative, the *WUSCHEL*-related homeobox (*WOX*) genes so far characterized appear to be involved in several aspects of plant development. Analogously to the role played by *WUS* in the shoot stem cell niche organizer, its close relative *WOX5* is specifically expressed in root quiescent center (QC), from the formation of the hypophyseal cell during embryogenesis (Hacker *et al.*, 2004). A *wox5* mutant fails to maintain the abutting columella stem cells in an undifferentiated state, indicating that *WOX5* is required for a signal from the QC in order to repress differentiation of the columella stem cells (Sarkar *et al.*, 2007). Moreover, the same authors demonstrate that *WOX5* also function redundantly with *SCARECROW*, *SHORTROOT* and *PLETORA* genes to repress premature differentiation in other stem cells surrounding the QC. Therefore, the *WOX5* role in the root QC appears analogous to that of *WUS* in the SAM OC, namely keeping the surrounding stem cell population in an undifferentiated state. Remarkably, promoter swap experiments have demonstrated that *WUS* and *WOX5* are interchangeable between both stem cell niches, although they share homology only in conserved domains (Sarkar *et al.*, 2007), indicating that these genes do not provide shoot or root specific signals but rather a more general

signal that is able to maintain the organizers daughter cells in an undifferentiated state.

As for *WOX5*, *WUS* can also fully rescue *WOX3/PRS* defects when expressed under the WOX3/PRS promoter (Shimizu *et al.*, 2009). *WOX3/PRS*, similar to its maize duplicated orthologs *NARROW SHEATH1/2*, is expressed in a restricted number of L1 cells at the lateral regions of flower primordia, floral organ primordia, and young leaf primordia. Furthermore, mutation in these loci causes the loss of lateral domains of lateral organs (Matsumoto and Okada, 2001; Nardmann *et al.*, 2004). Thus, *WOX3* is also involved in a key plant developmental process. Moreover, the fact that *WUS* can take over the *WOX3* function suggests a similar meristematic fate acquired by cells expressing *WOX3* homologous genes.

WOX2 and *WOX8/9* also highlight the importance of *WOX* genes during embryogenesis. In *Arabidopsis,* the zygote expresses both *WOX2* and *WOX8* transcripts but their expression domains become separated after the first asymmetric zygotic division, probably providing each daughter cell with a specific transcription program, which confers them apical and basal fate, respectively (Hacker *et al.*, 2004; Wu *et al.*, 2007; Breuninger *et al.*, 2008). A *wox2* single mutant and a *wox8 wox9* double mutant display defects in cell division patterns during embryonic development. These defects, given the extremely precise stereotypic cell division pattern program occurring during *Arabidopsis* embryonic development, causes lethality of the mutants. The w*ox2* cell division phenotypes occur with low penetrance only in the apical lineage. The combination of *wox2* with mutations in other closely related *WOX* genes, such as *WOX1*, *WOX3*/*PRS* and *WOX5*, enhances the shoot patterning defect, indicating that several *WOX* genes act coordinately in shoot patterning. However, only in the absence of *WOX2* activity do *WOX1*, *WOX3*/*PRS* and *WOX5* become essential for normal development of the apical lineage, suggesting *WOX2* is the key *WOX* gene for shoot patterning (Breuninger *et al.*, 2008). *wox8 wox9* double mutant combinations display aberrant cell division throughout the embryo from the 2-cell stage onward, consistent with the loss of *WOX2* expression in the apical cell and with a broader auxin maxima (Wu *ey al.*, 2007; Breuninger *et al.*, 2008). This indicates that *WOX8/9* are upstream of *WOX2* apical-lineage specific expression and are crucial to establish correct auxin maxima during *Arabidopsis* embryogenesis.

Apart from *Arabidopsis*, expression of several *WOX* genes, among which also *WOX2* and *WOX9*

homologs, has also been detected in maize, suggesting that *WOX* genes might play a conserved role in angiosperm embryogenesis (Nardmann *et al.*, 2007). However, this work also revealed major differences between mono- and dicotyledons, such as the absence of *WOX1/6/7* relatives in grasses, the functional duplication of the *WOX3* and *WOX5* sub-clades and different *WOX4* ortholog expression in maize compared to *Arabidopsis* (Nardmann *et al.*, 2007). Moreover, there are also new data regarding *WOX* genes function in species other the maize and *Arabidopsis*. Recently, the Petunia *WOX9* ortholog *EVERGREEN* (*EVG*), which plays a key role in the correct development of the cymose inflorescence in *Petunia*, has been described (Rebocho *et al*. 2008). In addition, the characterization of a *WOX11*-like mutant in rice emphasizes its requirement in promoting crown root development (Zhao *et al.*, 2009). Therefore, it appears that the *WOX* gene family members are involved in key developmental aspects, often via promoting meristematic cell fate.

Due to the several facets of plant development in which the *WOX* genes are involved, it would be intriguing to pursue further research on up the *WOX* gene family evolution during the evolution of the plant kingdom. In this respect, a second aspect of this dissertation will deal with the evolution of the *WOX* gene family, with particular regard to the lycophyte clade.

1.3 Lycophytes in the context of plant evolution

The first evidence of plant ancestors moving onto land dates back to the mid-Ordovician, some 470 million years ago (mya). The combination of a decay-resistant cell wall, which implies the presence of sporopollenin, and a tetrahedral cellular configuration, which entails haploid meiotic production, renders the spores found in mid-Ordovician fossil records a good evidence for the appearance of land plants (Gray, 1993).

But the plant kingdom has a much longer story. Embryophytes (Figure 1) are clearly descended from a green algal-like ancestor (Smith, 1950). The green algae lineage originated as much as 1500 mya (Yoon *et al.*, 2004), and the divergence of land plants likely occurred 490-425 mya (Sanderson, 2003). The prasinophytes, which consist of primitive appearing unicells representative of early-

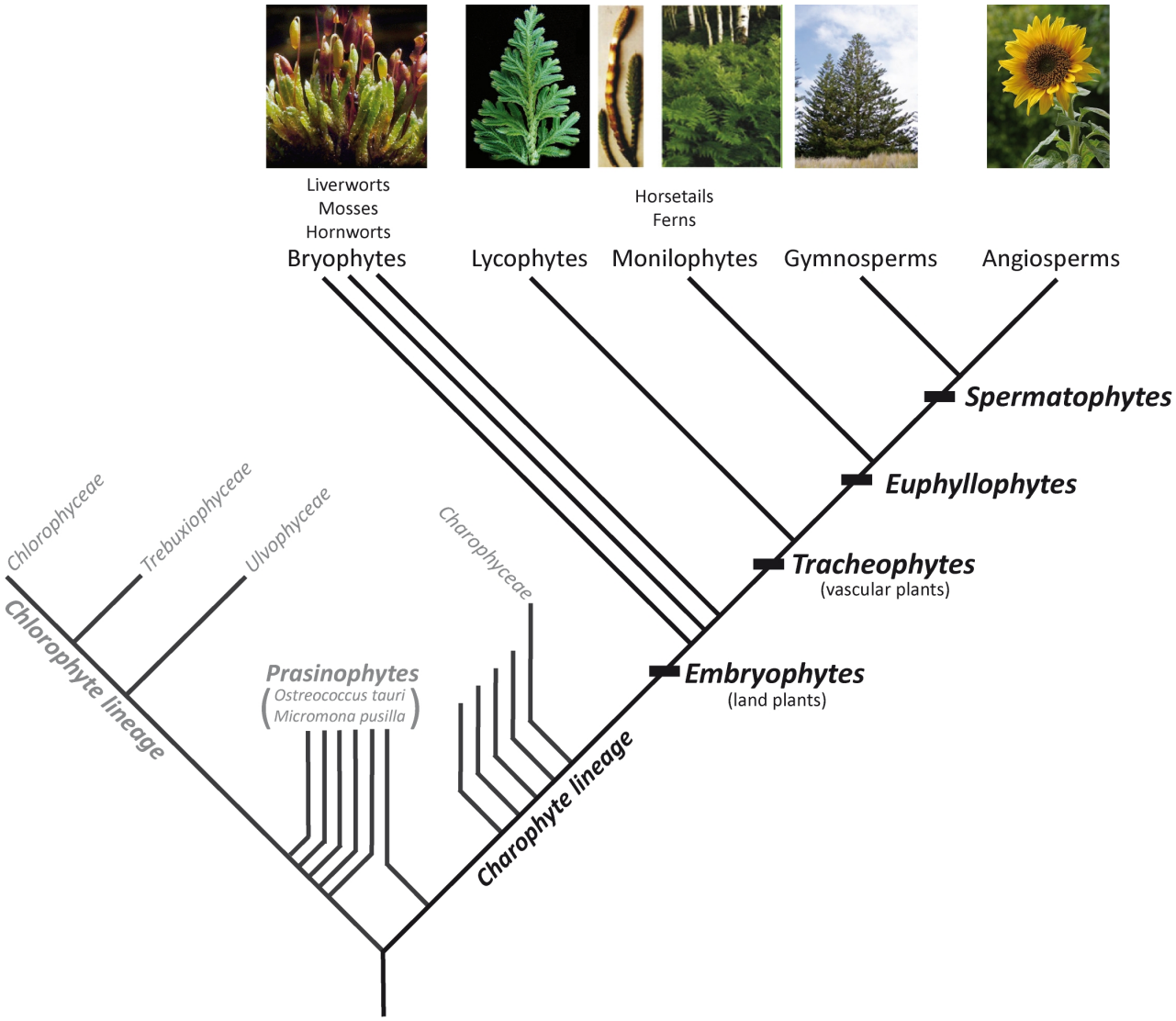

Fig. 1. Summary of the phylogenetic relationship among the major lineages of the plant kingdom. In grey the algae groups, in black the land plants ancestor lineage.

divergent algal clades (Fawley *et al.*, 2000), occupy the most basal position of the green algal tree of life and are viewed as the form of cell most closely representing the first green alga (Lewis and McCourt, 2004) (Figure 1). *Ostreococcus tauri* and *Micromonas pusilla*, whose genomes recently have been fully sequenced and annotated (Palenik *et al.*, 2007; Worden *et al.*, 2009), are prasinophytes of the order Mamiellales. Thereafter, the green algae have evolved into two major lineages. The chlorophyte clade, which comprises the classes Chlorophyceae, Ulvophyceae and Trebouxiophyceae (Figure 1), includes the majority of what have been traditionally called green

algae; the charophyte lineage contains a smaller number of green algal taxa as geographically widespread and as familiar as other green algae. Despite the antiquity of their shared common ancestor, ribosomal DNA and many plastid and mitocondrial genes are recognizable as homologues in green algae and land plants and identify the charophytes, and the Charophyceae class among them, as the algal sister group to land plants (Karol *et al.*, 2001; Turmel *et al.*, 2003) (Figure 1).

Paleobotanical studies on the earliest known fossil evidence of terrestrial colonization by plants suggest the first appearing flora were liverwort-like plants (reviewed by Kenrick and Crane, 1997). Indeed, a large scale molecular analysis on bryophyte relationships resolves the liverworts as the most basal group among land plants, and the hornworts as the most likely sister group of the vascular plants (Qiu *et al.*, 2006), thus rendering the bryophytes (liverworts, mosses and hornworts) as a paraphyletic group (Figure 1) that probably separated from the tracheophyte lineage over 420 mya, based on the fossil record for the first traces of prototracheal elements (Edwards and Feehan, 1980).

Thus, mosses and vascular plants share a common ancestor with a bryophyte-like life cycle. This implies that, before the separation of the lycophyte and euphyllophite lineages, the late Silurian/early Devonian flora (420-400 mya) must have undergone a gradual shift from a gametophyte-dominant to sporophyte-dominant life cycle, which are characteristic of briophytes and vascular plants, respectively. Indeed, the extinct genera *Aglaophyton* and *Nothia*, for which fossil evidence has been found in sediments dated back to early Devonian, had a diplohaplontic life cycle in which the sporophyte no longer greew parasitically on the gametophyte but rather independently from it (Kenrick, 2000). Therefore, these two extinct genera could represent a possible link between bryophytes and tracheophytes. The gametophyte of modern vascular plants is highly reduced but, interestingly, some basal groups such the licophyte family Lycopodiaceae and the monylophyte family Ophioglossaceae retain vestiges of the diplohaplontic life cycle (Kenrick, 1994).

Once plants had reached the land, they had to face the lack of water of the new environment and possible desiccation stresses. Most bryophytes avoid it by restricting their habitat to moist environments, or by drying out and putting their metabolism into a quiescent state until more

water is available. On the other side, to reduce water loss, tracheophytes developed a waterproof outer cuticle layer (as some bryophytes also do). Since a complete covering would isolate land plants from CO_2 in the atmosphere, in turn they have been compelled to evolve structures to maintain vital gas exchange, the stomata (Kenrick and Crane, 1997). Furthermore, in order to supply their photosynthetic apparatus with water, the early plants were forced to develop systems to transport water from the moist soil to the site of photosynthesis. Therefore, specialized water transport tissues soon evolved in the form of hydroids, tracheids, then secondary xylem, followed by an endodermis and ultimately vessels (Sperry, 2003). All these innovations, together with the appearance of branching sporophytes (Crane *et al.*, 2004), were acquired after the divergence of bryophytes from the higher plant lineage but before the lycophyte-euphyllophyte divergence.

Since the extant lycophytes, although they are the result of approximately 400 mya of independent evolution, retain most of the features of the trachephyte ancestor, including simple bifurcating meristems and naked sporangia (Banks, 2009), the establishing of a lycophyte plant model organism could provide new insight into the evolution of the earliest vascular plants. To this purpose, the genome sizes of several species of lycophytes ware surveyed in order to find the most suitable lycophyte species for a genome assembly project, and *Selaginella moellendorffii* was identified as the best candidate (Wang *et al.*, 2005).

The phylum Lycopodiophyta, which includes the three extant classes Lycopodiopsida, Isoetopsida and Selaginellopsida, constitute a monophyletic plant group (Raubeson and Jansen, 1992; Duff and Nickrent, 1999; Qiu *et al.*, 2007). They differ from the other vascular plants in having mycrophylls, namely leaves that have only a singular vascular trace and no leaf gaps, rather than the much more complex megaphylls found in ferns and seed plants. Although the KNOX-ARP antagonism is involved in euphyllophyte as well as in lycophyte leaf formation (Harrison *et al.*, 2005), the differences in vasculature architecture and the fossil evidence suggesting that the common ancestor of lycophytes and fern/seed plants clades lacked any leaves has led to the belief that leaves evolved independently in these two lineage and that the KNOX-ARP interaction has been recruited at least twice independently during land plant evolution (Kenrick and Crane, 1997; Harrison *et al.*, 2005). Similarly, the root is widely considered to have evolved independently in

lycophyte and euphyllophyte lineages (Raven and Edwards, 2001), emphasizing how similar structural adaptation for terrestrialization and, in the case of leaves, also conserved molecular strategies, have been recruited in several independent lineages in the course of plant evolution. Therefore, a comparative study of lycophytes and euphyllophytes could elucidate developmental mechanisms, such as those governing the formation of microphyll/megaphyll anlage, which were probably already present in their common ancestor more then 400 mya.

As mentioned above, *S.moellendorffii* was chosen among lycophytes by the DOE Joint Genome Institute for a genome assembly project (http://genome.jgi-psf.org/Selmo1/ Selmo1.home.html). *S.moellendorffii* has a genome size of only ~110Mbp, which is the smallest genome size of any plant reported (Wang *et al.*, 2005), with the exception of two species in the Lentibulariaceae (Greilhuber *et al.*, 2006). Unfortunately, *S.moellendorffii* has several unfavorable characteristics that hinder its use as a model organism. It is reported that cultivated specimens lack sexual reproduction due to megosporangia abortion (Little *et al.*, 2007). Moreover, *S.moellendorffii* appears to have extreme susceptibility to elevated light intensity that causes the plants to turn red and enter a kind of quiescent stage (J.A.Banks, Purdue University, Indiana; personal communication).

Although it has been picked among *Selaginella* species by the genome sequencing program mostly because of its extremely small genome size, *S.moellendorffii* has neither been extensively used in molecular biology nor botanically characterized until recently (Banks, 2009). On the other hand, another Selaginellaceae species, *S.kraussiana*, has been the object of several recent studies, making it a reliable model organism suitable for developmental investigations. Moreover, the Selaginellaceae family comprises the single genus *Selaginella*, which in turn includes approximately 700 different species (Banks, 2009). A molecular phylogentic study by Korall and Kenrick (2004) demonstrated that rates of molecular evolution among *Selaginella* species are remarkably high compared with those of angiosperm families. The same authors also characterized in detail the phylogenetic relationship among Selaginellaceae, revealing *S.moellendorffii* and *S.kraussiana* to be relatively distantly (Korall and Kenrick, 2002). Therefore, the parallel study of *S.moellendorffii* and *S.kraussiana* would enable the use of molecular biology tools in order to investigate the *WOX* gene

family evolution in the case where they are not serviceable on *S.moellendorffii*, and simultaneously to uncover possible differences peculiar of one or the other *Selaginella* species.

1.4 Aims of the work

The dissertation will focus on two distinct aspects, shoot apical meristem homeostasis in monocots and the evolution of the *WOX* gene family.

In an attempt to elucidate further monocot SAM homeostasis, this work will take advantage of both molecular biology and a genetic approach. Phylogenetic tools were used to find the best putative candidates able to regulate the *ZmWUS1* activity in the maize SAM, and the transcripts expression patterns were analyzed. In addition, data from a *ZmWUS2* mutator insertion line will be also discussed.

The second part of the dissertation will address WOX gene family evolution, especially focused on the lycophyte genus Selaginella. The work is centered on the identification of *WOX*-like genes in both *S.kraussiana* and *S.moellendorffii* and their expression pattern characterization, together with a extended analysis of the *WOX13*-like sub-clade.

MATERIALS AND METHODS

2.1 Molecular biology methods

All standard molecular biology methodologies were performed following the respective manufacturer protocols.

- Genomic DNA purification: Macherey-Nagel NucleoSpin® Plant II
- DNA purification of PCR products from agarose: Macherey-Nagel Nucleospin® Extract II
- Plasmid DNA purification: Macherey-Nagel Nucleospin® Plasmid
- RNA purification: Peqlab PeqGOLD plant RNA kit
- cDNA synthesis: Invitrogen SuperScript™ III Reverse transcriptase, primed with oligo(dT)$_{12\text{-}18}$ or random primers (Invitrogen), always preceded by 15-45' DNAse I (Roche) digestion at 37°, followed by 10' inactivation step at 70°
- RACE (Rapid Amplification cDNA ends): Ambion Inc. FirstChoice® RLM-RACE kit
- Genome Walking: BD Bioscience Universal GenomeWalker™ kit
- DNA fragment cloning: Invitrogen TOPO TA Cloning® with pCR®II-TOPO® following the One Shot® chemical transformation protocol in the *E.coli* DH5α® strain

2.2 Oligonucleotides and PCR conditions

All PCRs were performed using TaKaRa LA Taq™ or Invitrogen recombinant Taq DNA polimarases, following the manufacturer protocols. The optimal primer (Sigma-Aldrich Co.) pair T_m were always determined via gradient-PCR.

Name	Sequence 5' → 3'	Comments
GSS1877 Fw2	GGGGCTTTGCTACTTGCACC	GRMZM2G072569 *In situ* hybridization probe
GSS1877 Re2	GCTGATGAGATCTGGAGGCG	
GSS2672 Fw2	GTACGAGTTCATGCCCAACG	GRMZM2G141517 *In situ* hybridization probe
GSS2672 Re3	CGCTTCAACAGATTCATCAGC	
GSS1729 Fw2	CGTCAAGTCCAACAACATCC	GRMZM2G043584 *In situ* hybridization probe
GSS1729 Re3	CGCTTCACTCAAAGAACAGG	
DGWox13 all+SelCD Fw	CIKCICRISARMGITGGASRCC	Degenerate primer PCR on *S.kraussiana*
DGWox13 SelAEG Fw	CIGKICRISARMGITGGGMRCC	
DGWox13 SelFH Fw	CICCICRISARMGITGGYTNCC	
DGWox13 all Re	GMICKIGRYYTRTTYTGRAACC	
DGWox13 Sel Re	TCICKIGRYYTRTTYTGRAACC	
DGWox13 SelAG Re	TCICKIGRYYTRTTIGSRAACC	
JN7	CARATICARCARATIACIGC	
JN9	TGGAAYCCIACIAARGAICA	
DGWox9 Fw1	CCIAARCCACGITGGAAYCC	
DGWox9 Fw2	CCIAARCCIAGRTGGAAYCC	
DGWox9 Re	TTYTGRAACCARTARAAIACRTT	
DGWox3 Fw	TGGTGYCCIACICCIGARGCA	
DGWox4 Fw1	GGIACIACICGITGGAAYCC	
DGWox4 Fw2	GGIACIACIAGRTGGAAYCC	
WHOM Re	GCYTTRTGRTTYTGRAACCARTARAA	
JN8	TGGAAYCCIACICCIGAICA	
SkWOX13A Fw1	CAGAGGATCAAAGAGATAACC	*SkWOX13A* 3'RACE
SkWOX13A Fw2	CACGGGCAAATCTCCGAGACC	
SkWOX13B Fw1	GACACAACTCAAGATTTTAGAGG	*SkWOX13B* 3'RACE
SkWOX13B Fw2	GATTTGGCTAAACACGGTCCC	
SkWOX13C Fw1	GCAACGGATCAAGGAGATCG	*SkWOX13C* 3'RACE
SkWOX13C Fw2	TACGGCGAGATCTCCGAGGCG	

SkKNOX1 Fw	CAGTAGCATGCCTCCTCACC	Positive control
SkKNOX1 Re	CGTGGTAAGTCCCAATCTCC	
SmWOX13A Fw1	GCCTCTACGACGTTGGAATGG	*SmWOX13A* 3'RACE
SmWOX13A Fw2	GCGAGTGCGAGAGATCACGGC	
SmWOX13B Fw1	CCACCACAAGCCAACGTCGC	*SmWOX13B* 3'RACE
SmWOX13B Fw2	GGATCAAGGAGATCACGAGC	
SmWOX13C Fw1	GGCTGTTCGAGGAGGAGGGC	*SmWOX13C* 3'RACE
SmWOX13C Fw2	GCTCGCCAAGGTGATGTTACG	
SmWOX13C Fw3	GGCTCGAGCCAAGCGCAAGC	
SmH3 Fw	ATTTCTCAATGGCGCGTACC	Positive control
SmH3 Re	TTCGTGTCCTCGAAAAGACC	
SmWOX13A Fw6	GATTTTGGGATCGTGATGAGC	*SmWOX13A* RT-PCR and *in situ* hybridization probe
SmWOX13A Re1	GTCTTAGTTCGAGAGGACGACC	
SmWOX13B Fw3	CTCCCTCCTCCCAATCTTCC	*SmWOX13B* RT-PCR and *in situ* hybridization probe
SmWOX13B Re2	GCAACCGTGTAGCTTCCACC	
SmWOX13C Fw5	CGAGAATGCGGAGCCTGAGG	*SmWOX13C* RT-PCR and *in situ* hybridization probe
SmWOX13C Re1	GATTTTTTGTTACCTTGTTGAGG	
SelKra13A Re2	TTATCTCTTTGATCCTCTGCCTGTTTGG	Genome Walking
SelKra13C Re3	TCTCGCCGTATTGGACCAAGTCGGTTGC	
SelKra13B Re3	CGTAATCTCACTCACTCTCCTCTTATTTGG	
SkWOX13A Fw5	CCAGTGCAATGTCCTGTGGC	
SkWOX13A Re3	GGCATGTGGGGTGTTCCCGC	
SkWOX13A Re4	CCTCATGTCATGGTAAGAACTTGG	
SkWOX13C Fw3	TGGTTAAAATGTGTCGTAATGTCG	
SkWOX13C Re4	CGTAGTTTCGGACTTCGTTTGG	
SkHD2probe Fw	CTGTTCTCCTCCAGCTCTGC	Positive control for *in situ* hybridization
SkHD2probe Re	GGAAGCACTCGACTTTCTGC	
SkWOX13B Fw4	CTTACCATCCTCATTACGGC	*SKWOX13B in situ* hybridization probe
SkWOX13B Re1	CGAGAAGGACACAAAAGTTG	
SkWOX13A Fw6	CCCTCCCTCTCGCCTCTTGAGC	*SKWOX13A in situ* hybridization probe
SkWOX13A Re5	CGTCGATTGGAAAAAGCTGTCC	

SkWOX13C GWFw7	CTAGAACGGCTCTTCAAGCAGGGAACCG	*SKWOX13C in situ* hybridization probe
SkWOX13C Re1	GCTCTAGTATAGAACATCAGCCCC	
AtWOX13 Fw2	CCAAATTAGGAACTAAAATAACCG	*WOX13* genotyping
AtWOX13 genFw	CCCATTTGGACGTGAAGTAGACAC	
AtWOX13 Re2	TCAATTACCCATACACCAAAGTGA	
AtWOX13 Fw1	TTTACCTTTCCTTCTACTCCCG	*WOX13* RT-PCR
AtWOX13 Re1	TCACAAGACGATTCAACAATCC	
AtGAPDH Fw	ATGGCCGGGACTGGATTGTTTGCTG	*Arabidopsis* RT-PCR positive control
AtGAPDH Re	CACGATTTCTGAGCTGATTTCGCCA	
ZmWUS2 genFw	GCAGATCAGGATGCTGAAGG	ZmWUS2 *Mu* insertion lines genotyping
ZmWUS2 genRe3	GGAAGAGAGGGAGTGTCTCG	
ZmWUS2 Mu	GCCTCCATTTCGTCGAATC	

Wobbles:	A+C+T+G	N
	A+G	R
	C+T	Y
	A+C	M
	T+G	K
	C+G	S
	Desoxyinosin	I

2.3 Non-radioactive *in situ* hybridization

The freshly excised plant material is firstly infiltrated in 4% paraformaldehyde solution (in PBS + 0.1% Tween-20) under vacuum for at least 20', and anyway until the specimens sink, and then fixated o/n in the same solution. The day after the specimens undergo a dehydration procedure, as following:

- 50% Ethanol, 90', in ice
- 70% Ethanol, 90', in ice
- 85% Ethanol, 90', 4°
- 90% Ethanol, 90', 4°
- 100% Ethanol + 0.1 Eosin Y, 90', 4°

- 100% Ethanol + 0.1 Eosin Y, o/n, 4°

The following day is used to wash the excess of Eosin Y and to prepare the specimen for paraffin embedding.

- 100% Ethanol, 90', 4°
- 100% Ethanol, 60', RT
- 50% Ethanol: 50% Rotihistol, 60', RT
- 3x 100% Rotihistol, 60', RT
- 50% Rotihistol: 50% melted Paraplast Plus® (Sigma-Aldrich), o/n, 50°

The specimen are kept in liquid Paraplast Plus® (60°) for the next three days, and old Paraplast Plus® is exchanged at least twice a day with new one.

After solidification, the specimen have been oriented as preferred and subsequently sectioned using a Leica RM 2145 microtome. The sections were 7 µm in thickness.

The sections were then deparraffinized, dehydrated and prepared for hybridization as follows:

- 100% Rotihistol, 10'
- 100% Rotihistol, 10'
- 100% Ethanol, 1'
- 100% Ethanol, 1'
- 95% Ethanol, 1'
- 85% Ethanol, 1'
- 50% Ethanol, 1'
- 30% Ethanol, 1'
- dH_2O, 1'
- 0.2M HCl, 10'
- dH_2O, 5'
- PBS, 5'
- Pronase (0.125mg/ml; Sigma-Aldrich), 10'
- 0.2M Glycine in PBS, 10'

- PBS, 2'
- 4% Paraformaldehyde in PBS, 10'
- 2x PBS, 2'
- acetic anhydride (1ml in 100ml of 0.1M triethanolammine), 10'
- PBS, 2'
- rapid dehydration with consecutive and increasing ethanol concentration solutions

To prepare the antisense probe, the DNA fragment of interest cloned into the pCR®II-TOPO vector was linearized by a single cut opposite to the T7 or Sp6 promoter chosen for the RNA polymerization.

- 8.5 µl H_2O
- 2.5 µl 10x transcription buffer
- 1 µl RNAse inhibitor
- 2,5 µl 5mM ATP
- 2,5 µl 5mM CTP
- 2,5 µl 5mM GTP
- 2,5 µl 1mM DIG-UTP
- 2 µl linearized plasmid
- 1 µl T7/Sp6 RNA polymerase
- 37°, 60-120'

To stop the polymerization, were added 75 µl of TMS buffer (0.01M Tris-HCl, 0,01 M $MgCl_2$, 0,05 M NaCl), 2 µl of 100mg/ml tRNA, and 1 µl of DNAse I (10U/µl), for 10' at 37°. In order to precipitate the RNA, 100 µl of 3.8 M ammonium acetate and 600 µl of ethanol were added. After at least 60' at -20°, the RNA was precipitated by a centrifugation step (10' at 14000 rpm). The pellet was washed with ice cold 70% ethanol/0.15 M NaCl and subjected to a centrifugation step as above. The RNA pellet was the dissolved in 50 µl of DEPC-treated water.

In order to facilitate the penetration of the DIG-labeled probe, the length of this was reduced to approximately 150 bases as follows:

- 1 vol of carbonate buffer (0,08 M $NaHCO_3$, 0,12 Na_2CO_3) was added to labeled probe RNA
- the probe was then hydolyzed at 60° for t min, where:

$$t = \frac{L_0 - L_f}{k \cdot L_0 \cdot L_f}$$

L_0 = starting length of probe RNA (in kb)

L_f = desired length of probe RNA (in kb)

k = rate constant (0.11 kb/min)

t = hydrolysis time in min

After hydrolysis, the probe RNA was purified by addition of 10 µl of acetic acid, 12 µl of sodium acetate 3 M, and 312 µl of ethanol, and kept for at least 60' at -20°. Then RNA was pelleted by 14000 rpm centrifugation for 10', supernatant was discarded and pellet resuspended in 50 µl DEPC-treated water. Previous to each hybridization, the probe RNA specific activity was always analyzed via dot blot.

Probe at desired concentration was added to 1 vol formamide such that the finale volume is 16 µl for each slide, heated at 80° for 2', and immediately put on ice. 80 µl of hybridization buffer were then added to the denaturized probe and spread over the slide. The hybridization buffer for 24 slides was prepared as follows:

- 200 µl of 10x salts solution (3M NaCl, 0,1M Tris-HCl pH 6.8, 0.1M PBS, 0.05M EDTA)
- 800 µl formamide
- 400 µl 50% dextran sulfate
- 20 µl 100mg/ml tRNA
- 40 µl 50x Denhardt's (2g BSA, 2g Ficoll, 2gg Polyvynilpyrrolidone in 100ml H_2O)
- 140 µl H_2O

Every slide was then covered with a Sigma Hybri-slip, put in a humid chamber, and then incubated o/n at 50°.

After hybridization, the excess of probe was eliminated by three washing (15', 60', 60') steps with warmed (50°) 2x SSC/50% formamide. To remove the unhybridized probe, a RNAse step was also included (20 µg/ml RNAse A in NTE buffer; 0.5M NaCl, 0.01M Tris-HCl, 1µM EDTA). The subsequent step were performed:

- 0.1M Tris-HCl pH 7.5, 0.15M NaCl, 0.5% Boehringer-blocking reagent, 60'
- 0.1M Tris-HCl pH 7.5, 0.15M NaCl, 1% BSA, 0.3% Triton X 100, 60'
- 0.1M Tris-HCl pH 7.5, 0.15M NaCl, 1% BSA, 0.3% Triton X 100, anti-DIG antibodies coupled with alkaline phosphatase 1:3000
- 0.1M Tris-HCl pH 7.5, 0.15M NaCl, 0.3% Triton X 100, 4x 20'
- 0.1M Tris-HCl pH 7.5, 0.15M NaCl, 5'
- 0.1M Tris-HCl pH 9.5, 0.1M NaCl, 0.05M $MgCl_2$, 5'
- 0.1M Tris-HCl pH 9.5, 0.1M NaCl, 0.05M $MgCl_2$, 1,5 µl NBT and 1,5 µl BCIP, 10% polyvynilalcohol, up to 3 days in dark

The developing reaction with NBT/BCIP can last up to three days and was stopped by two washing steps in water for 5'.

The slide were then mounted with Entellan® new (Merck) and inspected with Nomarsky (DIC) optics on a Zeiss Axioskop microscope and captured by a Zeiss Axiocam coupled with it.

RESULTS

3. CLAVATA1 orthologs in maize

In contrast to *Arabidopsis*, where *WUS* expression is tightly linked to the SAM Organizing Center (OC), none of the grass *WUS* orthologs displays a stable OC-type expression domain but they are rather related to the specification of new phytomers (Nardmann and Werr, 2006).

The difference between *Arabidopsis* and grass *WUS* orthologs in terms of transcription domains acquires more relevance when correlated to the *TD1/FON1* expression pattern in maize and rice (Bommert *et al*., 2005; Suzaki *et al*., 2004). Both *TD1* and *FON1* are expressed at the flank of the meristem in cells recruited into the leaf primordia, overlapping the *ZmWUS2/OsWUS* transcription domains. In contrast, *TD1/FON1* transcripts are absent in the center of the SAM, where *ZmWUS1* and *OsWUS* can be transiently detected. Therefore, the *CLV1* orthologs *TD1* and *FON1* probably act to antagonize *ZmWUS2* and *OsWUS* activity in leaf primordia cells, but not the *ZmWUS1* and *OsWUS* activity observed in the SAM. The absence of *TD1* and *FON1* expression in the center of the shoot apex leads to the question of how *ZmWUS1* and *OsWUS* activity within the SAM is controlled.

3.1. Phylogenetic analysis

Assuming that *WUS* function and expression is under the control of *CLV1*-dependent signaling, it becomes obvious to look for close *CLV1* orthologs in maize other then *TD1*, supposing them to be the best putative candidates able to regulate *ZmWUS1* activity.

To estimate phylogenetic relationships between *CLV1*-related receptor-like kinases, a screening of four fully sequenced genome species databases other then maize, namely *A.thalana*, *Populus trichocarpa*, *O.sativa* and *Sorghum bicolor*, have been performed. The ten best hits from each TBLASTN results for the kinase domain primary sequence of *CLV1* (*Arabidopsis* and Poplar), *FON1* (Rice) and *TD1* (Maize and Sorghum), were taken into a first raw analysis. The putative kinase domains were identified from those sequences by similarity with the known kinase domain. These kinase domains were aligned then using the CLUSTALW2 algorithm (http://www.ebi.ac.uk/Tools/clustalw2/). Subsequently, the most distant results from *CLV1* and its closest orthologs were discarded. In order to strengthen the analysis, the phylogeny was constructed with the remaining 26 sequences using three different algorithms, namely maximum likelyhood (PHYLIP version 3.6, Felsenstein 2005), maximum parsimony and neighbor joining (MEGA 4, Tamura et al, 2007). The resulting phylogenies from each of the three methods has been tested with 1000 bootstrap replicates. Because of the different environment in which leucine-rich repeats (LRR) and kinase domains are embedded, and due to the different functions (ligand-binding and phosphorylation) they perform (Hunter, 1995), these two distinct domains might have been subjected to different evolutionary forces. To evaluate this eventuality, the same phylogenetic analysis described above has been performed on the LRR domains.

This phylogenetic reconstruction enables the analysis of possible differences among dicots and monocots and within the Poaceae family, by the comparison of one Bambusoideae species (Rice) and two Panicoideae grasses (maize and sorghum). Furthermore, since the entire *Z.mays* genome sequence has been completed only recently, the annotation process has not been completed yet (http://maizesequence.org/version.html - Release 3a.50, December 2008). Therefore, the evaluation of putative *Z.mays* candidates against *S.bicolor CLV1* orthologs might help to more deeply understand the phylogeny and to discriminate between real differences and any annotation-caused artifacts.

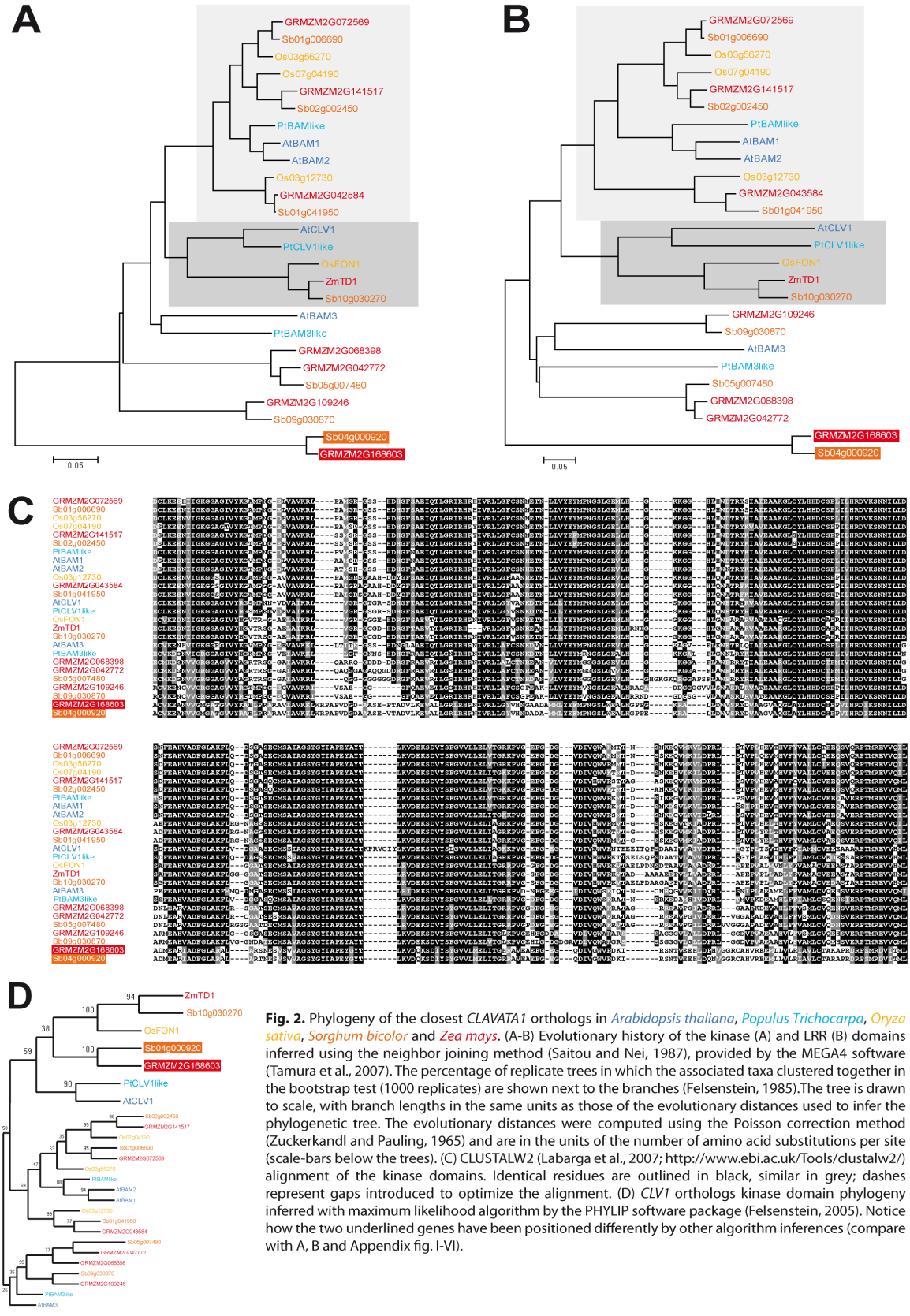

Fig. 2. Phylogeny of the closest *CLAVATA1* orthologs in *Arabidopsis thaliana*, *Populus Trichocarpa*, *Oryza sativa*, *Sorghum bicolor* and *Zea mays*. (A-B) Evolutionary history of the kinase (A) and LRR (B) domains inferred using the neighbor joining method (Saitou and Nei, 1987), provided by the MEGA4 software (Tamura et al., 2007). The percentage of replicate trees in which the associated taxa clustered together in the bootstrap test (1000 replicates) are shown next to the branches (Felsenstein, 1985).The tree is drawn to scale, with branch lengths in the same units as those of the evolutionary distances used to infer the phylogenetic tree. The evolutionary distances were computed using the Poisson correction method (Zuckerkandl and Pauling, 1965) and are in the units of the number of amino acid substitutions per site (scale-bars below the trees). (C) CLUSTALW2 (Labarga et al., 2007; http://www.ebi.ac.uk/Tools/clustalw2/) alignment of the kinase domains. Identical residues are outlined in black, similar in grey; dashes represent gaps introduced to optimize the alignment. (D) *CLV1* orthologs kinase domain phylogeny inferred with maximum likelihood algorithm by the PHYLIP software package (Felsenstein, 2005). Notice how the two underlined genes have been positioned differently by other algorithm inferences (compare with A, B and Appendix fig. I-VI).

The resulting phylogenetic reconstruction, inferred by the neighbor joining algorithm and based on the kinase domain (Figure 2A) and the LRR-domain (Figure 2B), is shown. In both trees, *CLV1* groups together with its orthologs *OsFON1* and *ZmTD1*, and one gene each of *P.thricocarpa* and *S.bicolor*, highlighting a discrete *CLV1*-related clade (dark-grey box in Figures 2A and B), as well as a clear split between eudicot and monocot sequences within the clade. Closer to the *CLV1*-related group, a sister clade comprising *Arabidopsis BAM1* and *BAM2* occurs in both phylogenetic trees (light-grey box in Figure 2A and B). Within this sub-family there are three different maize LRR-kinases, which create three small monocot-only sub-clades comprising one ortholog each from rice and sorghum. The genes *BAM1*, *BAM2* and a *PtBAMlike* group together in a fourth, eudicot specific sub-clade. Phylogenies constructed with maximum parsimony and maximum likelihood algorithms gave rise to similar trees with the same topology. Furthermore, in all trees the phylogenetic reconstruction was supported by high bootstrap values (appendix A, Figures I-V), with one exception. When the estimation of the kinase domain phylogeny has been performed with maximum likelihood algorithm, the genes *GRMZM2G168603* (highlighted in red) and *Sb04g000920* (highlighted in orange), originally used to root the tree due to their large evolutionary distance from *CLV1* relatives, moved within *CLV1*-like clade (Figure 2D, appendix A, Figure VI). This maize gene was not considered for further studies because it is clear that its position close to *CLV1* relatives is unlikely to be real: (1) the bootstrap value that should support *GRMZM2G168603* positioning in the maximum likelihood tree is poor, (2) the alignment among the kinase domain of the 26 sequences included in the phylogenetic analysis shows clearly those two genes to be the most divergent among all (Figure 2C) and (3) it has been reported that maximum likelihood can become strongly biased and statistically inconsistent when the rates at which sequence sites evolve change non-identically over time (Kolaczkowski and Thornton, 2004), and probably this might have been the case.

In light of this findings, it can be assumed that the proposed phylogenetic reconstruction should give the best approximation of the evolution of the closest *CLV1* orthologs in the five species under analysis. The clear dichotomy present between mono- and eudicot genes within all the sub-clades, as well as the concurrence between the gene trees and the known evolutionary distance among the screened species, strengthens the trees' validity. Furthermore, the molecular

evolutionary situation with respect to the *WUS*/*CLV* interaction in mono- and eudicot suggests a monocot-specific way to regulate a monocot-specific gene, *ZmWUS1*. Within the *BAMs* sub-clade, indeed, a monophyletic monocot-specific duplication has been reconstructed, as well as a paraphyletic outgroup including single rice, maize and sorghum sequences.

With this in mind, the presented phylogeny identified the genes *GRMZM2G072569*, *GRMZM2G141517* and *GRMZM2G043584* as the most likely candidates for further studies. Due to their closer phylogentic relationship to *Arabidopsis BAM1/2* genes, these three maize genes will be renamed *BAM-like Receptor-like* (*BLR*) *kinase 1*, *BLR2* and *BLR3*, respectively.

3.2. *ZmBLR1*, *ZmBLR2* and *ZmBLR3* gene structure

The predicted coding sequences of the genes *ZmBLR1*, *ZmBLR2* and *ZmBLR3* are aligned against their orthologs in rice and *Arabidopsis*, as well as *CLV1*, *TD1* and *FON1* (Figure 3). As expected, all these genes share common features. The leucine-rich repeat domain is found in the N-terminal region of all proteins, and it contains 21 or 22 imperfect tandem repeats of a 24 amino acid leucine-rich motif, arranged in a single block (in contrast to the arrangement of other LRRs domains in 2 or more discontinuous blocks, i.e. *CLV2*, *BRI1*; review by Shiu and Bleecker, 2001), as for *CLV1* closest orthologs. The consensus sequence that can be compiled from this alignment involves leucines at positions 1, 4, 6, 11 and 15, the latter often substituted by an isoleucine residue, an asparagine at position 9, a glycine at position 13 and a proline at position 16. Thus, the common consensus sequence among the LRR can be schematically drawn as LxxLxLxxNxLxGxI/LPx$_{7\text{-}9}$, which do not differ from the one already annotated for *CLV1* (Zhang, 1998). The LRR extracellular domains are flanked in all genes by pairs of highly conserved spaced cysteines (red asterisks) and followed by putative transmembrane domains (underscored in dark blue) and the C-terminal intracellular serine/threonine kinase domains (underscored in red). All these genes have a single intron located in a conserved position within the kinase domain (black arrowhead).

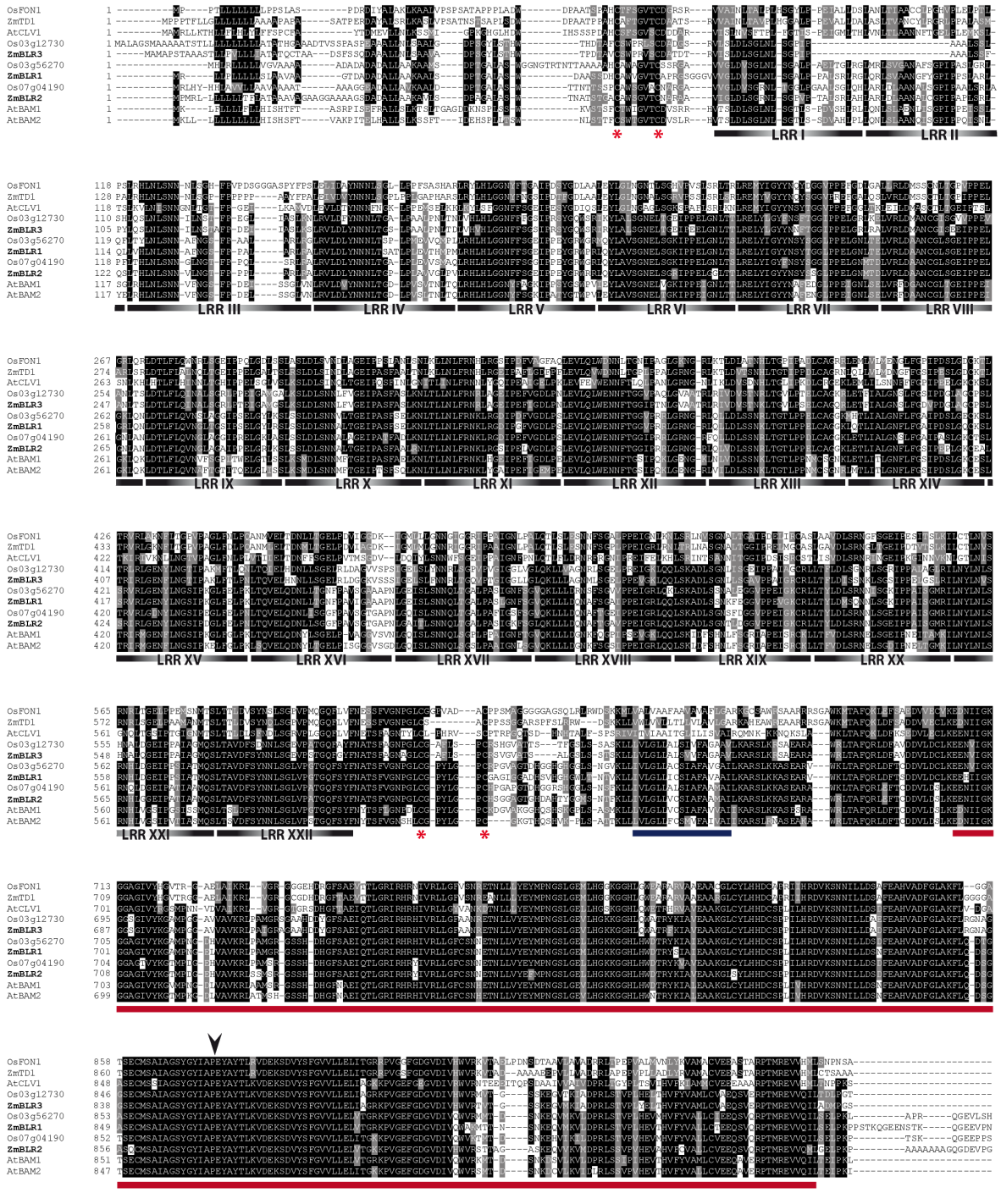

Fig. 3. Molecular characterization of the three maize candidate genes. CLUSTALW2 alignment of *TD1*, *CLV1*, *FON1*, *BAM1*, *BAM2* and their rice and maize closest orthologs. Identical residues are outlined in black, similar in gray; dashes represent gaps introduced to optimize the alignment. Domains are labeled below the respective sequences: black to white shaded, extracellular LRRs motifs; dark blue, transmembrane domain; red, serine/threonine kinase domain; red asterisks, conserved spaced cysteines. The black arrowhead indicates the conserved position of the single intron splicing site.

3.3. *ZmBLR1*, *ZmBLR2* and *ZmBLR3* expression patterns

3.3.1. *ZmBLR1* expression is associated with the growing region of leaf primordia

The predicted *ZmBLR1* transcript is 3880bp in length, containing an open reading frame of 3102bp, that includes a single 462bp intron and encodes for 1034 amino acid predicted protein (Figure 4A, http://maizesequence.org/index.html). This gene is positioned on chromosome 1. To analyze finely the expression pattern of this candidate gene, an *in-situ* hybridization analysis with a 697bp specific probe designed against the carboxy-terminus sequence of the gene was performed (underscored in pale orange in fig. 3A).

Expression of the maize *CLV1* ortholog *ZmBLR1* is mainly focused on the apical tip of the newly established leaf primordia, either the primordium is discretely distinguishable beside the SAM (P_2) or it is still protruding from the SAM flank (P_1) (Figure 4B). In older leaf primordia, the gene transcripts are detected in the vascular bundles (Figure 4B), but just inside the growing leaf (arrowhead in Figure 4B). A further clarification of the pattern is provided by cross-sections, depicted in Figure 3 (C-I). The signal within the P_2 is more intense at the very primordial tip (Figure 4D-E), while it wanes deeper in the shoot meristem (Figure 4F-I). Opposite to P_2, at the same height the SAM is losing is typical circular shape, the staining label the outgrowing P_1 (Figure 4G-I), partially overlapping the *ZmWOX3A/B* expression (Nardmann *et al.,* 2007). Furthermore, another expression pattern feature is evident in transverse view. In older leaves, the *ZmBLR1* transcripts are detected not only in the vascular strands, but in lateral leaf margins as well (dark-gray arrowhead in fig. 3D-F). Notably, the latter feature resembles the *ZmNS1/2* expression pattern (Nardmann *et al.,* 2004). Then, the gene *ZmBLR1* expression is associated with the meristematic active regions of the leaf primordia and it partially overlaps the expression of the four WOX3 orthologs in maize, *ZmNS1/2* and *ZmWOX3A/B*.

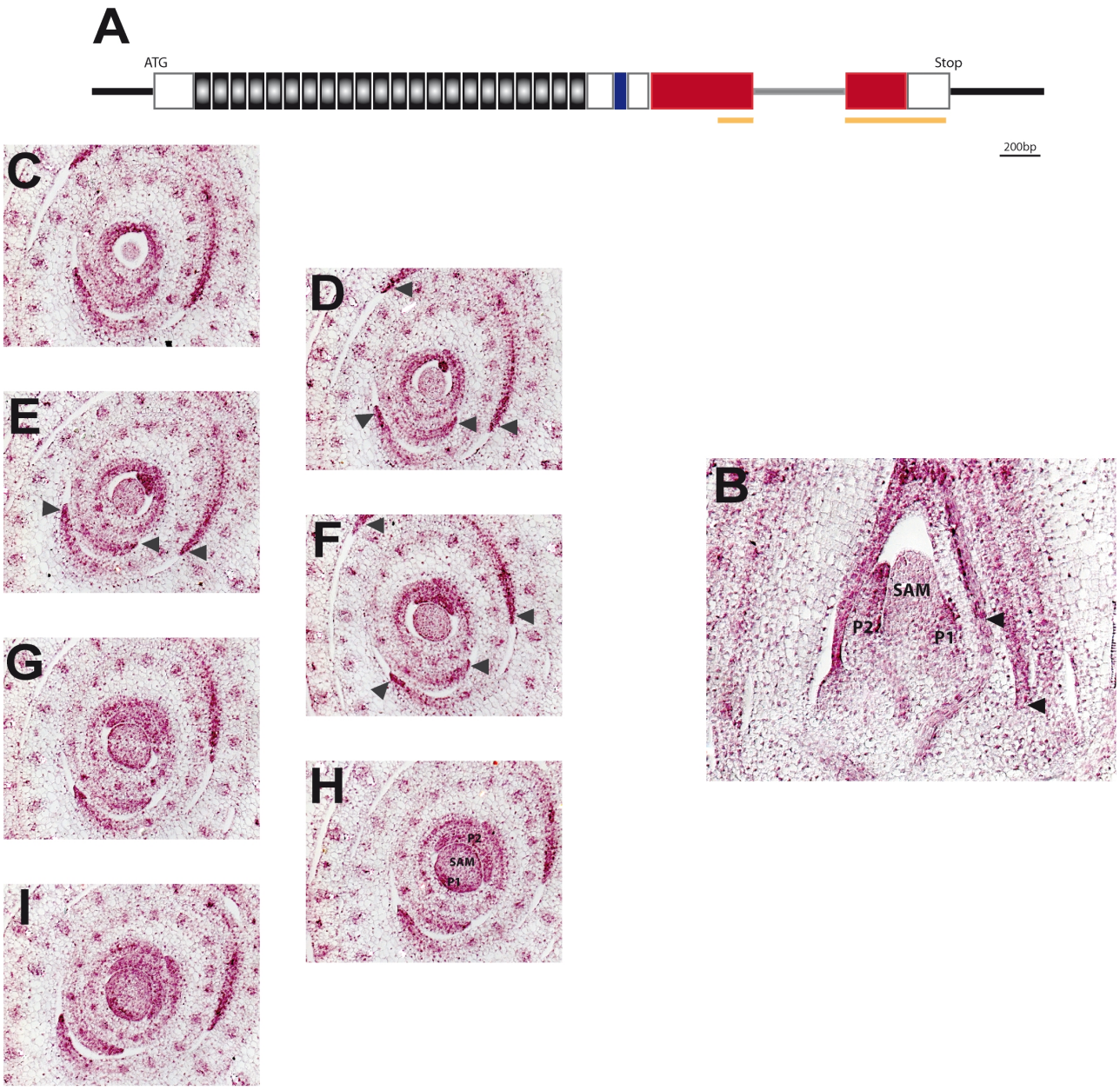

Fig. 4. *ZmBLR1* expression patterns. (A) In scale schematic representation of the gene showing the 22 LRRs (black-to-white shaded boxes), the transmembrane domain (dark blue box) and the kinase domain (red boxes) split by the single intron (dark grey line). In orange is underscored the probe annealing site. (B) Longitudinal section of a vegetative meristem, showing expression in the incipient P1 and in the tip of slightly older P2, as well as in leaf primordia vasculature bundle. The section shows a vascular strand coming from the stem and going inward the leaf primordia, in which the expression starts just when it has reached the leaf primordia itself (black arrowheads). (C-I) Transverse sections series through a vegetative meristem. Dark gray arrowheads mark the lateral domain of P3 and P4 where signal can also be detected.

However, these expression patterns highlight the absence of *ZmBLR1* transcripts within the SAM, where *ZmWUS1* is transcribed, leaving open the main question about the presence of a putative *CLV1* ortholog able to regulate *ZmWUS1* function.

3.3.2. *ZmBLR2* expression is associated with procambial cells

The predicted gene *ZmBLR2* is located on chromosome 7 and its mRNA is 3722bp in length. It codes for a predicted protein of 1037 amino acids, split by a single 257bp intron (Figure 5A, http://maizesequence.org/index.html). As for *ZmBLR1*, the expression pattern of the candidate gene *ZmBLR2* was analyzed via *in-situ* hybridization with a 727bp specific probe against the C-terminal region of the coding sequence (underscored in pale orange in Figure 5A).

From the *in situ* pictures depicted in Figures 4B and C, a transverse section at the height of P_1 anlage and a lateral median section respectively, it is easy to associate the expression pattern of *ZmBLR2* with the typical monocot vascular system architecture, made up of parallel veins lying along the leaf proximodistal axis. The expression pattern of gene *ZmBLR2* becomes more clear when singular vascular bundles are inspected. In Figures 5D-F are depicted vascular bundles stages I, III and IV (according to Sakaguchi and Fukuda, 2008). In its early developmental stage, procambial cells differentiate in the middle layer of the leaf ground tissue. The bundle outermost cells immediately form the circular layer that, eventually, differentiates into the final vascular bundle sheet (Stage I, Figure 5D). Subsequently, a primary protoxylem vessel and phloem cells are juxtaposed at the adaxial and abaxial sides, respectively. After the primary protoxylem vessel has differentiated, an adjacent cell acquires the protoxylematic fate (Stage III, Figure 5E). Later, two metaxylem vessels start to differentiate to the side of to the protoxylem elements (Stage IV, Figure 5F). Finally, protoxylem vessels collapse in the protoxylem lacuna, the vascular bundle sheet cells enlarge remarkably, and the differentiation of the vascular bundle is complete. During vascular bundle development, the procambial cells proliferate in the middle cell layer (Sakaguchi and Fukuda, 2008). Bearing in mind the developmental stage of monocot vascular bundles (insets in Figure 5D-F) and comparing those with the expression patterns show by *in situ* hybridization with the *ZmBLR2* specific probe, the correlation between *ZmBLR2* expression and procambial cells becomes clear.

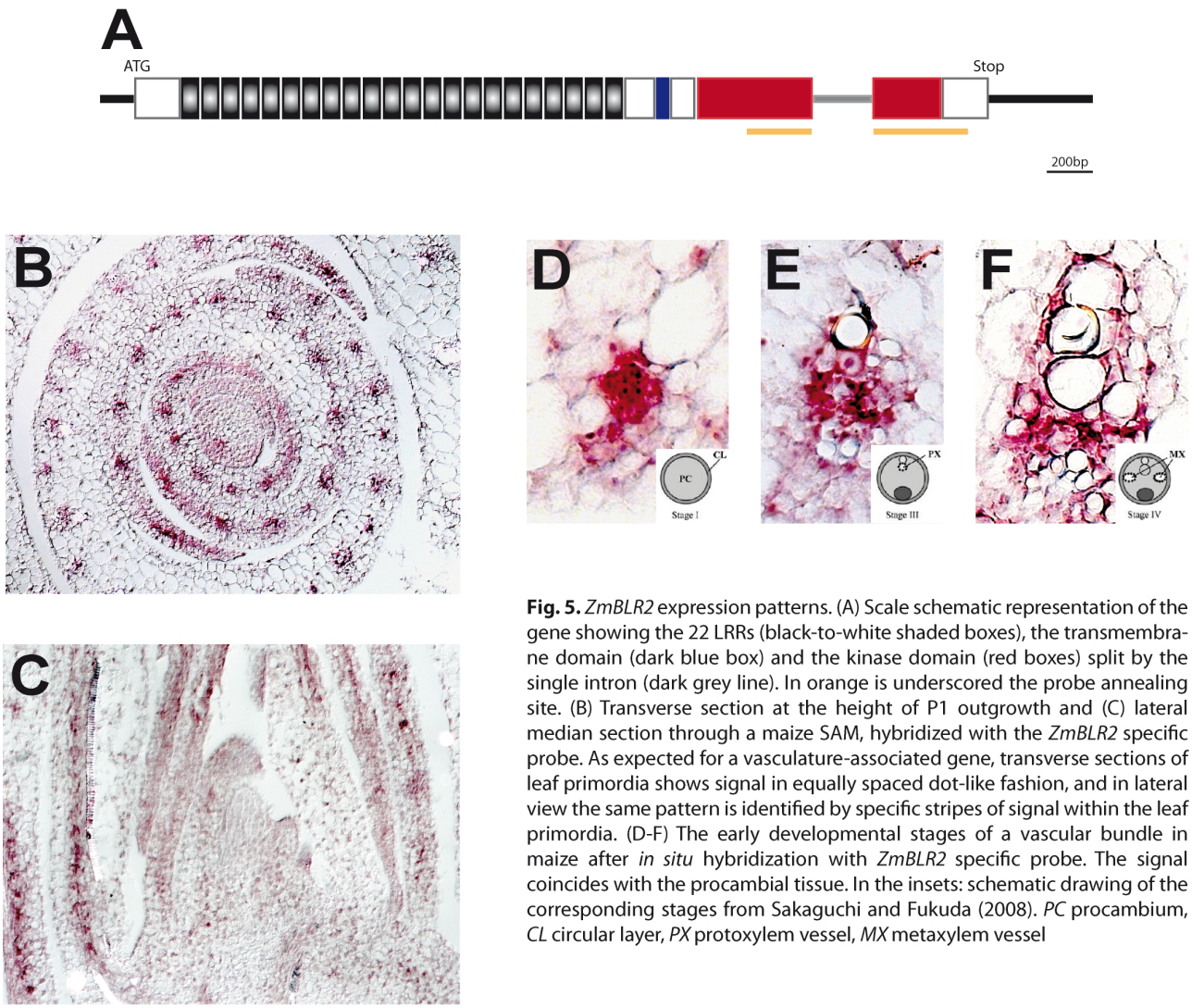

Fig. 5. *ZmBLR2* expression patterns. (A) Scale schematic representation of the gene showing the 22 LRRs (black-to-white shaded boxes), the transmembrane domain (dark blue box) and the kinase domain (red boxes) split by the single intron (dark grey line). In orange is underscored the probe annealing site. (B) Transverse section at the height of P1 outgrowth and (C) lateral median section through a maize SAM, hybridized with the *ZmBLR2* specific probe. As expected for a vasculature-associated gene, transverse sections of leaf primordia shows signal in equally spaced dot-like fashion, and in lateral view the same pattern is identified by specific stripes of signal within the leaf primordia. (D-F) The early developmental stages of a vascular bundle in maize after *in situ* hybridization with *ZmBLR2* specific probe. The signal coincides with the procambial tissue. In the insets: schematic drawing of the corresponding stages from Sakaguchi and Fukuda (2008). *PC* procambium, *CL* circular layer, *PX* protoxylem vessel, *MX* metaxylem vessel

Unfortunately, as for *ZmBLR1*, *ZmBLR2* expression is excluded from the SAM, thus ruling out the hypothesis that this gene might be a potential regulator of *ZmWUS1* activity.

3.3.3. *ZmBLR3* is expressed in primary thickening meristems

The gene *ZmBLR3* is located on chromosome 1. After splicing of the single 559bp intron, the mature transcript is translated into a 1002 amino acid predicted protein (Figure 6A, http://maizesequence.org/index.html). As for its close relatives, *in situ* hybridization analysis on

this gene has been performed using a 674 bp probe complementary to the end of the coding sequence, including part of the 3' UTR (underscored in pale orange in Figure 6A).

In lateral view, the *ZmBLR3* transcripts are detectable just beneath the SAM dome and in the most recently formed leaf primordium, but they are excluded from the SAM dome itself. the expression pattern then extends in a pyramid-like fashion that follows the insertion points of each leaf primordium on the stem (Figure 6B). In consecutive transverse sections, the expression of the gene is detectable in the ground tissue of the newly detached leaf primordia (Figure 6C-E) whereas, going deep in the meristem, the expression pattern acquires a doughnut-like shape, leaving a hole in expression where eventually the pith will form (Figure 6G-I). Moreover, the *in situ* hybridization staining never includes the most epidermal cell layers and shows some round gaps within the expression domain, which probably coincide with the vascular strands growing toward the leaf primordia (Figure 6I).

Interestingly, *ZmBLR3* marks regions of the shoot meristem that will be responsible, later in development, for the growth in thickness of the plant. As a monocot, in maize the thickening growth does not depend on the secondary meristem activity but rather on a monocot peculiar primary meristem, the primary thickening meristem (PTM). Indeed, according to Esau (1965, Figure 6J), the PTM is located beneath the leaf primordia. It produces rows of cells by periclinal divisions and its derivatives differentiate into ground parenchymatic cells traversed by procambial strands. Therefore, the PMT features described by Esau correspond almost entirely with the expression patterns shown by *ZmBLR3*.

As for the *ZmBLR1* and *ZmBLR2* expression patterns described above, *ZmBLR3* transcripts are excluded from the SAM, where *ZmWUS1* is expressed. In summary, although each of the candidate genes identified by the proposed phylogenetic analysis has a clear and distinct expression pattern, probably correlated with cell types which keep meristematic activity, none of them overlap *ZmWUS1*'s expression domain.

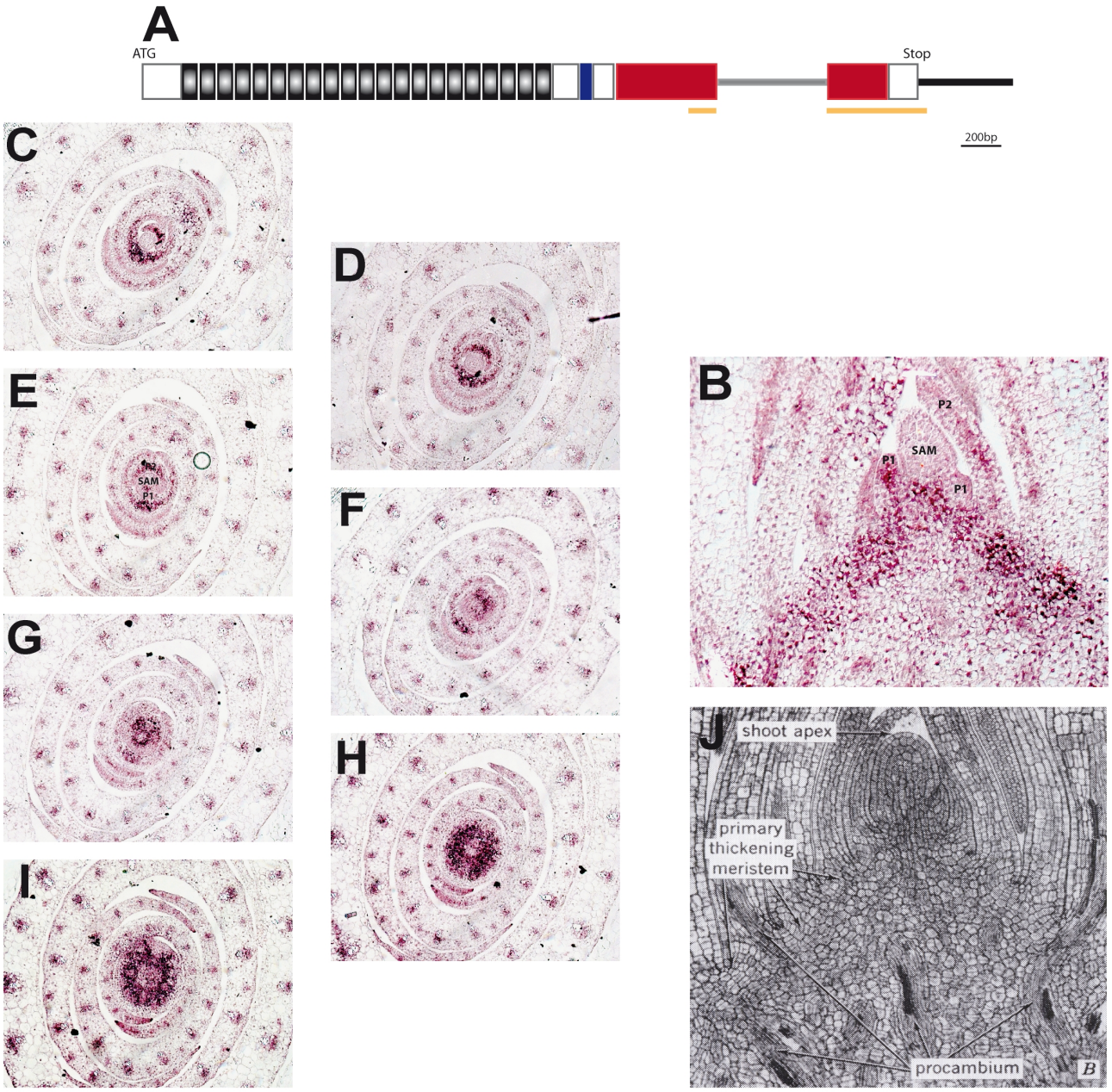

Fig. 6. *ZmBLR3* expression patterns. (A) Scale schematic representation of the gene showing the 21 LRRs (black-to-white shaded boxes), the transmembrane domain (dark blue box) and the kinase domain (red boxes) split by the single intron (dark grey line). In orange is underscored the probe annealing site. (B) Lateral view of a vegetative meristem, showing expression in the P1 and, beneath each leaf primordia, giving rise to a specific pyramid-like pattern. (C-I) Transverse sections series through a vegatative meristem. Going downward with the sections, the expression of gene *ZmBLR3* shifts from young leaf primordia to a ring-shaped domain in the stem, starting beneath the SAM dome. In (I) a few small non-expressing islands can be recognized within the compact ring-shaped expression. (J) Microphotography of a maize SAM pointing out the supposed location of primary thickening meristems, closely resembling the expression pattern shown in (B). From Esau (plate 58, p.598, 1965)

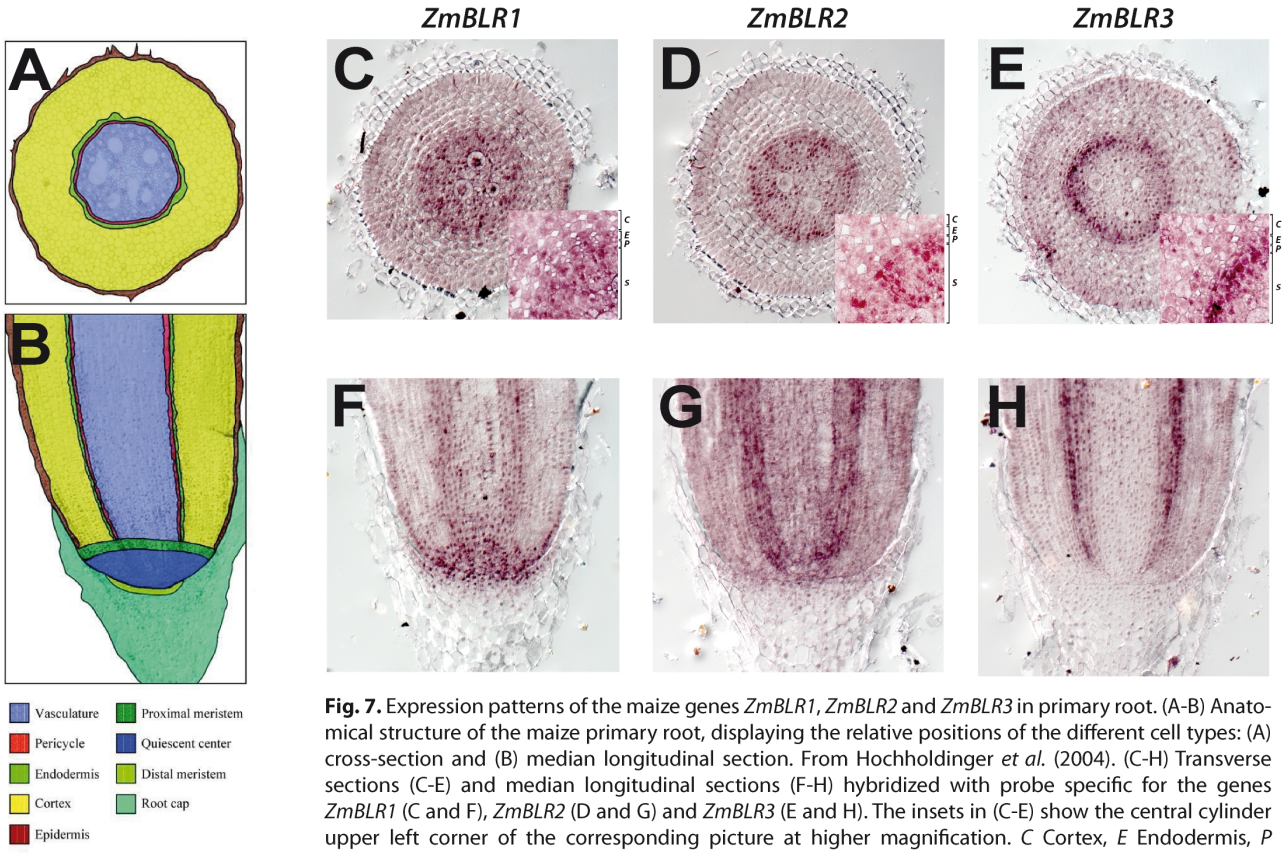

Fig. 7. Expression patterns of the maize genes *ZmBLR1*, *ZmBLR2* and *ZmBLR3* in primary root. (A-B) Anatomical structure of the maize primary root, displaying the relative positions of the different cell types: (A) cross-section and (B) median longitudinal section. From Hochholdinger *et al.* (2004). (C-H) Transverse sections (C-E) and median longitudinal sections (F-H) hybridized with probe specific for the genes *ZmBLR1* (C and F), *ZmBLR2* (D and G) and *ZmBLR3* (E and H). The insets in (C-E) show the central cylinder upper left corner of the corresponding picture at higher magnification. *C* Cortex, *E* Endodermis, *P* Pericycle, *S* Stele

3.3.4. *ZmBLR1*, *ZmBLR2* and *ZmBLR3* expression in root

Since *AtBAM1/2* are expressed also in roots (DeYoung *et al*. 2006), the expression of the three candidate genes in maize primary root was investigated as well in order to complete the data set about their expression patterns during the vegetative phase.

The three genes under study show different expression patterns. *ZmBLR1* has a peak of expression over the entire quiescent center and the calyptrogen (compare Figure 7B and F), whereas a less intense signal is observed within the stele (Figure 7C and F). Although in lateral sections *ZmBLR2* is expressed in the 4-5 outermost stele cell layers, corresponding to those which will develop into phloematic tissue (fig. 6G), in fact in transverse section the gene expression is excluded from the most central part of the stele, where the wider protoxylem vessels reside, and it

is non-continuous through the pericycle and its subtending cell layers (Figure 7D and its inset). This particular expression pattern probably prefigures the future phloem arches. The expression of *ZmBLR3* starts just above the quiescent center and is strong in the endoderm and pericycle cell layers (Figure 7E and H). Notably, the primary thickening meristem is not restricted to above ground meristem but has importance in roots as well, where it is known to cooperate in the production of a vascular network peripheral to the central cylinder, linking root, stem and leaf vasculature (Rudall, 1991). Moreover, a study on *A.cepa* positioned the PTM in root between cortex and central cylinder (DeMason, 1980), and a more recent work identified pericycle and endoderm cell layers as the source of meristematic activity involved in the monocotyledonous growth in thickness (De Menezes *et al.* 2005), the same region where *ZmBLR3* expression has been found in maize roots. Additionally, De Menezes and co-authors believe that the endodermis could maintain PTM identity in stem and leaves, mainly in the innermost ground layer, where the expression of gene *ZmBLR3* is found (Figure 6). Thus, *ZmBLR3* might mark the PTM in roots as well as in shoots.

4. ZmWUS2 insertion line

In order to better understand the SAM homeostasis in maize, a genetic approach was also followed. The Maize Target Mutagenesis DataBase (http://mtm.cshl.org/), which is a Robertson's *Mu* transposon insertions library stabilized by the using of a genetic inhibitor of *Mu* activity (May *et al*. 2003), was screened for transposon insertions in the maize genes *WUS1* and *WUS2*, and an insertion line for the latter was present. The obtained lines, termed MTM 48148, 48240 and 48242, all carry a single *Mu* insertion in the gene *ZmWUS2*. By sequence analysis, the three lines have *Mu* inserted in the same position, more precisely 284bp downstream to the gene's start codon, only 5bp after the homeodomain (Figure 8A).

The plants homozygote for the *Mu* insertion were apparently non phenotypic and their vegetative growth was not impaired, as well as their reproduction phase. Just in recent in-depth screening of possible phenotypes caused by the *Mu* insertion an interesting alteration was noticed. A wild-typic developing maize ear (Figure 8B) is characterized by a smooth apical inflorescence meristem (IM in Figure 8B), which produces several rows of short, determinate branches, termed spikelet-pair meristems (SPM in fugure 8B), which in turn divide to develop two spikelet meristems (SMs in Figure 8B) that further develop in the maize female flowers (Kiessekbach, 1949; Volbrecht *et al*, 2005). In *ZmWUS2* insertion lines, the inflorescence meristem appears bifurcated, split at least into two major, equally growing branches that are still apparently capable to produce spikelet-pair meristems and spikelet meristems (Figure 8C and D). Interestingly, *ZmWUS2* is expressed predominantly in the L1 layer of the IM where it appears to have a unique contribution (Nardmann and Werr, 2006).

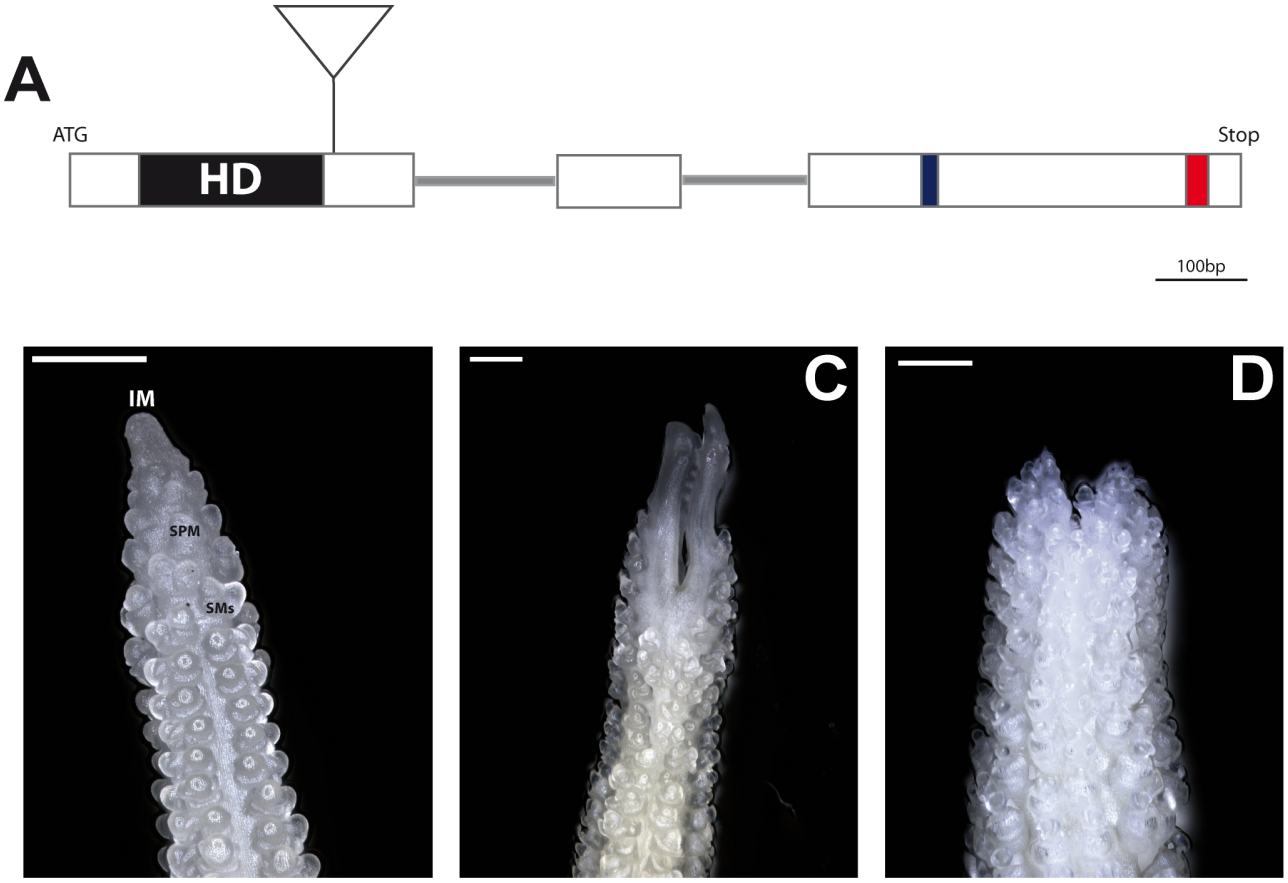

Fig. 8. *ZmWUS2* mutant phenotype. (A) In scale schematic representation of gene *ZmWUS2* showing the intron-exon pattern, the position of the conserved homeodomain (black box in the first exon), WUSCHEL box (blue box in the third exon), and EAR-like domain (red box in the third exon). In grey the *mu* insertion site as deduced by sequencing, right after the homeodomain. (B) Wild-typic immature ear showing the usual development of the female maize inflorescence. (C) Homozygote mutant immature ear showing split inflorescence apical meristem. (D) Older stage compared to (C).

Due to the peculiarity of the phenotype, and its very recent discovery, only a small population, namely 19 individuals, could be analyzed prior to phenotype loss due to ear maturation. All three analyzed homozygote plants for the *Mu* insertion in the gene *ZmWUS2* had this female inflorescence specific phenotype, whereas it was never observed in the remaining 16 wild-typic and heterozygotic plants. Obviously, this phenotypic data needs to be reinforced by a wider population analysis. Anyway, the fact that three homozygote plants out of three bears altered ear inflorescence meristem is a good indication that the *Mu* insertion in the gene *ZmWUS2* is the cause of the observed phenotype.

5. Evolution of the WOX Gene Family

The *WOX* gene family is involved in several plant developmental processes. These roles might be carried out via timing and orientation control of cell division planes, as demonstrated by the abnormal apical embryo development observed in the *wox2* mutant (Brueninger *et al*., 2008), through the control of cell cycle, as suggested by the *WOX9/STIP* mutant analysis in embryonic and adult tissues (Wu *et al*., 2005; Wu *et al*., 2007), or through interaction with auxins, as indicated by altered auxin maxima in *wox8 wox9* embryos (Breuninger *et al.*, 2008) or by the direct interaction of *WUSCHEL* with *WSIP/TOPLESS* (Kieffer *et al.*, 2006), which plays a crucial role in mediating the inhibitory effect of *IAA12/BDL* on *ARF5/MP*-regulated transcription (Szemenyei *et al.*, 2008).

Since the implication of *WOX* genes in a broad spectrum of developmental decisions is clear, it is intriguing to investigate the origin and evolution of this gene family. The recent completion of the sequencing projects of the moss *Physcomitrella patens* (Rensing *at al.*, 2008) and the Lycophyte *Selaginella moellendorffii* (http://genome.jgi-psf.org/Selmo1/Selmo1.home.html), which belong to the most basal plant kingdom divisions, have given a solid starting point to pursue this project further. Due to the breadth of the overall project, this study will focus on the evolution of the *WOX* gene family in two *Selaginella* species and initial characterization of possible *Arabidopsis WOX13* mutants.

5.1. Identification of the most basal *WOX* clade

After BLASTing the first-released versions of both *P.patens* and *S.moellendorffii* genome databases using the highly conserved *WOX* homeodomain, it became clear that the most basal

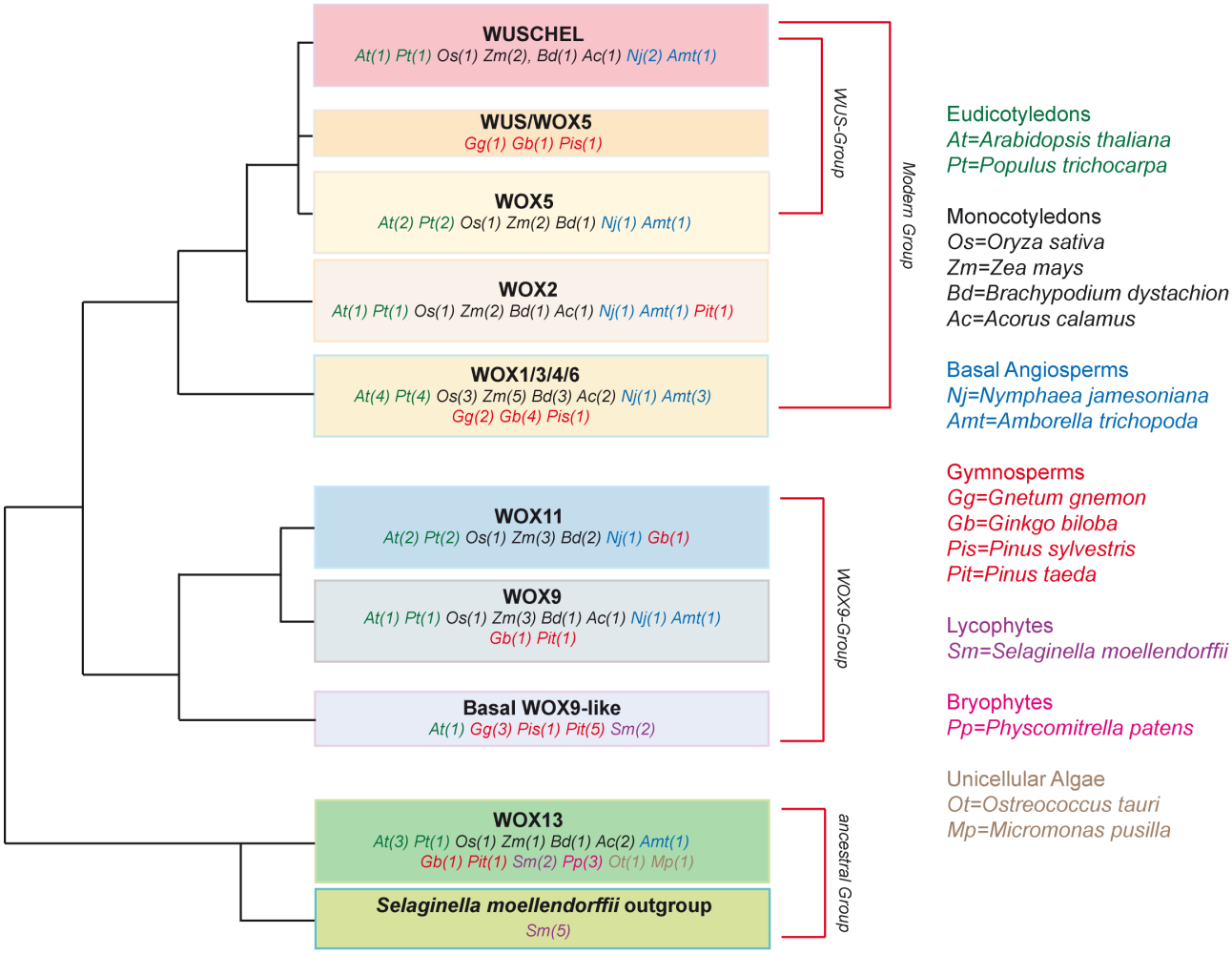

Fig. 9. Phylogeny of the *WOX* gene family. The scheme summarizes the evolutionary relationship among the homeodomain sequences of *WUSCHEL*-related genes present or predicted in the plant species listed and color coded.

WOX clade corresponds with the *WOX13* branch. The evolutionary relationship among the *WOX* gene family, comprising all the known and putative genes discovered so far, was inferred by the comparison of 122 known and predicted homeodomain sequences. It shows three distinct clades (Figure 9): (1) a modern clade, grouping together the *WUSCHEL* homologs genes from spermatophyte species and their closest orthologs *WOX1/2/3/4/5/6*; (2) a *WOX9*-like group which includes two *S.moellendorffii* predicted genes as well as angiosperm and gymnosperm genes that, in addition to the homeodomain, share a C-terminal conserved domain of unknown function; a clade including *WOX*-like genes from both *P.patens* and *S.moellendorffii*, as well as the unique

WOX genes found in the genomes of the unicellular algae *Ostreococcus tauri* and *Micromonas pusilla*, grouped together with spermatophyte *WOX13*-like genes.

The screening of the *S.moellendorffii* genomic database helped identify the sequences of nine putative *WOX* homeodomains. However, one of the supposed *WOX* genes in the *WOX9*-like clade, initially named *WOXB*, cannot be considered as a *WOX* gene. Indeed, although the genomic data suggest a putative homeodomain, this gene's transcript lacks a stretch of amino acids within the homeodomain that putatively encodes for the first homeodomain α-helix, as supported by both EST and RT-PCR data. Obviously, the lack of that helix would irremediably affect the functionality of the homeodomain itself. Therefore, the gene *SmWOXB* has been excluded from the phylogenetic analysis. In absence of *WOXB*, the phylogenetic algorithms move the other S.*moellendorffii WOX9* related gene into the *WOX13* clade. This gene was then named *SmWOX13C* and has been further studied along with *SmWOX13A* and *B*.

5.2. The *WOX13*-like Genes in *S.moellendorffii* and *S.kraussiana*

In contrast to *S.*moellendorffii, there are little or no genomic data available for *S.kraussiana*. Therefore, the potential *WOX*-like genes were first identified via degenerate primer PCR. Using the *S.moellendorffii* homeodomain sequences as templates, and comparing those to the known *WOX* genes, the most conserved sequences that could be used as anchor points within the homeodomain were determined to design degenerate primers to survey the *S.kraussiana* genome. None of the primer combinations specific to the *WOX* modern clade members or *WOX9* group produced positive results. Similarly, only non-specific amplicons were obtained with all the possible combinations of two forward and three reverse primers specific for the predicted *S.moellendorffii* outgroup genes. In contrast, the *WOX13* and the *S.moellendorffii WOX13*-like *s*pecific primers amplified three putative homeodomains. This suggests that, as for *S.moellendorffii*, in the *S.kraussiana* genome, and thus probably even among all Selaginellaceae, only *WOX13*-like genes are present. On the other hand, if the expansion of *WOX*-like genes observed in *S.moellendorffii,* which gave rise to a specific *S.moellendorffii* outgroup, would be

present in *S.kraussiana* as well, then it might be so divergent as to be undetectable by a degenerate primer PCR strategy based upon *S.moellendorffii* sequences.

The phylogeny of the *WOX13* clade, based on the homeodomain sequences as well as on the whole coding sequence (reported in appendix B), is shown in Figure 10. In both trees, the dichotomy between basal land plant/algae species and angiosperms is clearly distinguishable, as is the distinct separation within angiosperms between mono- and eudicotiledonous species. On the other hand, the evolution of *WOX* genes within *Selaginella* (yellow and orange colored in Figure 10) is less clear from the trees, which never show a discrete *Selaginella* clade. Moreover, clades

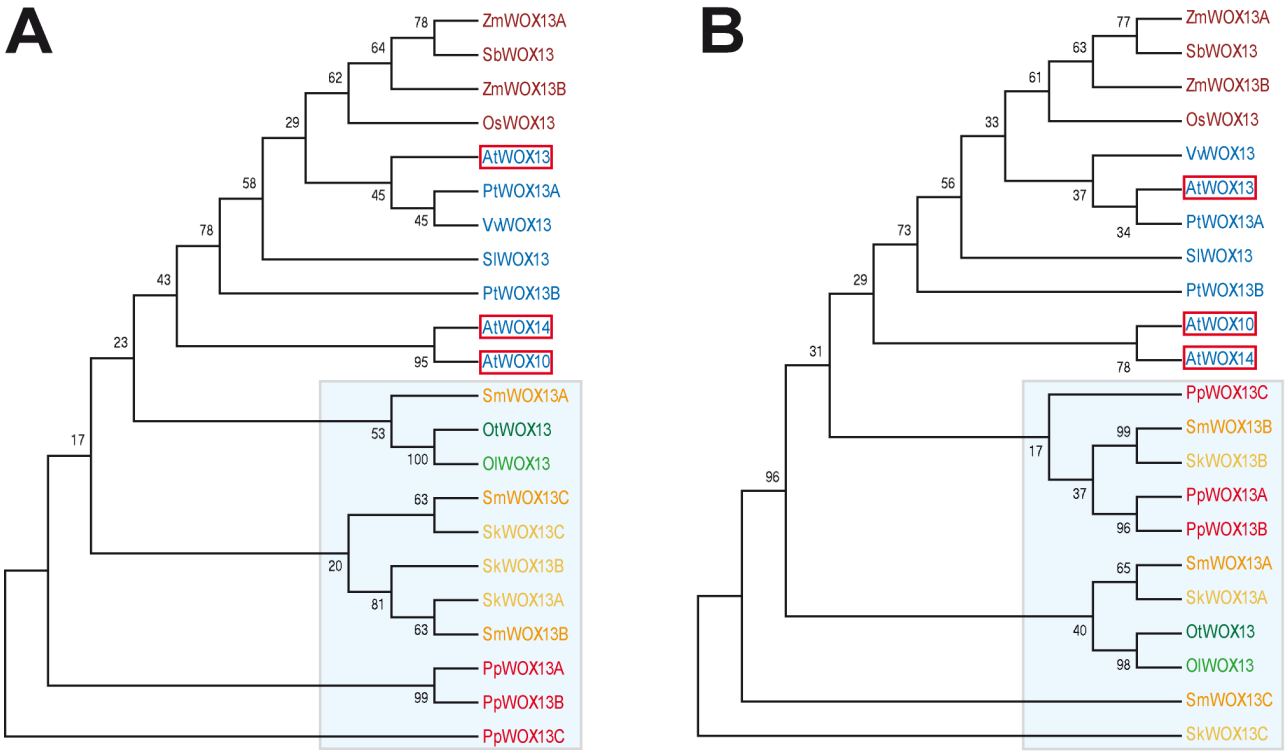

Fig. 10. Phylogeny of the *WOX13* clade. The evolutionary history based on the homeodomain (A) and the full coding sequence (B) was inferred using the neighbor joining method (Saitou and Nei, 1987), provided by the MEGA4 software (Tamura et al., 2007). The percentage of replicate trees in which the associated taxa clustered together in the bootstrap test (1000 replicates) are shown next to the nodes (Felsenstein, 1985). The light blue box demarcates the basal land plant *WOX13* genes, which includes algal (green), bryophyte (red) and lycophyte (orange) relatives. The angiosperm *WOX13*-like genes are clearly divided in two sub-branches, corresponding to monocots (dark red) and dicots (blue) At, *Arabidopsis thaliana*; Ol, *Ostreococcus lucimarinus*; Os, *Oryza sativa*; Ot, *Ostreococcus tauri*; Pp, *Physcomitrella patens*; Pt, *Populus trichocarpa*; Sb, *Sorghum bicolor*; Sk, *Selaginella kraussiana*; Sl, *Solanum lycopersicon*; Sm, *Selaginella moellendorffii*; Vv, *Vitis vinifera*; Zm, *Zea mays*.

that include *Selaginella* genes are often supported by low bootstrap values, reflecting uncertainty in their positions.

5.3. *WOX13*-like genes share unique features among the *WOX* gene family

A deeper *WOX13* clade analysis revealed two evolutionarily conserved motifs present in all the *WOX13*-like genes annotated so far, in addition to highly conserved homeodomain (Figure 11). A domain enriched in acidic residues (dark blue in Figure 11), conserved in *P.patens* and in angiosperms but not in three *Selaginella* genes (*S.moellendorffi WOX13A*, *S.kraussiana WOX13A* and *B*) or the genes *AtWOX10/14*, lies right after the homeodomain. A second highly conserved motif (in red in Figure 11), present in almost all *WOX13*-like genes, was identified in the first exon, which also has a conserved glycine that marks the first intron splicing site (arrowhead in Figure 11B). Conserved domains other then the homeodomain are quite uncommon among the *WOX* gene family members. All the known genes belonging to the *WOX9* sub-clade have a moderately conserved C-terminal domain (Hacker *et al.*, 2004; Deveaux *et al.*, 2008) but it is not as conserved as the *WOX13* N-terminal domain. All *WOX* genes apart from *WOX13* share a short stretch of six amino acids, the WUSCHEL-box (Hacker *et al.*, 2004). All closer *WUS* relatives also have an EAR-like domain composed of 6-8 residues at the C-terminus. Thus, the domains observed in the *WOX13*-like genes are specific to and characterize this *WOX* gene family clade.

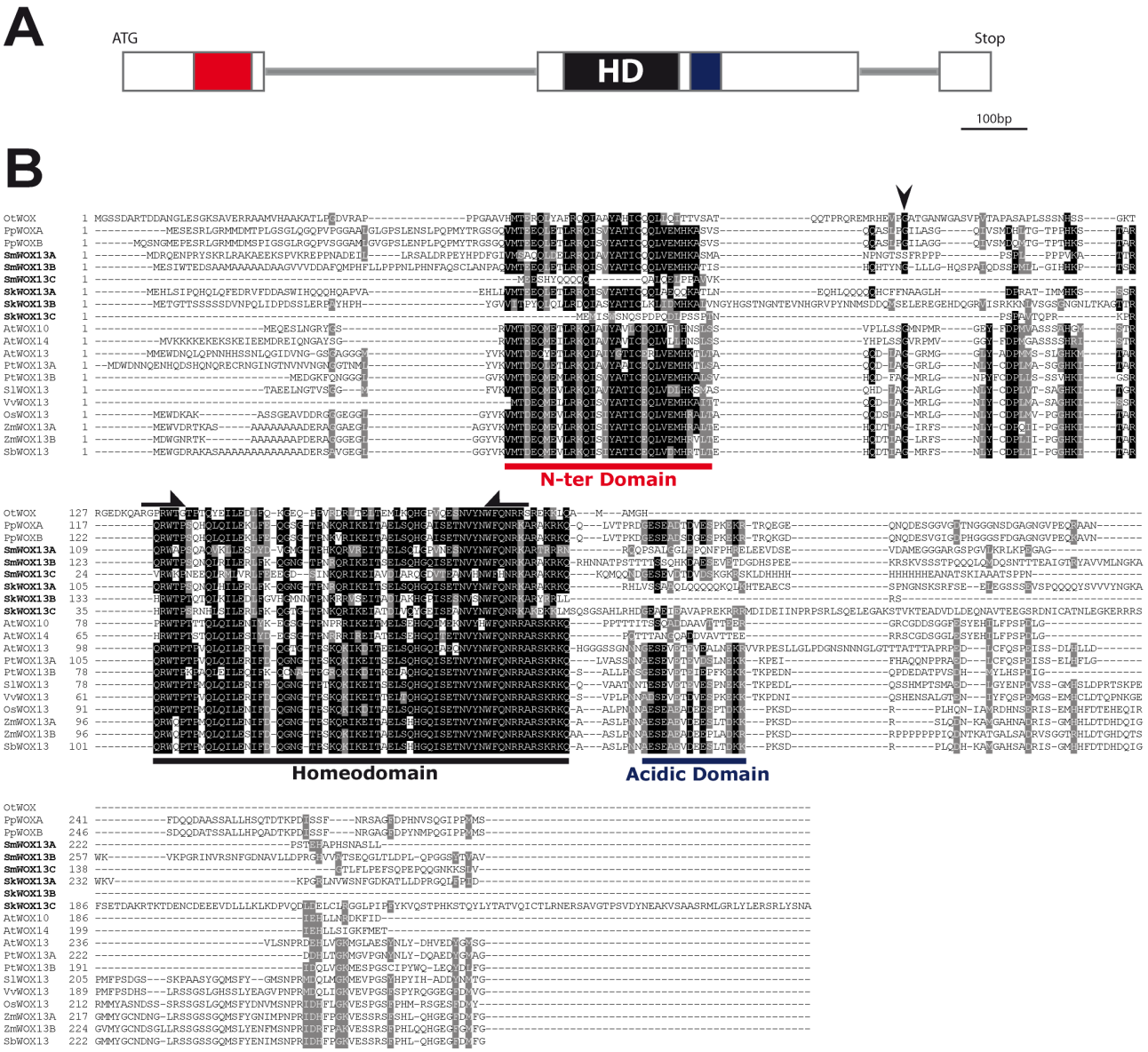

Fig. 11. *WOX13*-like gene structure. (A) *Arabidopsis WOX13* scale schematic representation showing the common exon-intron pattern among *WOX13*-like genes and the position of the amino-terminal domain (red), homeodomain (black) and acidic domain (dark blue) in the coding sequence. (B) Sequence characterization of annotated, complete coding *WOX13*-like gene sequences. Identical residues are outlined in black, similar in gray; dashes represent gaps introduced to optimize the alignment. Domains are labeled below the respective sequences: red, amino-terminal domain; black, homeodomain; dark blue, acidic domain. The *Selaginella Kraussiana* and *S.moellnedorffii* are emphasized by bold font. The black arrowhead indicates the conserved splicing position of the first intron; the half arrows over the homeodomain mark the anchor point used to design degenerate PCR primers. At, *Arabidopsis thaliana*; Os, *Oryza sativa*; Ot, *Ostreococcus tauri*; Pp, *Physcomitrella patens*; Pt, *Populus trichocarpa*; Sb, *Sorghum bicolor*; **Sk**, *Selaginella kraussiana*; **Sm**, *Selaginella moellendorffii*; Zm, *Zea mays*.

According to protein secondary structure prediction algorithms, the amino-terminal domain should fold as an amphipathic single helix or perhaps as a coiled coil domain. Four different algorithms, namely DSC (King and Stemberg, 1996), MLRC (Guermeur *et al.*, 1999), PHD (Rost and

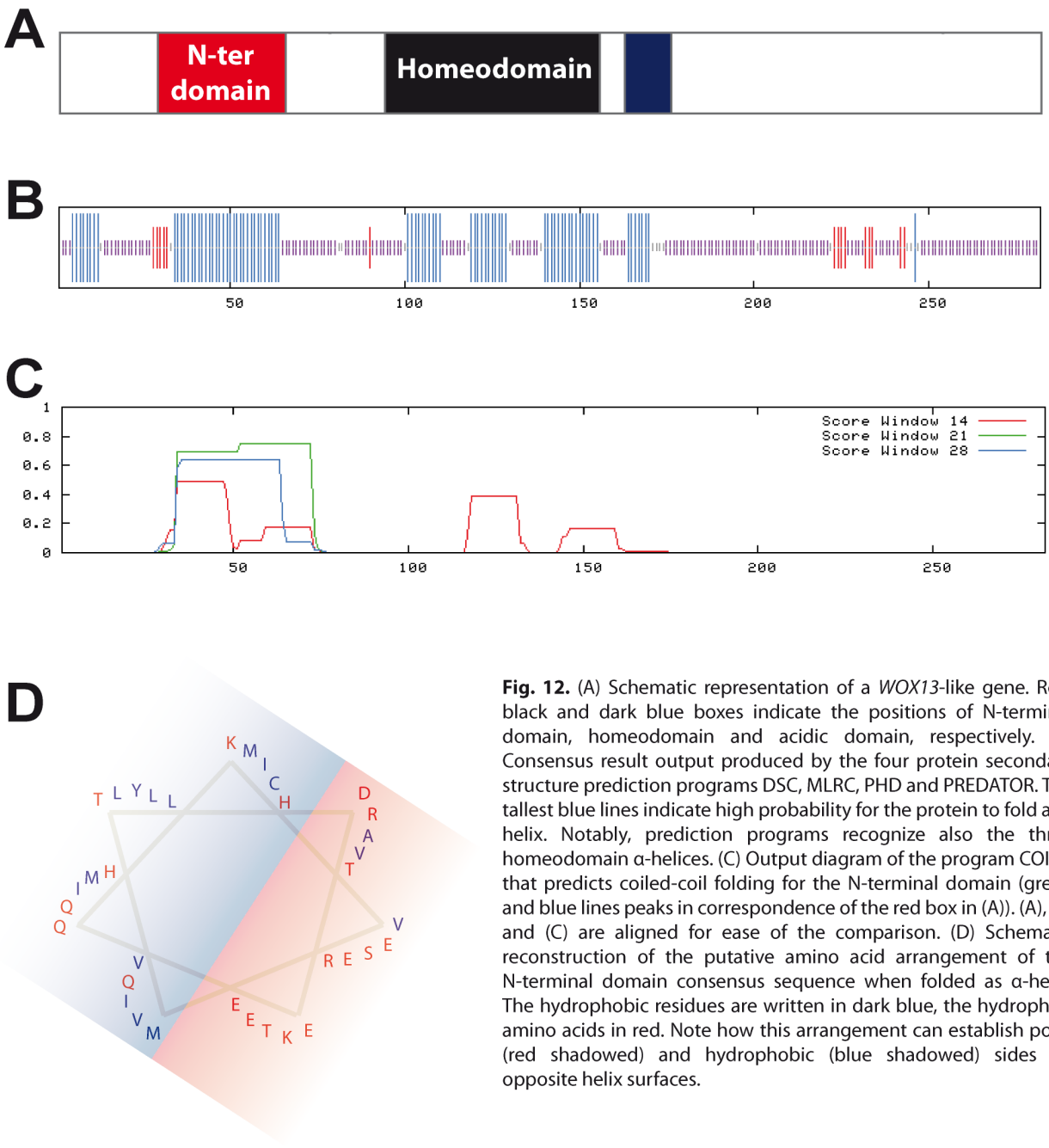

Fig. 12. (A) Schematic representation of a *WOX13*-like gene. Red, black and dark blue boxes indicate the positions of N-terminal domain, homeodomain and acidic domain, respectively. (B) Consensus result output produced by the four protein secondary structure prediction programs DSC, MLRC, PHD and PREDATOR. The tallest blue lines indicate high probability for the protein to fold as a helix. Notably, prediction programs recognize also the three homeodomain α-helices. (C) Output diagram of the program COILS, that predicts coiled-coil folding for the N-terminal domain (green and blue lines peaks in correspondence of the red box in (A)). (A), (B) and (C) are aligned for ease of the comparison. (D) Schematic reconstruction of the putative amino acid arrangement of the N-terminal domain consensus sequence when folded as α-helix. The hydrophobic residues are written in dark blue, the hydrophilic amino acids in red. Note how this arrangement can establish polar (red shadowed) and hydrophobic (blue shadowed) sides on opposite helix surfaces.

Sander, 1993) and PREDATOR (Frishman and Argos, 1996), predict with high probability that the amino-terminal domain primary sequence folds in a helix (compare Figure 12A and B). This putative helix might have an amphipathic nature due to the arrangement of the amino acid residues around the typical α-helix fold (Figure 12D). Furthermore, the program COILS (Lupas *et al.*, 1991) hypothesizes the amino terminal domain to be capable of folding as a coiled coil with more

than 70% probability (compare Figure 12 A to C). Therefore, the conserved amino-terminal domain possibly folds in a discrete three-dimensional structure never found in any known *WOX* gene other then *WOX13s*, which suggests the potential to establish specific protein-protein interactions.

5.4. *WOX* gene expression patterns in *S.kraussiana*

Different functional contributions of the *S.kraussiana WOX* genes became more clear after *in situ* hybridization analysis (Figure 13). Longitudinal sections of the *S.kraussiana* SAM shows *SkWOX13A* transcripts in the outgrowing microphylls primordia (black arrowheads in Figure 13A) and the meristem flanks (red arrowheads), probably marking the merophytes of the outer two distal-most cells of SAM (Lyndon, 1998; Harrison *et al.*, 2007). Differently, when similar sections were screened for peaks of expression, *SkWOX13A* transcripts were found at the very apical tip of the minor shoot SAM (Figure 13B), where the apical initials should be (Harrison *et al.*, 2007). The staining was detectable only in three sections of the series, marking that specific minor SAM initial(s) but not the initials of the other two visible meristems (appendix Figure VII). This *SkWOX13A* expression pattern was seen twice overall, probably reflecting a very dynamic and transient expression and therefore hard to detect. Moreover, this staining was particularly intense and required a short staining-development reaction time to be detected, which was possibly not long enough for the enzymatic reaction to fully reproduce the pattern observed in Figure 13A, thus explaining why the previous *SkWOX13A* expression pattern is not visible in Figure 13B.

Similar to its expression pattern in the SAM, the *SkWOX13A* expression pattern observed in median diagonal-longitudinal section of a developing strobilus coincides with the younger and incipient sporophylls primordia and the meristem flanks (Figure 13C, black and red arrowheads, respectively). Moreover, during the reproductive phase, *SkWOX13A* expression was detectable from the very early microsporangia developmental stages in both the tapetum and sporogenous mass as well as in the ligule (definitions according to Horner and Beltz, 1970), whereas later the expression is confined just to the tapetum.

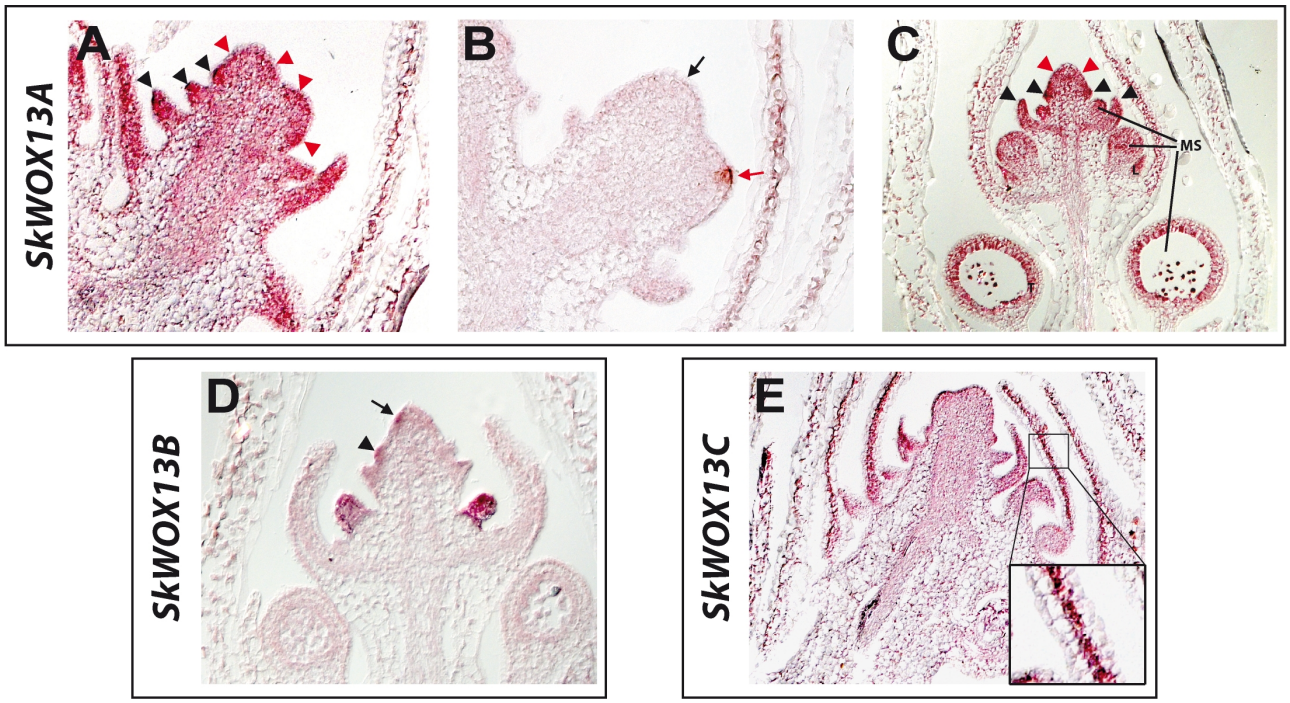

Fig. 13. *WOX* gene expression in *Selaginella kraussiana*. (A) Vegetative SAM hybridized with *SkWOX13A* specific probe shows expression of the gene within the young microphyll primordia (black arrowhead) and the lateral sides of the SAMs (red arrowhead). (B) Higher magnification of a bifurcating SAM displaying a different expression pattern of gene *SkWOX13A* compared to (A), in which the signal is detectable apparently in one apical inital of the minor shoot SAM (red arrow) but not where the apical initials of the major shoot SAM are suppose to lie (black arrow). (C) Strobili apical meristem hybridized with *SkWOX13A* probe: black arrowheads point to sporophylls, red arrowheads indicate the expression at the meristem flanks. L, ligule; MS, microsporangia; T, tapetum. (D) Expression of *SkWOX13B* in a strobilus diagonal-longitudinal section coincides with microsporangial early developmental stages. The arrowhead points to a slight protuberance at the axil of a sporophyll, where new microsporangia are developing, whereas the arrow emphasizes few cells expressing *SkWOX13B* on the flank of the meristem, possibly marking the next microsporangia primordium. (E) *SkWOX13C* expression in median longitudinal section of SAM, marking the mesophyll of older microphylls.

In contrast to *SkWOX13A*, *SkWOX13B* signal was never detected during vegetative stages but exclusively in strobili. During the reproductive phase, the *SkWOX13B* gene appears to be transcribed solely in the very young stage of microsporangia development but not later, when differentiated tissues within the microsporangia, as sporogenous mass and tapetum, can be distinctly visible (Figure 13D). *SkWOX13B* expression is high in the most recently formed microsporangia and detectable also in the slight bulge protruding at the axil of a sporophyll primordium, which is the position where sporangia usually are established (arrowhead in Figure 13D). Moreover, a small group of cells stained on the flank of the meristem, possibly marking the future, and not yet histologically visible, sporangium primorda (arrow in Figure 13D).

In situ hybridization with a *SkWOX13C* specific probe yielded a mesophyll-associated expression pattern. As depicted in Figure 13E, the most distal portion of the shoot apical meristem is free of staining, whereas weak staining is detectable in the younger microphyll primordia. In the older expanding microphylls, *SkWOX13C* transcripts are never found in both adaxial and abaxial epidermis but only in the mesophyll (inset in Figure 13E). No signal could be detected when *in situ* hybridization was performed on strobili sections.

5.5. *WOX* gene expression patterns in *S.moellendorffii*

The *S.moellendorffii WOX* genes appear to behave similarly to their *S.kraussiana* orthologs. Diagonal-longitudinal sections of the *S.moellendorffii* SAM hybridized with a *SmWOX13A* specific probe show expression of the gene in young microphyll primordia (black arrowheads in Figure 14A) and both lateral sides of the meristem (red arrowheads in Figure 14A), as for *SkWOX13A* (compare to Figure 13A). Likewise, *SmWOX13A in situ* hybridization on diagonal sections cut through strobili stains in developing sporangia, sporophylls and ligules (Figure 14B), and a better in-plane view of the strobilus apex shows the transcripts detected also in the earlier stages of development of both sporangia and sporophylls, besides a clear signal marking the flank of the meristem (inset in Figure

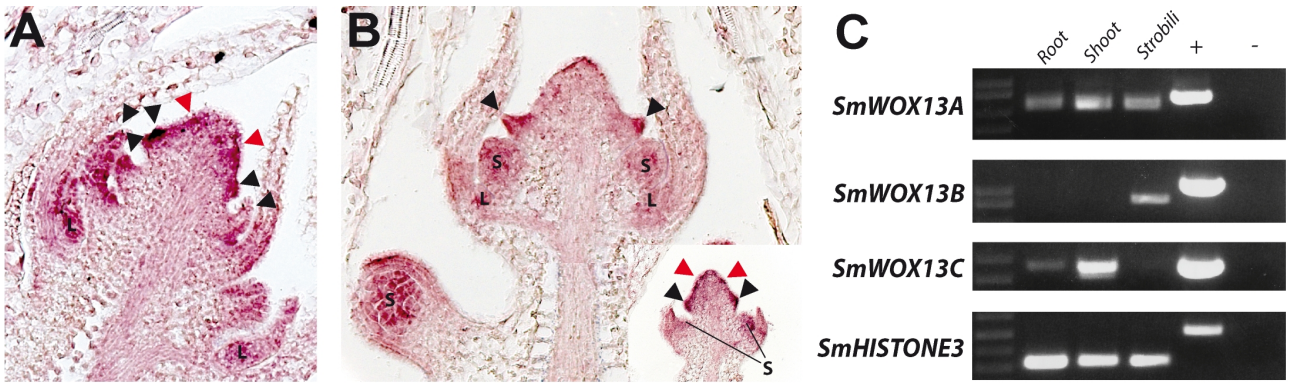

Fig. 14. *WOX* gene expression in *Selaginella moellendorffii*. (A) Median diagonal-longitudinal section hybridized with *SmWOX13A* probe showing expression of the gene in the younger microphyll primordia (black arrowheads) and meristem flanks (red arrowheads), as well as in ligules. (B) Expression of *SmWOX13A* in strobili is focused in sporophyll primordia (black arrowheads), flank of the meristem (red arroheads, inset) and developing sporangia. The inset is a median diagonal-longitudinal section of the very tip of the strobili meristem. (C) RT-PCR adressing the expression of the three *WOX13*-like genes in *S.moellendorffii* roots, shoots and strobili. *SmHistone3* was used as positive reference. + , genomic DNA; - , negative control. L, ligule; S, sporangia.

14B). Thus, the expression pattern of *SmWOX13A* resembles that observed for its close *S.kraussiana* ortholog *SkWOX13A*.

Although several attempts to obtain distinct expression patterns of the genes *SmWOX13B* and *SmWOX13C* were performed, none of them produced reliable patterns. Therefore the expression of these genes has been addressed via reverse transcriptase PCR.

RT-PCR analysis on *SmWOXs* indicates some possible analogies with their *S.kraussiana* orthologs (Figure 14C). Indeed, the expression of *SkWOX13B* was never found in vegetative SAM and, similarly, *SkWOX13B* is expressed just in strobili (Figure 13D). Likewise, expression of *SkWOX13C* was never detectable in strobili and *SmWOX13C* RT-PCR also shows no expression of the *S.moellendorffii* ortholog in strobili.

Therefore, the three *S.moellendorffii WOX13*-like genes probably share common expression patterns, and possibly the related function(s), with their *S.kraussiana* counterparts.

6. AtWOX13 insertion line

In *Arabidopsis* the *WOX13* gene is encoded by the locus At4g35550. In order to understand the putative function(s) of *WOX13*-like genes, a screening for mutated alleles of the At4g35550 locus was performed. According to the TAIR website (www.arabidopsis.org) and the NCBI database, the GABI-Kat line 922B03 should carry a T-DNA insertion in the *WOX13* 5'UTR, 7bp in front of the translation start codon. In fact, the sequence of the genotyping amplicon positioned the T-DNA insertion upstream of the annotated site by 176bp, 43bp before the supposed transcription start, therefore situated within the predicted core promoter of the gene (Figure 15A). Moreover, the T-DNA insertion caused a 23bp deletion. Thus, although the insertion is outside the transcript, the T-DNA could affect the *WOX13* transcriptional process. To evaluate whether the T-DNA insertion may compromise the expression of *WOX13* even if located inside the promoter instead of directly affect the transcript itself, inflorescences of homozygote plants were screened for the presence of

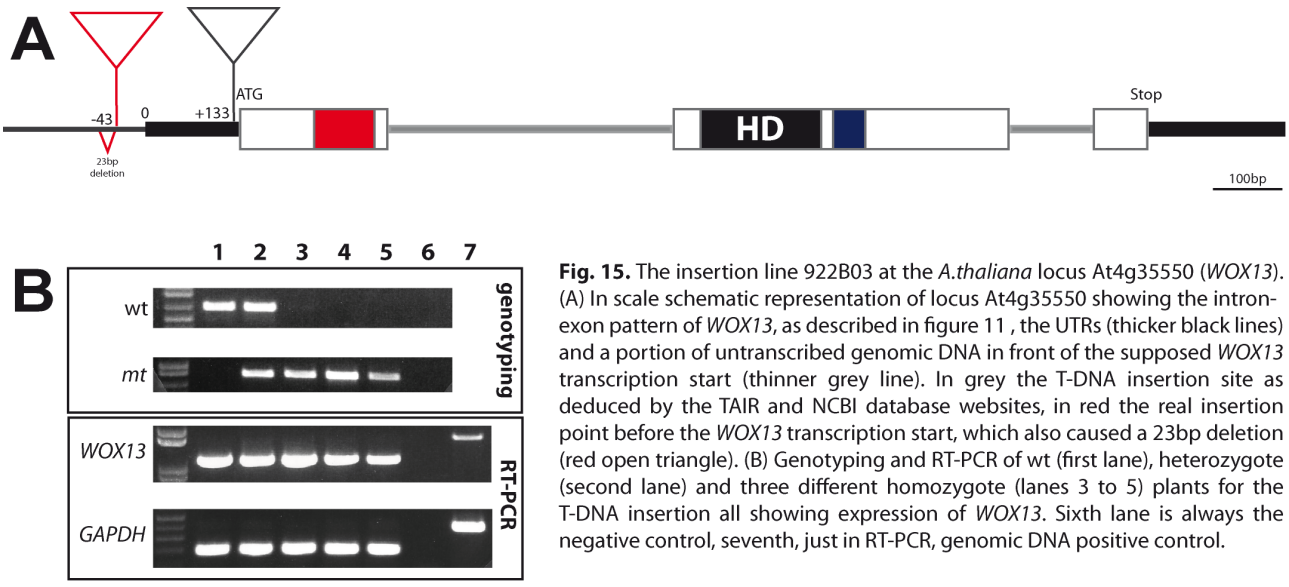

Fig. 15. The insertion line 922B03 at the *A.thaliana* locus At4g35550 (*WOX13*). (A) In scale schematic representation of locus At4g35550 showing the intron-exon pattern of *WOX13*, as described in figure 11 , the UTRs (thicker black lines) and a portion of untranscribed genomic DNA in front of the supposed *WOX13* transcription start (thinner grey line). In grey the T-DNA insertion site as deduced by the TAIR and NCBI database websites, in red the real insertion point before the *WOX13* transcription start, which also caused a 23bp deletion (red open triangle). (B) Genotyping and RT-PCR of wt (first lane), heterozygote (second lane) and three different homozygote (lanes 3 to 5) plants for the T-DNA insertion all showing expression of *WOX13*. Sixth lane is always the negative control, seventh, just in RT-PCR, genomic DNA positive control.

WOX13 transcripts (Devaux *et al.*, 2008). Unfortunately, it appeared that although the T-DNA insertion should affect the supposed core promoter sequence, the expression of *WOX13* is maintained in plants homozygote for the insertion (Figure 15B), which might also explain the lack of phenotype observed in the line 922B03 compared to published *wox13* mutant phenotype (Devaux *et al.*, 2008).

DISCUSSION

7.1. The *CLAVATA1* phylogeny identifies three LRR receptor-like kinases closely related to *TD1* in maize

To find the best candidate that might be able to control *ZmWUS1* activity in the SAM, the phylogeny of the closest *CLAVATA1* orthologs was reconstructed, taking advantage of four fully sequenced and annotated genomes, that could be compared with maize. The recent achievement of the complete sequencing of the maize genome does not substantially alter the initial phylogenetic inference, except for the disappearance of a putative gene closely similar to *ZmBLR1.* Thus, although the newest maize genome release slightly modified the entry sequences, the topology of the phylogenetic tree did not differ from that obtained previously.

In order to strengthen the phylogenetic reconstruction, the evolutionary relationship among the *CLV1* relatives was inferred with three different algorithms: neighbor joining, which relies on the genetic distance between the analyzed sequences, namely the fraction of mismatches at aligned positions (Saitou and Nei, 1987); maximum parsimony, that calculates the potential phylogenetic tree with the smallest total number of evolutionary events needed to explain the observed sequence data; and maximum likelihood, which uses standard statistical techniques coupled with a specific substitution model to assess the probability of a particular mutation, which evaluates the probability of possible phylogentic trees. All these methods have different weak points in inferring phylogenies. Neighbor joining is a greedy algorithm, that is the algorithm makes the local optimal choice at each stage with the hope to eventually find the global optimum, but

this do not assure neighbor joining will certainly find the true tree topology (Gascuel and Steel, 2006). Maximum parsimony is instead prone to “long branch attraction” (Felsenstein, 1978), whereas maximum likelihood becomes statistically inconsistent and converges to the wrong tree as the amount of data grows when heteretachous genes are analyzed, that is the functional constrains on sites in a gene sequence changes through time, causing shifts in site-specific evolutionary rates (Philippe and Lopez, 2001; Kolaczkowski and Thornton, 2004).

Although these differences between the phylogenetic algorithms used, the phylogenies inferred by the three methods are highly similar overall and identical for the *CLV1* clade and its sister clade (appendix figure 1-6), with the exception of the tree inferred by maximum likelihood for the kinase domain data set. In this case, the sorghum gene *Sb04g000920* and the maize model gene *GRMZM2G168603* switch from their position at the base of the tree to a sister branch of monocot *CLV1* orthologs (Figure 2D and appendix Figure VI). The poor bootstrap value and the marked divergence between these gene sequences and the rest of the kinase domains data set support the idea that the phylogenetic reconstruction from the maximum likelihood method was erroneous.

Interestingly, when the phylogeny was inferred from the LRRs domains data set, the topology of the trees did not vary considerably compared to those obtained from the analysis of kinase domains. Although the gene distances computed are often higher, most likely reflecting less conservation in the LRRs domain compared to the kinase domain, the topology of the trees identifies in both cases distinct *CLV1*-like and *BAM1/2*-like clades, and within the latter three different sub-groups. Thus, the extracellular LRRs domain and the cytoplasmatic serine/threonine kinase domain probably co-evolved, even if at different rates, although they are embedded in distinct cellular compartments and they have to carry out different functions.

Within the *BAM1/2* clade, several sub-clades are clearly distinguishable: a eudicot-specific sub-clade comprising the *P.trichocarpa BAM-like* gene and *AtBAM1/2*, its monophyletic sub-clade in which a monocot specific duplication occurred during evolution, and finally a monocot-specific outgroup. Three different maize genes sit within this clade and were chosen for further study in

order to evaluate whether a strong candidate could be found among them that is able to regulate *ZmWUS1* activity within the maize meristem.

7.2. None of the closest *CLAVATA1* orthologs appears able to regulate *ZmWUS1* activity

As expression in a pattern similar to *ZmWUS1* would be suggestive of a role in *ZmWUS1* regulation, the expression patterns of the three candidates genes *ZmBLR1*, *ZmBLR2* and *ZmBLR3* were determined. Unfortunately, none of the candidates has transcript expression in the SAM dome as *ZmWUS1*.

ZmBLR1 is expressed mostly in the apical tip of young leaf primordia and in lateral domains of older leaves. In comparison, *Arabidopsis BAM1* and *BAM2* are widely expressed, with strong signal detected on the meristem's flanks, in a pattern that excludes and surrounds *CLV1* expression (DeYoung *et al.*, 2006). Interestingly, *TD1* transcripts were detected in leaf primordia and leaves (Bommert *et al.*, 2005), like *ZmBLR1*, whereas *CLV1* expression is found in SAM L3 layer, surrounding and overlapping the organizing center (Clark *et al.*, 1997). Then, BAMs expression is centrifugal compared to *CLV1* and, similarly, *ZmBLR1* gene is expressed centrifugal compared to the *TD1* expression pattern, possibly highlighting once more the different concept of organizing center in monocots versus dicots. Although the *ZmBLR1* expression might overlap with *ZmWOX3A/B* expression in young leaf primordia (Nardmann *et al.*, 2007) and with *ZmNS1/2* expression in the lateral domain of leaves (Nardmann *et al.*, 2004), there is no further support for this speculation, neither from BAM expression patterns that are unclear except for anthers (Hord *et al.*, 2006), nor for *WOX3* patterns in *Arabidopsis* that appear to be expressed only in lateral leaf domains (Matsumoto and Okada, 2001).

As can be inferred by the phylogeny shown in Figure 2, the gene *ZmBLR2* is a monocot specific duplication and its transcription is strictly correlated to procambial cells in vascular bundles (Figure 5). Putative LRR-RLK proteins are required for differentiation events during vascular development (Clay and Nelson, 2002) and to regulate the correct cell division plane in order to achieve the exact

xylem and phloem positioning (Fisher and Turner, 2007). Several studies have also implicated *CLE* peptides in vascular development (reviewed by Fukuda *et al.*, 2007). Thus, LRR-RLKs play a role in vascular development, and together with the strong correlation between *ZmBLR2* expression and developing vascular bundles, it suggest that this gene might have a role in vascular development. The monocotyledonous vascular tissue arrangement gives rise to closed collateral bundles, which lack the stable cambium activity that allows secondary growth. This is in contrast to open collateral bundles, typical of eudicot species, which maintain cambium seasonal activity. Since procambial cells within monocot vascular strands do not share a common fate with their dicot counterparts, it might be that in maize the gene *ZmBLR2* has a role in defining this monocot-specific vascular tissue.

The *CLV1* phylogeny positioned the gene *ZmBLR3*, and its closest rice and sorghum orthologs, in a branch that includes only monocotyledonous genes, and the *ZmBLR3* expression pattern supports this inference. Indeed, the particular expression detected by *in situ* hybridization on maize shoot and root overlaps almost perfectly with the supposed primary thickening meristems (PTM) position. In this respect, the meristematic identity of all the tissue marked by *TD1* and its closest orthologs in maize seems to be a common feature. Thus, the phylogeny supports a link for *ZmBLR3* to a monocot-exclusive meristem, as PTM is, and on the other hand the expression pattern of *ZmBLR3* corroborates the grouping of this gene in a monocot-specific branch.

In summary, unfortunately none of the screened candidates show an expression domain that might overlap with *ZmWUS1* expression. So, is there a gene able to regulate *ZmWUS1* activity? And, if it does, which might this be?

CORYNE is a recently characterized gene that encodes a receptor kinase involved in shoot meristem homeostasis (Müller *et al.*, 2008). Mutation in *CRN* phenocopies *CLAVATA* mutant phenotypes and the genetic interaction between *CRN* and *CLAVATA* genes, together with the highly similar phenotypes of *CLAVATA2* and *CORYNE,* led Müller and colleagues to postulate two parallel *CLV3*-perceiving pathways involving separately *CLV1* and *CLV2/CRN,* the latter as a heterodimer. The root phenotype of *sol2* mutant, which was later found to be a *CORYNE* allele, may support this theory (Miwa *et al.*, 2008). This mutant was isolated in a screen for suppressors of short root

phenotype in transgenic plants constitutively overexpressing the *CLE19* gene, which is known to trigger the root meristem consumption through a *CLV2*-dependent pathway (Fiers et al. 2005). *sol2* mutant displays a very similar spectrum of sensitivity to *CLE* peptides when compared to *clv2,* whereas *clv1-4* and *clv1-6* mutations, which are a *CLV1* dominant-negative and a weak allele, respectively, display poor or no root response to *CLE* peptide treatment, suggesting functional similarities between *CLAVATA2* and *SOL2,* and functional distinctions from *CLAVATA1,* in both root and shoot meristem maintenance. Moreover, the additive effect, rather then an epistatic relationship, found in *td1/fea2* double mutants (Bommert *et al*., 2004), further corroborates the assumption of separate but parallel pathways in shoot and inflorescence meristem homeostasis, also in monocotyledons. Therefore, a possible next attempt to isolate the putative regulator of *ZmWUS1* activity should follow these new assumptions and screen for the closest maize *CORYNE* orthologs.

The phenotype observed in the *ZmWUS2 Mu* insertion line emphasizes another aspect of the *WUSCHEL-CLAVATA* antagonism in monocots compared to dicots. Indeed, mutations affecting either *WUS* or one of the three *CLV* genes in *Arabidopsis* lead to both vegetative and reproductive meristem defects (Clark *et* al., 1993; Clark *et* al., 1995; Laux *et al.*, 1996; Jeong *et al.*, 1999). In contrast, the described mutant *td1* and *fea2* of maize and *fon1*, *fon2* and *fon4* of rice show severe defects exclusively during reproductive phase, with only slightly increase in size of the vegetative meristem (Taguchi-Shiobara *et* al., 2001; Bommert *et al*, 2004; Suzaki *et al.*, 2004; Chu *et al.*, 2006; Moon *et al.*, 2006; Suzaki *et al.,* 2006). In this respect, the *ZmWUS2* insertion line described do not show any visible defect during the vegetative stages, but consistently with *td1* mutation, only the apical inflorescence meristem appears affected. Therefore, the *ZmWUS2* mutant corroborates the assumption that *WUSCHEL* and *CLAVATA* interaction in monocots affects predominantly the ear development and only marginally the vegetative growth.

The maize *CLAVATA1* orthologs identified and characterized for transcript expression in this work deserve further study. Firstly, the phylogenetic relationship among *CLAVATA1* closest relatives shows expansion of *BAM*-like relatives in monocotyledonous species that could correlate with

developmental features typical of monocots. In this respect, investigation of possible phenotypes caused by mutations in these genes might help to understand the different evolutionary events that shaped extant monocotyledons. Secondly, both phylogeny and expression analysis highlight unique features of each gene, suggesting limited functional redundancy. Finally, the *ZmBLR3* expression pattern is clearly related to meristematic tissue involved in monocotyledons primary thickening growth. A recent publication by Kashiwagi *et al.* (2008) demonstrates how, in rice, the stem diameter is potentially the most interesting target for increase lodging resistance. Lodging is the permanent displacement of cereal shoots from an upright position (Pinthus, 1973). It affects all cereals worldwide and causes a large reduction in grain yield (up to 80%) and quality (Fischer and Stapper, 1987; Easson *et al.*, 1993). Due to its strict correlation with the primary thickening meristem, mutants analysis of the gene *ZmBLR3* could identify a possible target for increased lodging resistance breeding programs in cereals.

7.3. The *WOX* gene family ancestor was a *WOX13*-like gene

Embedded inside a wider project devoted to the investigation of the *WOX* gene family evolution, this study has analyzed the lycophyte scenario. The complete annotation of the S.*moellendorffi* genome and the more extensive use of *S.kraussiana* as a molecular biology model organism were the basis which this study could be built on.

The evolutionary relationship among the homeodomains of the *WOX* gene family members showed the unique presence of the bryophyte *P.patens* and unicellular algae *O.tauri* and *M.pusilla* *WOX*-like genes in the *WOX13* clade. This clade also includes most of the *S.moellendorffii* *WOX*-like genes. Five *S.moellendorffii* *WOX*-like genes group together defining a sister clade to *WOX13*-like genes. Although the loss of other *WOX*-like genes cannot be excluded, this finding identifies the *WOX13*-like group as the common ancestor of the whole *WOX* gene family.

The Mamiellales *O.tauri* and *M.pusilla* genomes annotations each contains one *WOX*-like gene. The order Mamiellales (prasinophyte) diverged very early in evolution from the chlorophyte clade, one of the two major lineage of green algae, whereas the second, named charophytes, is the

lineage that leads to land plants (Lewis and McCourt, 2004). Therefore, the common ancestor of prasinophytes and embryophytes must be traced back to the very base of algae phylogeny. Then, since both prasinophyte and embryophyte genomes have at least one *WOX*-like gene, it is reasonable to suppose that their common ancestor, and thus the common ancestor of the plant kingdom as a whole, had at least one *WOX*-like gene.

Of the three known *WOX*-like genes present in the *P.patens* genome, *PpWOXC* transcripts were never found, thus supporting the idea that *PpWOXC* could be a pseudogene (Deveaux *et al.*, 2008). *PpWOXA* and *PpWOXB* are probably products of the genome duplication event which the moss *P.patens* underwent between 30 and 60 mya (Rensing *et al.*, 2007), an inference supported by the high degree of sequence identity between *PpWOXA* and *PpWOXB* that spreads throughout their entire coding sequence, rising to 92% (Reisewitz, unpublished data). Thus, probably the bryophyte lineage had a single *WOX*-like gene, like the sequenced genomes of prasinophytes. Therefore, it is probable that the most basal plant and algal lineages, as well as their common ancestor, had a unique *WOX*-like gene.

Going from bryophytes toward lycophytes, the *WOX* gene family possibly underwent an expansion from one to three different *WOX13*-like genes, or even more. In contrast to *P.patens*, in both *S.moellendorffii* and *S.kraussiana*, *WOX13*-like genes show limited sequence similarity outside of the three conserved domains, a common feature of all known *WOX13* genes. The expansion in *WOX* gene number observed in the lycophyte lineage may be explained as the starting point of a gradual evolution toward the variety seen in the spermatophyte's *WOX* modern clade, or by an independent evolution of the lycophyte lineage itself. The phylogenetic reconstruction of the *WOX13* subfamily does not help to clarify the relationship between *Selaginella* and *P.patens*/*O.tauri WOX13*, since none of the *Selaginella WOX13s* forms a sister clade to the spermatophyte, in contrast to the species phylogeny. Rather they are located within various basally-branching groups, along with basal plant species in the reconstructed trees. This may suggest that *Selaginella WOX13*-like genes have evolutionary distance comparable to *P.patens*/*O.tauri WOX13* genes when compared to spermatophyte relatives. Besides, the homeodomain, the acidic domain and the amino-terminal domain are *WOX13* peculiar motifs

always present in all *WOX13*, from the bryophyte *P.patens* to the eurosid *Arabidopsis*. Interestingly, the genes *SkWOX13C* and *SmWOX13C*, the only ones which have the acidic domain besides *SmWOX13A*, lack the characteristic first exon and thereby miss the amino-terminal domain. On the other hand, both *SmWOX13B* and *SkWOX13B* have only the amino-terminal domain but they lack the acidic domain. Thus, during the evolution of the *Selaginella* lineage, the *WOX* genes probably have been duplicated, releasing evolutionary pressure and thereby permitting subfunctionalization of the amino-terminal and acidic domains between different genes, as happened in *S.kraussiana* and just partially in *S.moellendorffii*. In this respect, probably the expansion of the *WOX* genes observed in *Selaginella* results from 400 million years of independent and fast evolution of the lycophyte lineage, already demonstrated by Koral and Kenrick (2004), rather then depending on the gradual evolution of the *WOX* family in the direction of the *WOX* gene complexity observed in spermatophytes.

This suggests that tracheophytes common ancestor probably still had a single *WOX*-like gene and therefore that the expansion of the *WOX* gene family occurred later during euphyllophytes evolution, thus after the separation of the lycophyte lineage from the seed plant-leading lineage. Consistently, other transcription factors families showed a strong increase in gene number after the lycophytes-euphyllophytes divergence. In angiosperms, PEPB (phosphatydylethanolammine-binding) proteins, such as *FLOWERING LOCUS T* and *TERMINAL FLOWER 1*, are involved in the control of shoot meristem identity and flowering time (Bradley *et al.*, 1997; Ohshima *et al.*, 1997; Kardailsky *et al.*, 1999; Kobayashi *et al.*, 1999), and form a highly conserved small gene family composed by six different genes in *Arabidopsis*, that can be sub-grouped in three distinct clades (Kobayashi *et al.*, 1999). A deep phylogenetic analysis involving *P.patens* and *S.moellendorffii* revealed that the whole family derives from the duplication of a single clade, which likely occurred after the lycophytes divergence (Hedman *et al.*, 2009). A similar evolution pattern was followed also by the *KNOX* (Harrison *et al.*, 2005; Sakakibara *et al.*, 2008), *HDIII-ZIP* (Floyd *et al.*, 2006) and *DOF* (Moreno-Risueno *et al.*, 2007) gene families, which all show an expansion in gene number from basal to higher plant that starts after the separation of the lycophyte lineage. Therefore, the postulated *WOX* gene family onset of expansion during euphyllophytes evolution, but still limited

prior to tracheophytes appearance, seems to be a common evolutionary process followed by several plant transcription factor gene families.

7.4. *Selaginella WOX* expression patterns have been conserved during Selaginellaceae evolution

Although the expression pattern data on *S.moellendorffii* are incomplete, RT-PCR data obtained on different tissues suggest a conserved expression, and possibly function, of the three *WOX* genes present in both analyzed species.

SmWOX13A and *SkWOX13A* appear to be expressed broadly. Their expression patterns always occur in cells supposed to be still in an undifferentiated and active cell division state, as merophytes, early microphyll primordia and, sole of the reproductive phase, the sporangia primordia from very early stages. In this respect, the strict correlation with meristematic cells is a common feature that *SmWOX13A* and *SkWOX13A* share with the *WOX* modern clade members. Interestingly, a peak of *SkWOX13A* expression can be detected in a single apical cell of a minor branching SAM, probably in a dynamic and transient fashion. This expression could be related to the new establishment of the minor branching SAM, which depends on a single initial in contrast to the two initials sitting on the very tip of the major SAM (Harrison *et al.*, 2007). A hypothesis could be that this transient signal confers to the single marked cell the ability to divide, producing a daughter cell with initial fate to re-establish the usual number of SAM initials in *S.kraussina*. Alternatively, the transient expression of *SkWOX13A* might mark the cell that will acquire the initials cell fate among all the cell field on the SAM distal portion. In any case, *SmWOX13A* and *SkWOX13A* do not appear to be constantly expressed in all SAM initials.

RT-PCR demonstrated that *SmWOX13B* is transcribed only in strobili. Similarly, *SkWOX13B* is expressed only in the very early stages of sporangia anlage, possibly even before the sporangia is hystologically visible. *SmWOX13B* and *SkWOX13B* demonstrate a clear subfunctionalization when compared to *SmWOX13A* and *SkWOX13A*. Moreover, although the lack of functional data, it is

reasonable to speculate over *SmWOX13B* and *SkWOX13B* function as directly involved in sporangial cell fate. Thus, these two closer homologs appears to share similar expression domains strongly related to sexual reproduction.

SkWOX13C is distinctly expressed in the mesophyll cell layer within the microphylls but no expression has been detected in strobili. Equally, RT-PCR data show expression of *SmWOX13C* in root and shoot, but not in strobili. Interestingly, *SkWOX13C* does not have the N-terminal domain and its expression pattern does not coincide with actively dividing cells. Therefore, possibly the coiled-coil amino-terminal domain could be linked to the meristematic activity. As an alternative, as both *SmWOX13B* and *SkWOX13B* carry just the amino-terminus, whereas *SmWOX13C* and *SkWOX13C* homologs hold only the acidic domain, it could be possible that the amino-terminus and acidic domains have crucial function during reproductive and vegetative stages, respectively. Moreover, those functions could be separated over different genes as happened during the Selaginellaceae evolution.

Therefore, the three *WOX* genes present in both *Selaginella* genomes analyzed have distinct expression patterns, often associated with developing organs where cell division occurs. Moreover, these expression domains appear to be conserved between the two species, indicating that their common ancestor probably already had three *WOX* genes with distinctive expression patterns and, possibly, functions.

This study on the lycophytes *S.moellendorffii* and *S.kraussiana* further substantiated the hypothesis that the *WOX13* clade is the most basal among the *WOX* gene family and the only *WOX* gene present in basal land plants, bryophytes and lycophytes. Fossil records show how the common ancestor of euphyllophytes and lycophytes was a small and morphologically simple plant, with terminal sporangia and without leaves or roots (reviewed by Kenrick and Crane, 1997). Probably, this extinct plant group already held a *WOX*-like gene prior to the divergence of the lycophyte and euphyllophyte lineages more then 400 million years ago. Therefore, in order to

follow up the *WOX* gene family evolution to better understand the implications for plant developmental processes, it would be useful to study early euphyllophytes plants, such as ferns.

The presence of two distinct highly conserved domains besides the homeodomain in all *WOX13* relatives, prompts the idea of a crucial function for them in a highly conserved plant process, common from the moss *P.patens* and to the most evolved mono- and eudicots. Moreover, the nature of these two domains, namely the putative coiled-coil and the acid domain, suggests a possible protein-protein interaction for *WOX13s*. In this respect, a yeast two-hybrid screening would be the best tool to attempt to find whether interaction partner(s) do exist and what could they be.

Further study to improve our knowledge about the *WOX* gene family would help us in understanding, at least in part, the evolution of the plant kingdom and development of land plants, to whom all of us owe the Earth as we know it and our life.

Literature Cited

Abbe E.C., Phinney B.O. and Baer D.F. (1951) The growth of the shoot apex in maize: internal features. *American Journal of Botany 38: 744–752*

Abbe E.C. and Stein O.L. (1954) The growth of the shoot apex in maize: embryogeny. *American Journal of Botany 41: 285-293*

Banks J.A. (2009) Selaginella and 400 million years of separation. *Annual Review of Plant Biology 60: 223-238*

Bommert P., Lunde C., Nardmann J., Vollbrecht E., Running M., Jackson D., Hake S. and Werr W. (2005) *thick tassel dwarf1* encodes a putative maize ortholog of the *Arabidopsis CLAVATA1* leucine-rich repeat receptor-like kinase. *Development 132: 1235–1245*

Bradley D., Carpenter R., Copsey L., Vincent C., Rothstein S. and Coen E. (1996) Control of inflorescence architecture in *Antirrhinum. Nature 379: 791–797*

Brand U., Fletcher J.C., Hobe, M. Meyerowitz, E.M. and Simon, R. (2000) Dependence of stem cell fate in *Arabidopsis* on a feedback loop regulated by *CLV3* activity. *Science 289:617-619*

Brueninger H., Rikirsch E., Hermann M., Ueda M. and Laux T. (2008) Differential expression of *WOX* genes mediates apical-basal axis formation in the *Arabidopsis* embryo. *Developmental Cell 14: 867-876*

Byrne M.E., Barley R., Curtis M., Arroyo J.M., Dunham M., Hudson A. and Martienssen R.A. (2000) *ASYMMETRIC LEAVES1* mediates leaf patterning and stem cell function in *Arabidopsis*. *Nature 408: 967–971*

Chu H., Qian Q., Liang W., Yin C., Tan H., Yao X., Yuan Z., Yang J., Huang H., Luo D., Ma H. and Zhang D. (2006) The floral organ number4 gene encoding a putative ortholog of *Arabidopsis* CLAVATA3 regulates apical meristem size in rice. *Plant Physiology 142: 1039-1052*

Clark S.E., Running M.P. And Meyerowitz E.M. (1993) *CLAVATA1*, a regulator of meristem and flower development in *Arabidopsis*. *Development 119: 397-418*

Clark S.E., Running M.P. And Meyerowitz E.M. (1995) *CLAVATA3* is a specific regulator of shoot and floral meristem development affecting the same process as *CLAVATA1*. *Development 121: 2057-2067*

Clark S.E., Williams R.W. and Meyerowitz E.M. (1997) The *CLAVATA1* gene encodes a putative receptor kinase that controls shoot and floral meristem size in *Arabidopsis*. *Cell 89: 575–585*

Clay N.K. and Nelson T. (2002) VH1, a provascular cell-specific receptor kinase that influences leaf cell pattern in *Arabidopsis*. *Plant Cell 14: 2707-2722*

Crane P.R., Herendeen P. and Friis E.M. (2004) Fossils and plant phylogeny. *American Journal of Botany 91: 1683-1699*

DeMason D.A. (1980) Localization of cell division activity in the primary thickening meristem in *Allium cepa L. American Journal of Botany 67: 393-399*

De Menezes N.L., Silva D.C., Arruda R.C.O., Melo-De-Pinna G.F., Cardoso V.A., Castro N.M., Scatena V.L. and Scremin-Dias E. (2005) Meritematic activity of the Endodermis and the Pericycle in the primary thickening in monocotyledons. Considerations on the "PTM". *Anais da Academica Brasileira de Ciências 77: 259-274*

DeYoung B.J., Bickle K.L., Schrage K.L., Muskett P., Patel K. and Clark S.E. (2006) The *CLAVATA1*-related *BAM1*, *BAM2* and *BAM3* receptor kinase-like proteins are required for meristem function in *Arabidopsis*. *Plant Journal 45: 1-16*

Deveaux Y., Toffalo-Nioche C., Claisse G., Thareau V., Morin H., Laufs P., Moreau H., Kreis M. and Lecharny A. (2008) Genes of the most conserved WOX clade in plants affect root and flower development in Arabidopsis. *BMC Evolutionary Biology 8:291*

Duff R.J. and Nickrent D.L. (1999) Phylogenetic relationship of land plants using mitochondrial small-subunit rDNA sequences. *American Journal of Botany 86: 372-386*

Easson D.L., White E.M. and Pickles S.J. (1993) The effects of weather, seed rate and cultivar on lodging and yield in winter wheat. *The Journal of Agricultural Science 121: 145-156*

Edwards D. and Feehan J. (1980) Records of *Cooksonia*-type sporangia from late Wenlock strata in Ireland. *Nature 287: 41-42*

Esau K. (1965) Plant Anatomy, Second Edition. *p.400-1, p.598, plate 58. John Wiley & Sons, Inc., New York.*

Evans M.M. and Barton M.K. (1997) Genetics of angiosperm shoot apical meristem development. *Annual Review of Plant Physiology and Plant Molecular Biology 48: 673–701*

Fawley M.W., Yun Y. and Qin M. (2000) Phylogenetic analysis of 18s rDNA sequences reveal a new coccoid lineage of the Prasinophyceae (Chlorophyta). *Journal of Phycology 31: 664-667*

Felsenstein J. (1978) Cases in which parsimony and compatibility methods will be positively misleading. *Systematic Zoology 27: 401-410*

Felsenstein J. (1985) Confidence limits on phylogenies: an approach using the bootstrap. *Evolution 39:783-791*

Felsenstein J. (2005) PHYLIP (Phylogeny Inference Package) version 3.6. Distributed by the author. *Department of Genome Sciences, University of Washington, Seattle.*

Fiers M., Golemiec E., Xu J., van der Geest L., Heidstra R., Stiekema W. and Liu C.M. (2005) The 14-amino acid CLV3, CLE19 and CLE40 peptides trigger consumption of the root meristem in *Arabidopsis* through a *CLAVATA2*-dependent pathway. *The Plant Cell 17: 2542-2553*

Fischer R.A. and Stapper M. (1987) Lodging effects of high yielding crops of irrigated semi-dwarf wheat. *Field Crop Research 17: 245-248*

Fisher K. and Turner S. (2007) PXY, a receptor-like kinase essential for maintaining polarity during plant vascular-tissue development. *Current Biology 17: 1061-1066*

Floyd S.K., Zalewski C.S. And Bowman J.L. (2006) Evolution of class III homeodomain-leucine zipper genes in streptophytes. *Genetics 173: 373-388*

Frishman D. and Argos P. (1996) Incorporation of non-local interactions in protein secondary structure prediction from the amino acid sequence. *Protein Engineering 9:133-142*

Fukuda H., Hirakawa Y. and Sawa S. (2007) Peptide signaling in vascular development. *Current Opinion in Plant Biology 10: 477-482*

Gascuel O. and Steel M. (2006) Neighbour-joining reveald. *Molecular Biology and Evolution 23: 1997-2000*

Gray J. (1993) Major paleozoic land plant evolutionary bio-events. *Paleogeography, Paleoclimatology and Paleoecology 104: 153-169*

Greilhuber J., Borsch T., Muller K., Worberg A., Porembski S. and Barthlott W. (2006) Smallest angiosperm genomes found in lentibulariaceae, with chromosomes of bacterial size. *Plant Biology 8: 770-777*

Guermeur Y., Geourjon C., Gallinari P. and Deleage G. (1999) Improved Performance in Protein Secondary Structure Prediction by Inhomogeneous Score Combination. *Bioinformatics 15: 413-421*

Guo M., Thomas J., Collins G., Timmermans M.C.P. (2008) Direct repression of *KNOX* loci by the ASYMMETRIC LEAVES1 complex of Arabidopsis. *The Plant Cell 20: 48-58*

Haecker A., Gross-Hardt R., Geiges B., Sarkar A., Breuninger H., Herrmann M. and Laux T. (2004) Expression dynamics of *WOX* genes mark cell fate decisions during early embryonic patterning in *Arabidopsis thaliana*. *Development 131: 657–66*

Harrison C.J., Corley S.B., Moylan E.C., Alexander D.L., Scotland R.W. and Langdale J.A. (2005) Independent recruitment of a conserved developmental mechanism during leaf evolution. *Nature 434: 509-514*

Harrison C.J., Rezvani M. and Langdale J.A. (2007) Growth from two transient apical initials in the meristem of *Selaginella kraussiana*. *Development 134: 881-889*

Hedman H., Källman T. and Lagercrantz U. (2009) Early evolution of the MTF-like gene family in plants. *Plant Molecular Biology in press.*

Hochholdinger F., Woll K., Sauer M. and Dembinski D. (2004) Genetic dissection of root formation in maize (*Zea mays*) reveals root-type specific developmental programmes. *Annals of Botany 93: 359-368*

Hord C.L., Chen C., DeYoung B.J., Clark S.E. and Ma H. (2006) The BAM1/BAM2 receptor-like kinases are important regulators of *Arabidopsis* early anther development. *The Plant Cell 18: 1667-1680*

Horner H.T. and Beltz C.K. (1970) Cellular differentiation of heterospory in *Selaginella*. *Protoplasma 71: 335-341*

Hunter T. (1995) Protein kinases and phosphatases: The ying and yang of protein phosporylation and signaling. *Cell 80: 225-236*

Irish V.F. and Sussex I.M. (1992) A fate map of the *Arabidopsis* embryonic shoot apical meristem. *Development. 115: 745–753*

Jeong S., Trotochaud A.E. and Clark S.E. (1999) The *Arabidopsis CLAVATA2* gene encodes a receptor-like protein required for the stability of the *CLAVATA1* receptor-like kinase. *The Plant Cell 11: 1925-1934*

Karol K.G., McCourt R.M., Cimino M.T. and Delwiche C.F. (2001) The closest living relatives of land plants. *Science 294: 2351-2353*

Kashiwagi T., Togawa E., Hirotsu N. and Ishimaru K. (2008) Improving of lodging resistance with QTLs for stem diameter in rice (*Oryza sativa* L.). *Theoretical and Applied Genetics 117: 749-757*

Kardailsky I., Shukla V.K., Ahn J.H., Dagenais N., Christensen S.K., Nguyen J.T., Chory J., Harrison M.J. and Weigel D. (1999) Activation tagging of the floral inducer FT. *Science 286: 1962–1965*

Kayes J.M. And Clark S.E. (1998) *CLAVATA2*, a regulator of meristem and organ development in *Arabidopsis*. *Development 125. 3843-3851*

Kenrick P. (1994) Alternation of generation in land plants: new phylogenetic and morphological evidence. *Biological Reviews 69: 293-330*

Kenrick P. and Crane P.R. (1997) The origin and early evolution of plants on land. *Nature 389: 33-39*

Kenrick P. (2000) The relationship of vascular plants. *Phylosophycal Transaction of the Royal Society B 355: 847-855*

Kieffer M., Stern Y., Cook H., Clerici E., Maulbetsch C., Laux T. and Davis B. (2006) Analysis of the transcription factor WUSCHEL and its functional homologue in *Antirrhinum* reveals a potential mechanism for their roles in meristem maintenance. *Plant Cell 18: 560-573*

Kiesselbach T.A. (1949) The structure and reproduction of corn. *University of Nebraska Press*

King R.D. and Sternberg M.J. (1996) Identification and application of the concepts important for accurate and reliable protein secondary structure prediction. *Protein Science 5: 2298-2310*

Kobayashi Y., Kaya H., Goto K., Iwabuchi M. and Araki T (1999) A pair of related genes with antagonistic roles in mediating flowering signals. *Science 286: 1960–1962*

Kolaczkowski B. and Thornton J.W. (2004) Performance of maximum parsimony and likelihood phylogenetics when evolution is heterogeneous. *Nature 431: 980–984*

Korall P. and Kenrick P. (2002) Phylogenetic relationship in Selaginellaceae based on *rbcL* sequences. *American Journal of Botany 89: 506:517*

Korall P. and Kenrick P. (2004) The phylogenetic history of Selaginellaceae based on DNA sequences from the plastid and nucleus: extreme substitution rates and rate heterogeneity. *Molecular Phylogenetics and Evolution 31: 852-864*

Labarga A., Valentin F., Andersson M. and Lopez R. (2007) Web Services at the European Bioinformatics Institute. *Nucleic Acids Research Web Services Issue July 2007: W6-W11*

Laux T., Mayer K.F., Berger J. and Jürgens G. (1996) The *WUSCHEL* gene is required for shoot and floral meristem integrity in *Arabidopsis*. *Development 122: 87-96*

Laux T., Wuerschum T. and Breuninger H. (2004) Genetic regulation of embryonic pattern formation. *Plant Cell 16: S190-S202*

Lewis L.A. and McCourt R.M. (2004) Green algae and the origin of land plants. *American Journal of Botany 91: 1535-1556*

Lupas A., van Dike M. and Stock J. (1991) Predicting coiled coils from protein sequences. *Science 252: 1162-1164*

Lyndon R.F. (1998) The shoot apical meristem – Its growth and development. *Cambridge University Press*

Mansfield S.G., Briarty L.G. and Erni S. (1991) Early embryogenesis in *Arabidopsis thaliana*. I. The mature embryo sac. *Canadian Journal of Botany 69: 447-460*

Mansfield S.G. and Briarty L.G. (1991) Early embryogenesis in *Arabidopsis thaliana*. II. The developing embryo. *Canadian Journal of Botany 69: 461-476*

Matsumoto N. and Okada K. (2001) A homeobox gene, *PRESSED FLOWER*, regulates lateral axis-dependent development of *Arabidopsis* flowers. *Genes & Development 15: 3355-3364*

May B.P., Liu H., Vollbrecht E., Senior L., Rabinowicz P.D., Roh D., Pan X., Stein L., Freeling M., Alexander D., and Martienssen R. (2003) Maize-targeted mutagenesis: A knockout resource for maize. *PNAS 100: 11541-11546*

Mayer K.F., Schoof H., Haecker A., Lenhard M., Jurgens G. and Laux T. (1998) Role of *WUSCHEL* in regulating stem cell fate in the *Arabidopsis* shoot meristem. *Cell 95: 805–815*

Miwa H., Betsuyaku S., Iwamoto K., Kinoshita A., Fukuda H. and Sawa S. (2008) The receptor-like kinase SOL2 mediates CLE signaling in *Arabidopsis*. *Plant Cell Physiology 49: 1752-1757*

Moon S., Jung K.H., Lee D.E., Lee D.Y., Lee J., An K., Kang H.G. and An G. (2006) The rice FON1 gene controls vegetative and reproductive development by regulating shoot apical meristem size. *Molecules and Cells 21: 147-152*

Moreno-Risueno M.Á., Martínez M., Vicente-Carbajosa J. and Carbonero P. (2007) The family of DOF transcription factors: from green unicellular algae to vascular plants. *Molecular Genetics and Genomics 277: 379-390*

Müller R., Bleckmann A. and Simon R. (2008) The receptor kinase CORYNE of *Arabidopsis* transmit the stem cell-limiting signal CLAVATA3 independently of CLAVATA1. *Plant Cell 20: 934-946*

Nardmann J., Ji J., Werr W. and Scanlon M.J. (2004) The maize duplicate genes *narrow sheath1* and *narrow sheath2* encode a conserved homeobox function in a lateral domain of shoot apical meristems. *Development 131: 2827-2839*

Nardmann J. and Werr W. (2006) The shoot stem cell niche in angiosperms: expression patterns of WUS orthologues in rice and maize imply major modifications in the course of mono- and dicot evolution. *Molecular Biology and Evolution 23: 2492–2504*

Nardmann J. and Werr W. (2007) The evolution of plant regulatory networks: what *Arabidopsis* cannot say for itself. *Current Opinion in Plant Biology 10: 653-659*

Nardmann J., Zimmermann R., Durantini D., Kranz E. and Werr W. (2007) *WOX* gene phylogeny in *Poaceae*: a comparative approach addressing leaf and embryo development. *Molecular Biology and Evolution 24: 2474-2484*

Ohshima S., Murata M., Sakamoto W., Ogura Y. and Motoyoshi F. (1997) Cloning and molecular analysis of the *Arabidopsis* gene terminal flower 1. *Molecular and General Genetics 254: 186–194*

Palenik B., Grimwood J., Aerts A., Rouzé P., Salamov A., Putnam N., Dupont C., Jorgensen R., Derelle E., Rombauts S., Zhou K., Otillar R., Merchant S.S., Podell S., Gaasterland T., Napoli C., Gendler K., Manuell A., Tai V., Vallon O., Pigeneau G., Jancek S., Heijde M., Jabbari K., Bowler C., Lohr M., Robbens S., Werner G., Dubchak I., Pazour G.J., Ren Q., Paulsen I., Delwiche C., Schmutz J., Rokhsar D., Van de Peer Y., Moreau H. and Grigoriev I.V. (2007) The tiny eukaryote *Ostreococcus* provides genomic insights into the paradox of plankton speciation. *Proceedings of the National Academy of Science USA 104: 7705-7710*

Phelps-Durr T.L., Thomas J., Vahab P. and Timmermans M.C.P. (2005) Maize ROUGH SHEATH2 and its Arabidopsis orthologue ASYMMETRIC LEAVES1 interact with HIRA, a predicted histone chaperone, to maintain knox gene silencing and determinacy during organogenesis. *Plant Cell 17: 2886–2898*

Philippe H. and Lopez P (2001) On the conservation of protein sequences in evolution. *Trends in Biochemical Science 26: 414-416*

Pinthus M.J. (1973) Lodging in wheat, barley and oats: the phenomenon, its causes and preventative measures. *Advances in Agronomy 25: 209-263*

Poethig S. (1984) Cellular parameters of leaf morphogenesis in maize and tobacco. *In: White R, Dickinson WC, editors. Contemporary problems in plant anatomy. New York: Academic Press. p. 235–259*

Qiu Y.L., Li L., Wang B., Chen Z., Knoop V., Groth-Malonek M., Dombrovska O., Lee J., Kent L., Rest J., Estabrook G.F., Hendry T.A., Taylor D.W., Testa C.M., Ambros M., Crandall-Stotler B., Joel Duff R., Stech M., Frey W., Quandt D. and Davis C.C. (2006) The deepest divergences in land plants inferred from phylogenomic evidence. *Proceedings of the National Academy of Science USA 103: 15511-15516*

Qiu Y.L., Li L., Wang B., Chen Z., Dombrovska O., Lee J., Kent L., Li R., Jobson R.W., Hendry T.A., Taylor D.W., Testa C.M. and Ambros M. (2007) A Nonflowering Land Plant Phylogeny Inferred from Nucleotide Sequences of Seven Chloroplast, Mitochondrial, and Nuclear Genes. *International Journal of Plant Science 168: 691-708*

Randolph L.F. (1936) Developmental morphology of the caryopsis in maize. *Journal of Agricultural Research 53: 881-916*

Raubeson L.A. and Jansen R.K. (1992) Chloroplast DNA evidence on the ancient evolutionary split in vascular plants. *Science 255: 1697-1699*

Raven J.A. and Edwards D. (2001) Roots: evolutionary origins and biogeochemical significance. *Journal of Experimental Botany 52 (Root Special Issue): 381-401*

Rebocho A.B., Bliek M., Kusters E., Castel R., Procissi A., Roobeek I., Souer E. and Koes R. (2008) Role of EVERGREEN in the development of the cymose Petunia inflorescence. *Developmental Cell 15: 437-447*

Rensing S.A., Ick J., Fawcett J.A., Lang D., Zimmer A., Van de Peer Y. and Reski R. (2007) An ancient genome duplication contributed to the abundance of metabolic genes in the moss *Physcomitrella patens*. *BMC Evolutionary Biology 7: 130*

Rensing S.A., Lang D., Zimmer A.D., Terry A., Salamov A., Shapiro H., Nishiyama T., Perroud P.F., Lindquist E.A., Kamisugi Y., Tanahashi T., Sakakibara K., Fujita T., Oishi K., Shin-I. T., Kuroki Y., Toyoda A., Suzuki Y., Hashimoto S., Yamaguchi K., Sugano S., Kohara Y., Fujiyama A., Anterola A., Aoki S., Ashton N., Barbazuk W.B., Barker E., Bennetzen J.L., Blankenship R., Cho S.H., Dutcher S.K., Estelle M., Fawcett J.A., Gundlach H., Hanada K., Heyl A., Hicks K.A., Hughes J., Lohr M., Mayer K., Melkozernov A., Murata T., Nelson D.R., Pils B., Prigge M., Reiss B., Renner T., Rombauts S., Rushton P.J., Sanderfoot A., Schween G., Shiu S.H., Stueber K., Theodoulou F.L., Tu H., Van de Peer Y., Verrier P.J., Waters E., Wood A., Yang L., Cove D., Cuming A.C., Hasebe M., Lucas S., Mishler B.D., Reski R., Grigoriev I.V., Quatrano R.S. and Boore J.L. (2008) The *Physcomitrella* genome reveals evolutionary insights into the conquest of land by plants. *Science 319: 64-69*

Rojo E., Sharma V.K., Kovaleva V., Raikhel N.V. and Fletcher J.C. (2002) CLV3 is localized to the extracellular space, where it activates the *Arabidopsis* CLAVATA stem cell signalling pathway. *Plant Cell 14: 969-977*

Rost B. and Sander C. (1993) Prediction of protein secondary structure at better than 70% accuracy. *Journal of Molecular Biology 232:584-599*

Rudall P. (1991) Lateral meristems and stem thickening growth in Monocotyledons. *The Botanical Review 57: 150-163*

Saitou N., Nei M (1987) The neighbor-joining method: A new method for reconstructing phylogenetic trees. *Molecular Biology and Evolution 4:406-425*

Sakaguchi J. and Fukuda H. (2008) Cell differentiation in the longitudinal veins and formation of commissural veins in rice (*Oryza sativa*) and maize (*Zea mays*). *Journal of Plant Research 121: 593-602*

Sakakibara K., Nishiyama T., Deguchi H. and Hasebe M. (2008) Class 1 KNOX gene are not involved in shoot development in the moss *Physcomitrella patens* but do function in sporophyte development. *Evolution & Development 10: 555-566*

Sanderson M.J. (2003) Molecular data from 27 proteins do not support a precambrian origin of land plants. *American Journal of Botany 90: 954-956*

Sarkar A.K., Luijten M., Miyashima S., Lenhard M., Hashimoto T., Nakajima K., Scheres B., Heidstra R. and Laux T. (2007) Conserved factors regulate signalling in *Arabidopsis thaliana* shoot and root stem cell organizers. *Nature 446: 811–814*

Schoof H., Lenhard M., Haecker A., Mayer K.F., Jurgens G. and Laux T. (2000) The stem cell population of *Arabidopsis* shoot meristems is maintained by a regulatory loop between the *CLAVATA* and *WUSCHEL* genes. *Cell. 100: 635–644*

Shimizu R., Ji J., Kelsey E., Ohtsu K., Schnable P.S. and Scanlon M.J. (2009) Tissue specificity and evolution of meristematic WOX3 function. *Plant Physiology 149: 841-850*

Shiu S.-H. and Bleecker A.B. (2001) Plant receptor-like kinases gene family: diversity, function, and signalling. *Science STKE RE22*

Smith G.M. (1950) The freshwater algae of the United States. *McGraw-Hill, New York, New York, USA*

Sperry J.S. (2003) Evolution of water transport and xylem structure. *International Journal of Plant Science 164(S3): 115-127*

Steffensen D.M. (1968) A reconstruction of cell development in the shoot apex of maize. *American Journal of Botany 55: 354–369*

Stuurman J., Jaggi F. and Kuhlmeier C. (2002) Shoot meristem maintenance is controlled by a GRAS-gene mediated signal from differentiating cells. *Genes & Development 16: 2213-2218*

Suzaki T., Sato M., Ashikari M., Miyoshi M., Nagato Y. and Hirano H.Y. (2004) The gene *FLORAL ORGAN NUMBER1* regulates floral meristem size in rice and encodes a leucine-rich repeat receptor kinase orthologous to Arabidopsis *CLAVATA1*. *Development. 131: 5649–5657*

Suzaki T., Toriba T., Fujimoto M., Tsutsumi N., Kitano H. and Hirano H.Y. (2006) Conservation and diversification of meristem maintenance in *Oryza sativa*: function of the FLORAL ORGAN NUMBER2 gene. *Plant Cell Physiology 47: 1591-1602*

Szemenyei H., Hannon M. and Long J.A. (2008) TOPLESS mediates auxin-dependent transcriptional repression during *Arabidopsis* embryogenesis. *Science 319: 1384-1386*

Szymkowiak E.J. and Sussex I.M. (1996) What chimeras can tell us about plant development. *Annual Review of Plant Physiology and Plant Molecular Biology 47: 351–376*

Taguchi-Shiobara F., Yuan Z., Hake S. and Jackson D. (2001) The *fascinated ear2* gene encodes a leucine-rich repeat receptor-like protein that regulates shoot meristem proliferation in maize. *Genes & Development 15: 2755–2766*

Tamura K., Dudley J., Nei M. and Kumar S. (2007) *MEGA4*: Molecular Evolutionary Genetics Analysis (MEGA) software version 4.0. *Molecular Biology and Evolution 24: 1596-1599*

Timmermans M.C., Hudson A., Becraft P.W. and Nelson T. (1999) *ROUGH SHEATH2*: a Myb protein that represses knox homeobox genes in maize lateral organ primordia. *Science 284: 151–153*

Tsiantis M., Schneeberger R., Golz J.F., Freeling M., Langdale J.A. (1999) The maize *rough sheath2* gene and leaf development programs in monocot and dicot plants. *Science 284: 154–156*

Turmel M., Otis C. and Lemieux C. (2003) The mitocondrial genome of *Chara vulgaris*: insight into the mitocondrial DNA architecture of the last common ancestor of green algae and land plants. *Plant Cell 15: 1888-1903*

Van Lammeren A.A.M. (1986) Developmental morphology and cytology of the young maize embryo (*Zea mays L.*). *Acta Botanica Neerlandica 35: 169-188*

Vollbrecht E., Springer P.S., Goh L., Buckler IV E.S. and Martienssen R. (2005) Architecture of floral branch system in maize and related grasses. *Nature 436: 1119-1126*

Waites R., Selvadurai H.R., Oliver I.R. and Hudson A. (1998) The *PHANTASTICA* gene encodes a MYB transcription factor involved in growth and dorsoventrality of lateral organs in *Antirrhinum*. *Cell. 93:779–789*

Wang W., Tanurdzic M., Luo M., Sisneros N., Kim H.R., Weng J.K., Kudrna D., Mueller C., Arumuganathan K., Carlson J., Chapple C., de Pamphilis C., Mandoli D., Tomkins J., Wing R.A. and Banks J.A. (20059 Construction of a bacterial artificial chromosome library from the spikemoss *Selaginella moellendorffii*: a new resource for plant comparative genomics. *BMC Plant Biology 5: 10*

Worden A.Z., Lee J.-H., Mock T., Rouzé P., Simmons M.P., Aerts A.L., Allen A.E., Cuvelier M.L., Derelle E., Everett M.V., Foulon E., Grimwood J., Gundlach H., Henrissat B., Napoli C., McDonald S.M., Parker M.S., Rombauts S., Salamov A., Von Dassow P., Badger J.H., Coutinho P.M., Demir E., Dubchak I., Gentemann C., Eikrem W., Gready J.E., John U., Lanier W., Lindquist E.A., Lucas S., Mayer K.F.X., Moreau H., Not F., Otillar R., Panaud O., Pangilinan J., Paulsen I., Piegu B., Poliakov A., Robbens S., Schmutz J., Toulza E., Wyss T., Zelensky A., Zhou K., Virginia Armbrust E., Bhattacharya D., Goodenough U.W., Van de Peer Y. and Grigoriev I.V. (2009) Green evolution and dynamic adaptations revealed by the genomes of the marine picoeukaryotes *Micromonas*. *Science 324: 268-272*

Wu X., Chory J. and Weigel D. (2007) Combinations of *WOX* activities regulate tissue proliferation during *Arabidopsis* embryonic development. *Developmental Biology 309: 306-316*

Xu, L., Xu Y., Dong A.W., Sun Y., Pi L.M., Xu Y.Q. and Huang H. (2003) Novel as1 and as2 defects in leaf adaxial-abaxial polarity reveal the requirement for ASYMMETRIC LEAVES1 and 2 and ERECTA functions in specifying adaxial identity. *Development 130: 4097–4107*

Yoon H.S., Hackett J., Ciniglia C., Pinto G. and Bhattacharya D. (2004) A molecular timeline for the origin of photosynthetic eukaryotes. *Molecular Biology and Evolution 21: 809-818*

Zhang X. (1998) Leucine-rich Repeat Receptor-like Kinases in Plants. *Plant Molecular Biology Reporter 16: 301-311*

Zhao Y., Yongfeng H., Mingqiu D., Huang L. and Zhou D.X. (2009) The WUSCHEL-related homeobox gene *WOX11* is required to activate shoot-borne crown root development in rice. *Plant Cell in press.*

Zuckerkandl E. and Pauling L. (1965) Evolutionary divergence and convergence in proteins. *Evolving Genes and Proteins: 97-166*

APPENDIX A: FIGURES

I

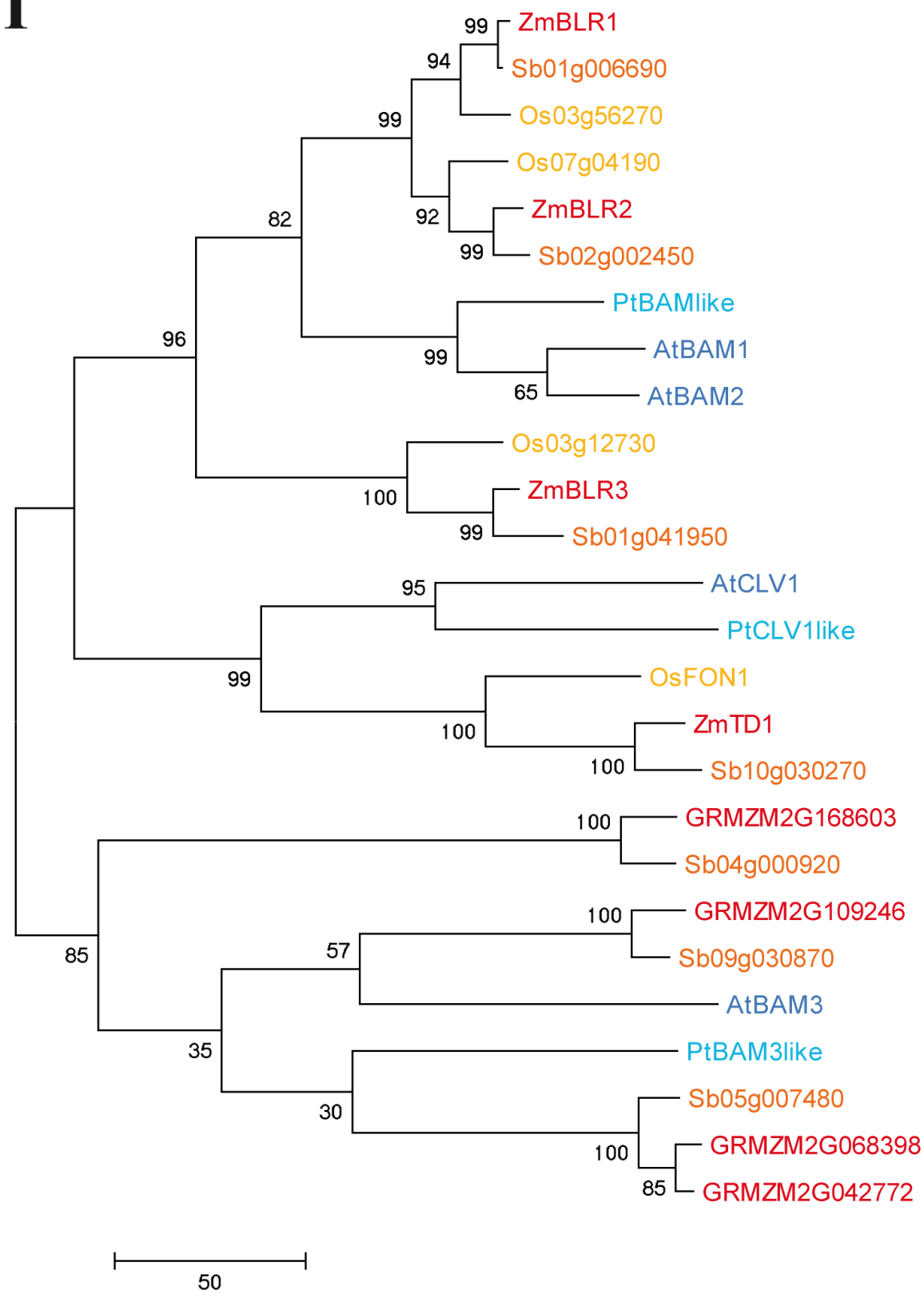
ZmBLR1
Sb01g006690
Os03g56270
Os07g04190
ZmBLR2
Sb02g002450
PtBAMlike
AtBAM1
AtBAM2
Os03g12730
ZmBLR3
Sb01g041950
AtCLV1
PtCLV1like
OsFON1
ZmTD1
Sb10g030270
GRMZM2G168603
Sb04g000920
GRMZM2G109246
Sb09g030870
AtBAM3
PtBAM3like
Sb05g007480
GRMZM2G068398
GRMZM2G042772
99
94
99
82
92
99
96
99
65
100
99
95
99
100
100
100
85
57
35
30
100
85
50

II

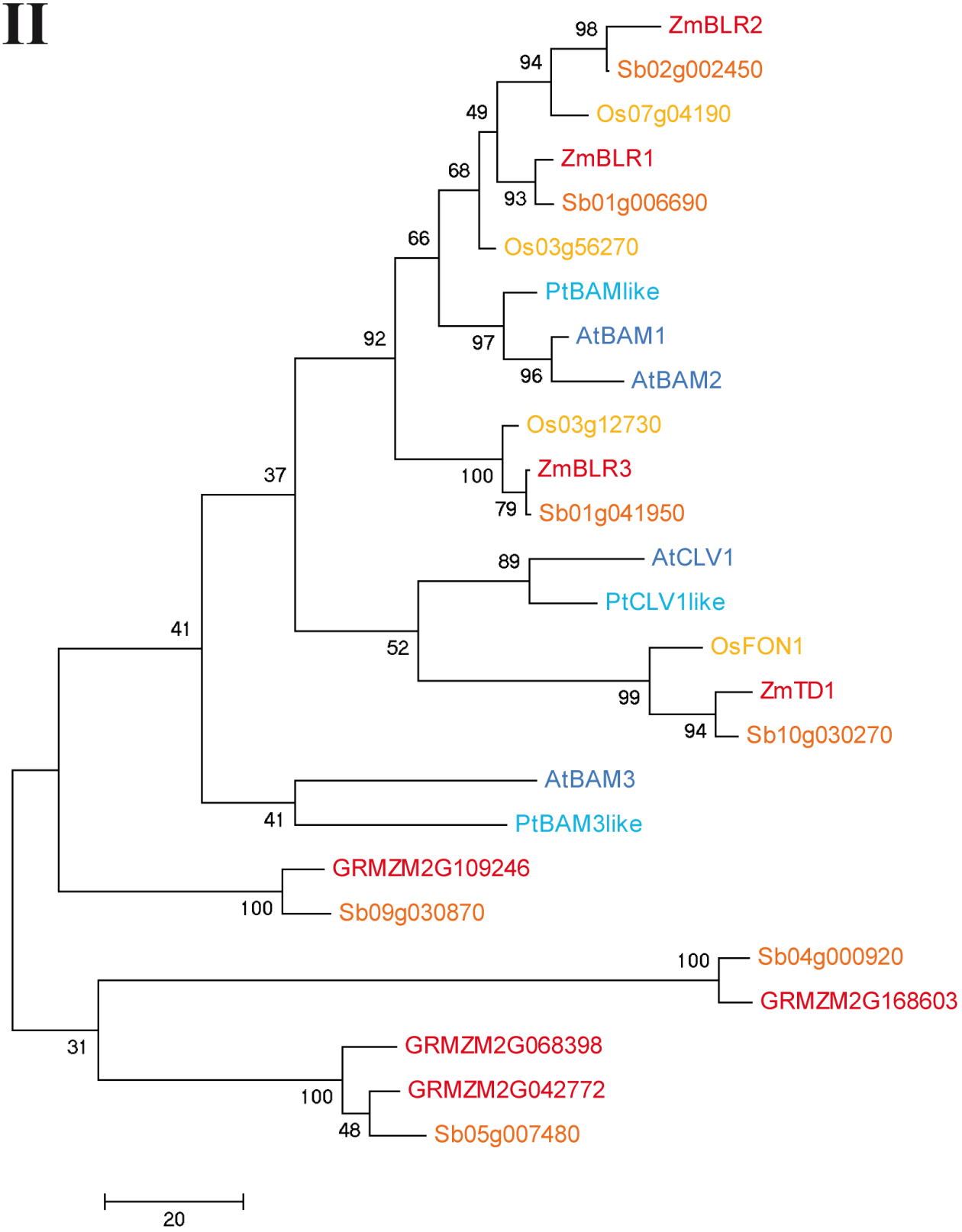
ZmBLR2
Sb02g002450
Os07g04190
ZmBLR1
Sb01g006690
Os03g56270
PtBAMlike
AtBAM1
AtBAM2
Os03g12730
ZmBLR3
Sb01g041950
AtCLV1
PtCLV1like
OsFON1
ZmTD1
Sb10g030270
AtBAM3
PtBAM3like
GRMZM2G109246
Sb09g030870
Sb04g000920
GRMZM2G168603
GRMZM2G068398
GRMZM2G042772
Sb05g007480
98
94
49
68
93
66
92
97
96
37
100
79
89
41
52
99
94
41
100
100
31
100
48
20

III

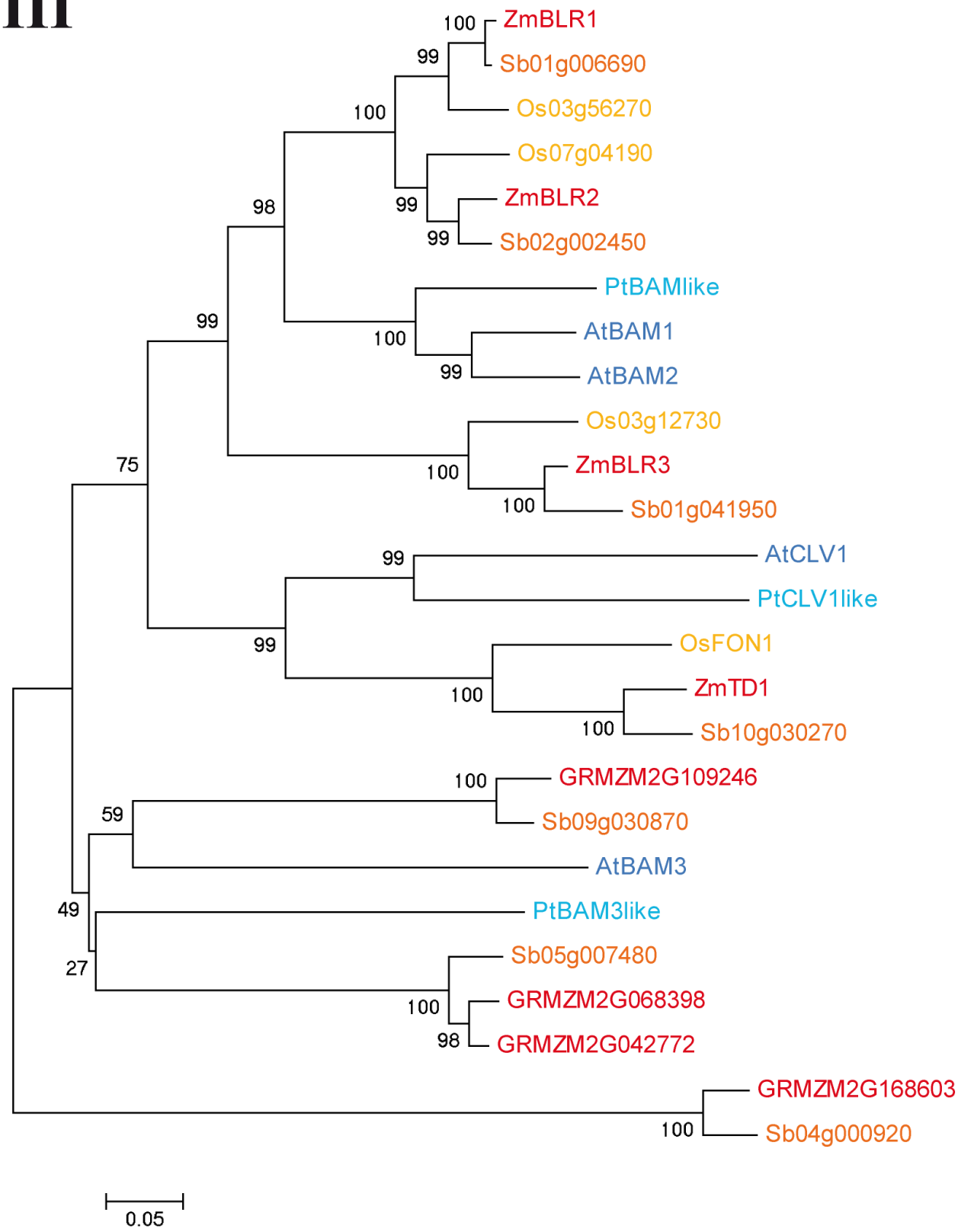
ZmBLR1
Sb01g006690
Os03g56270
Os07g04190
ZmBLR2
Sb02g002450
PtBAMlike
AtBAM1
AtBAM2
Os03g12730
ZmBLR3
Sb01g041950
AtCLV1
PtCLV1like
OsFON1
ZmTD1
Sb10g030270
GRMZM2G109246
Sb09g030870
AtBAM3
PtBAM3like
Sb05g007480
GRMZM2G068398
GRMZM2G042772
GRMZM2G168603
Sb04g000920
100
99
100
99
98
99
99
100
99
75
100
100
99
99
100
100
100
59
49
27
100
98
100
0.05

IV

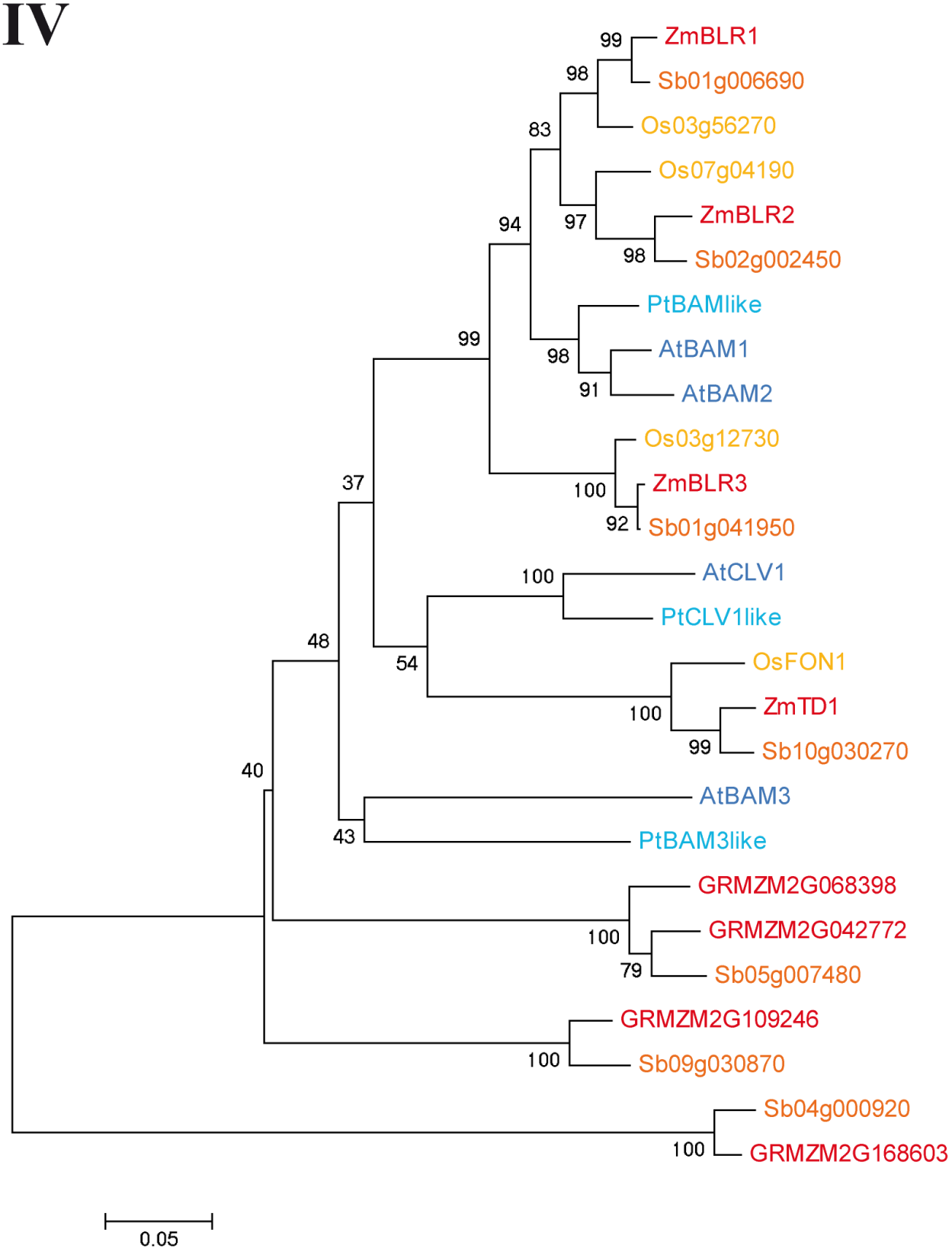
ZmBLR1
Sb01g006690
Os03g56270
Os07g04190
ZmBLR2
Sb02g002450
PtBAMlike
AtBAM1
AtBAM2
Os03g12730
ZmBLR3
Sb01g041950
AtCLV1
PtCLV1like
OsFON1
ZmTD1
Sb10g030270
AtBAM3
PtBAM3like
GRMZM2G068398
GRMZM2G042772
Sb05g007480
GRMZM2G109246
Sb09g030870
Sb04g000920
GRMZM2G168603
99
98
83
97
94
98
99
98
91
37
100
92
100
48
54
100
99
40
43
100
79
100
100
0.05

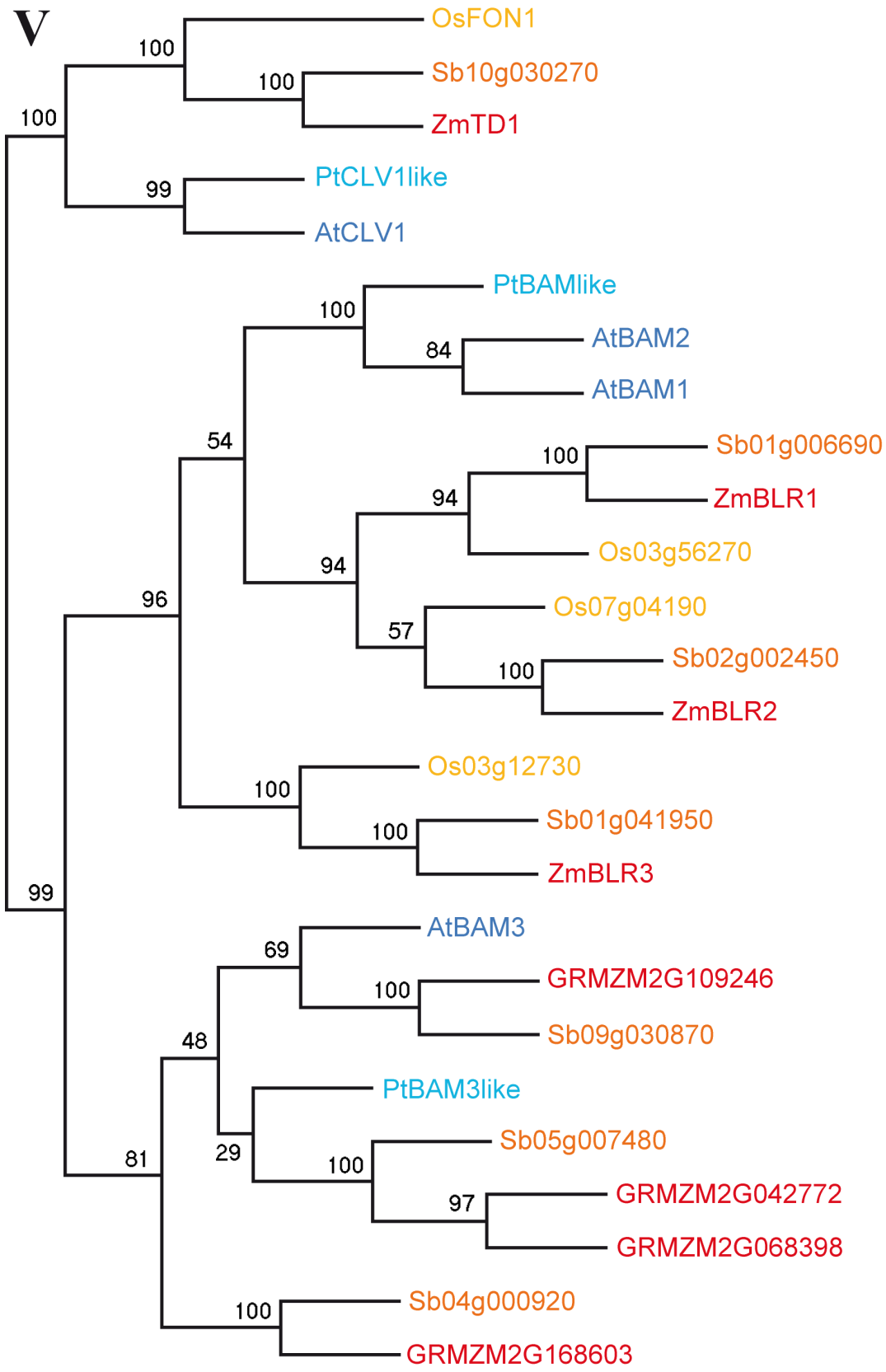
V
OsFON1
Sb10g030270
ZmTD1
PtCLV1like
AtCLV1
PtBAMlike
AtBAM2
AtBAM1
Sb01g006690
ZmBLR1
Os03g56270
Os07g04190
Sb02g002450
ZmBLR2
Os03g12730
Sb01g041950
ZmBLR3
AtBAM3
GRMZM2G109246
Sb09g030870
PtBAM3like
Sb05g007480
GRMZM2G042772
GRMZM2G068398
Sb04g000920
GRMZM2G168603
100
100
100
99
100
84
54
100
94
94
96
57
100
100
100
99
69
100
48
29
100
97
81
100

VI

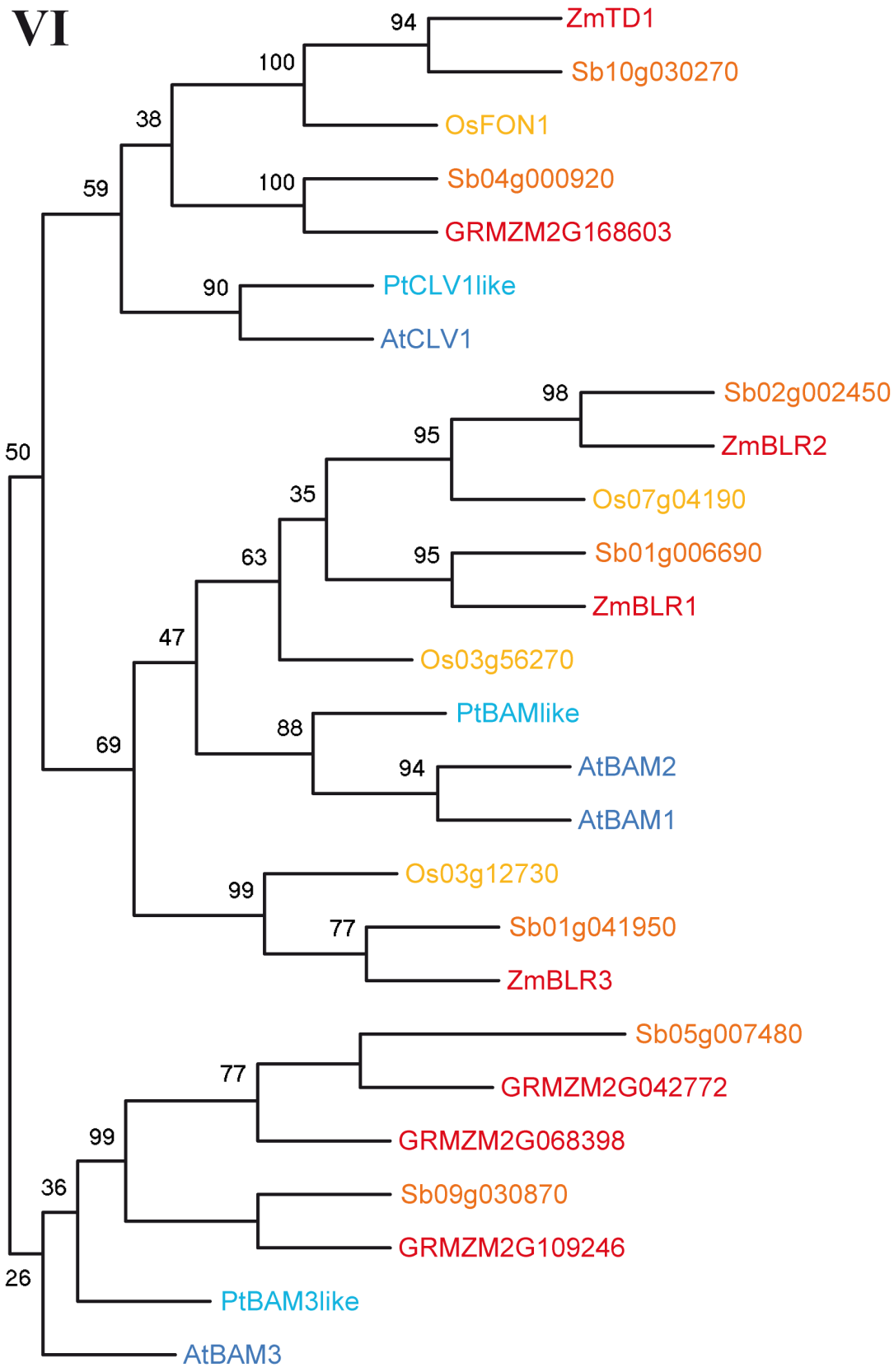
94
ZmTD1
100
Sb10g030270
38
OsFON1
100
Sb04g000920
59
GRMZM2G168603
90
PtCLV1like
AtCLV1
98
Sb02g002450
95
ZmBLR2
50
35
Os07g04190
95
Sb01g006690
63
ZmBLR1
47
Os03g56270
PtBAMlike
88
69
94
AtBAM2
AtBAM1
Os03g12730
99
77
Sb01g041950
ZmBLR3
Sb05g007480
77
GRMZM2G042772
99
GRMZM2G068398
36
Sb09g030870
GRMZM2G109246
26
PtBAM3like
AtBAM3

Appendix Fig. I-VI. Phylogeny of the closest *AtCLAVATA1* orthologs in *Arabidopsis thaliana*, *Populus Trichocarpa*, *Oryza sativa*, *Sorghum bicolor* and *Zea mays*. The evolutionary history of the LRR domains (I,III and V) and kinase domains (II, IV and VI) inferred using the maximum parsimony (I-II), the neighbor joining (III-IV) and the maximum likelihood methods (V-VI). The percentage of replicate trees in which the associated taxa clustered together in the bootstrap test (1000 replicates) are shown next to the branch nodes.The tree is drawn to scale, with branch lengths in the same units as those of the evolutionary distances used to infer the phylogenetic tree.

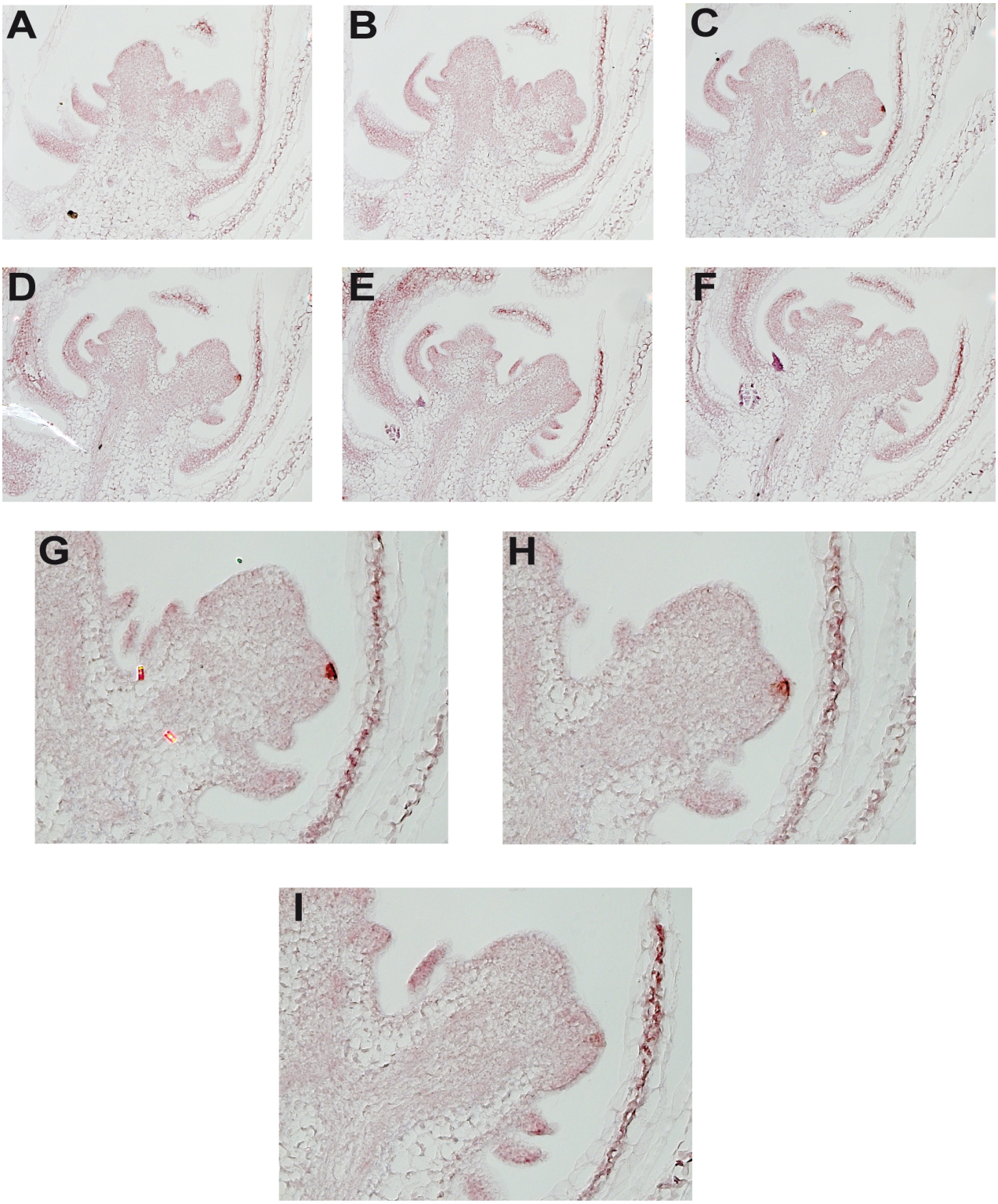

Appendix fig. VII. *SkWOX13A* expression pattern in minor branch meristem. (A-F) Longitudinal sections hybridized with a *SkWOX13A* specific probe. Note the three different shoot apical meristem depicted, but only one of them showing a distinct signal. (G-I) Magnification of pictures (C-E).

APPENDIX B: SEQUENCES

S.kraussiana WOX13A

- genomic locus

tttaaaacgacctagctgcccctagagctgtttatggtaatagtttaaccggtgacacgtttagcaattctgtgttgtttacattatga
taatgtaaaaaaaaacgaaagaaacttgatcattcagcttctaatagaaatcgaagcgggaatacatttttcaggcgttctcgtcc
ttggcctcagtggctccttcctcctgcacattacaacacagaatgggcgtgtcagtgctatggagtgaacacagtacctgcatgtcc
gaggtccagagagtgagattgtcacgcaggagctgcatgatgagcgtgctgtccttgtaagactcctcaccgatggtgtccaactc
cgcgatcgcttcatcgaacgcctgcaatcgtaaaaatgagctgcaaagctgacacaaaacggacctgcttggcaaggctgcatgc
ccggtccggcgagttgaggatctcgtagtaaaacacggagaagttgagggcaagacccaggcggatggggtgcgtcggtgccag
ctccaccagtgcaatgtcctgtggcccagataaccatggtttatcaaagaacttcaatgttaacctgggcggacttgtatgcaacga
gggtgctctcggcggcctctttgcgttcagcgcccgtcttgaactccgccaagtagcggtggtaatcgcccttcattttgaggtagaa
cacgcgcgactcgcccgctggggccgatggcacgaggtgggcgtcgagcaggttgaggatgccggcgcagatggtggatagctc
cgactcaatccggccacggtactcccggatcatcgccacatgctcctcgtttcccttgctctcctcctcctgctcgatcgaggagacg
atcctccacgacgcccgccgcgccccgatcacgttcttgtacgccacggagagcaggttgcgctcctccacgctgagaccctccct
ggagcccgtcactaccttctccatgtactccaccatctcgtcgtagcgctctncccgctcggccagcttcgccatgtacacgctctctt
ccctcgtcatgttcaccgccgtcgccgccatggaaacactcactcaattagggcccgaggagtgagaatatacccgggcacattct
catcccggcacgagaatattggtgggtatattcctagctcggctcgccgttgagccgggaaaggcaacatttttttctttttccggggc
ccgtttggtcattccccttggtgcgcacgcacacgcgcgcacgggcgctgccgnttcgatccgcagtcgcgggaacaccccacatg
cccccacacatgcaccttatattcctcctctcg**CCCTCCCTCTCGCCTCTTGAGCATGGTCGGCGCCTCATGAGC**
TTTCGATCATATGGAACACTTGAGCATCCCGCAGCACCAGCTTCAGTTCGAGGACCGTGTCTTCGA
CGATGCTTCCTGGATTCATCAACAGCAACATCAGGCGCCAGTGGCCGAGCATCTGCTGGTCATGA
CTGAGGAGCAACTGGAGACTTTGAGAAGGCAAATCTCCGTCTATGCAACAATCTGTCAGCAGCT
GGCGGAGCAGCAGAAAGCCACGCTGAACGAGCAGCACCTCCAGCAACAGCAGCAGCATTGCTTC
TTCAATggtacatacatctctgcggtcacgcccaggcctcgcatttttttgttttctttgcatgactgaa**GCTGCAGGACTTCA**
CGATCCAAGAGCCACTATCATGATGCACAAGTCGAGTTCAAGGCAGCGATGGACGCCCAGCCAG
AACCAGCTGCATATCCTTGAGCGCCTCTTCAAGCAAGGCAACGGTACTCCAAACAGGCAGAGGA

TCAAAGAGATAACCTCCGAGCTGAGCCAGCACGGGCAAATCTCCGAGACCAACGTTTACAACTG
GTTCCAGAACCGGAAGGCCCGTGCCAAGAGGAAACAGAGGCACTTGGTTAGCTCTGCAGCTCAA
CTACAACAGCAGCAGCAGAAACAGCTTAAGCACACCGAGGCCGAATGCAGTTCTCCAAACGGCA
ACAGCAAGTCGAGGTTCAGTGAAGAACTCGAAGGCTCTTCCTCCGAaggtaagtgccttataatggtatcg
gattgtacaaaatgcatatatatgcacttc**AGTGAGTCCGCAACAACAGCAATACTCGGTTGTTGTCTACAAT**
GGCAAGGCTTGGAAGGTGAAACCCGGAAGACTGAACGTATGGAGCAACTTTGGTGACAAAGCA
ACACTGCTTGATCCGAGAGGACAGCTTTTTCCAATCGACGagtgtggtatgacttgccagcctctgcagccggg
tgcagcctatactgttgccgggtataagacatacttgcatgctaagcgttaagctgatactcttgtccctttgacttgttgttacagta
ccggcctcagcgatggcacattggattgtgcgtgttaacattgtcaaggcctcatgcaatggtatgtacgcaaccttggcaagtcca
aatgtgtcatttaaaccacttacttggagatagtgcagtcatatcacaaaccaagagccctttccagtttctgtatttggttcaagaa
aatccaagtcatctgaaagacccacacttgaaacctgaattcctggccaagttcttaccatgacatgaggagctatccgtatacag
tacgttccgaatccagtatacaacttgaaaggcccgtgcttccgaattgtttggatggcacaatctagagaacctgaatacggatat
ttgccatcagctcccggctgcatcttttgtatttgagtcttgacataatcgaagggaaggctgcatgcagacgcaaagaatccgga
aacagcactggcacctgcatagagccaggacccgtacttatgctgtacaagtccgcacctatcacggtttgcacctcgggcaagtt
gagcgactctctaaagaactctaggctctgatcgtaggacgcgagcatccccatattaagagccattgcacgcacaacagtcggt
ccagcacctttccaaagggccaaaactccctcgtctttggttattctgtagagtgcatgcaaagcgtttctgtagttcctcctctgtgc
agcaggtaatagagcatcggcttgcattctgatgagagctaaatcggcgggacttccgacagtcgccccgatagcaccagctg

- <u>partial mRNA</u>

ccctccctctcgcctcttgagcatggtcggcgcctcatgagctttcgatcatatggaacacttgagcatcccgcagcaccagcttca
gttcgaggaccgtgtcttcgacgatgcttcctggattcatcaacagcaacatcaggcgccagtggccgagcatctgctggtcatga
ctgaggagcaactggagactttgagaaggcaaatctccgtctatgcaacaatctgtcagcagctggcggagcagcagaaagcca
cgctgaacgagcagcacctccagcaacagcagcagcattgcttcttcaatgctgcaggacttcacgatccaagagccactatcat
gatgcacaagtcgagttcaaggcagcgatggacgcccagccagaaccagctgcatatccttgagcgcctcttcaagcaaggcaa
cggtactccaaacaggcagaggatcaaagagataacctccgagctgagccagcacgggcaaatctccgagaccaacgtttacaa
ctggttccagaaccggaaggcccgtgccaagaggaaacagaggcacttggttagctctgcagctcaactacaacagcagcagca
gaaacagcttaagcacaccgaggccgaatgcagttctccaaacgacaacagcaagtcgaggttcagtgaagaactcgaaggctc
ttcctccgaagtgagtccgcaacaacagcaatactcggttgttgtctacaatggcaaggcttggaaggtgaaacccggaagactg
aacgtatggagcaactttggtgacaaagcaccactgcttgatccgagaggacagctttttccaatcgacg

- <u>predicted protein</u>

MEHLSIPQHQLQFEDRVFDDASWIHQQQHQAPVAEHLLVMTEEQLETLRRQISVYATICQQLAEQQK
ATLNEQHLQQQQQHCFFNAAGLHDPRATIMMHKSSSRQRWTPSQNQLHILERLFKQGNGTPNRQRI
KEITSELSQHGQISETNVYNWFQNRKARAKRKQRHLVSSAAQLQQQQQKQLKHTEAECSSPNGNSKS
RFSEELEGSSSEVSPQQQQYSVVVYNGKAWKVKPGRLNVWSNFGDKATLLDPRGQLFPID

S.kraussiana WOX13B

- genomic locus

tttaaattttaagtaacaagtgttgagatgtataaaatgctacgaacagcgtagaactgtatagacaatgtaattattgttggatac
aaataacgatacgttaaaccgtatcatctatcgatctatcgtaattcttcaagaagttgctatgtaggcgcgggattagtggattga
taattgctcaaagtcaatcttagaatatttctccggaaaaaataaattgcgccggaggtggcatctttctggcattttcatatttctat
tcaatcacttgcacggcaagcaggctcgttgttgttgtaagcacgacgctgagcatcaatctcccgcgcacattcctcgcgattcct
cgcagtgacgcttccaggttcgaaaagatttccctcaagaagttcaatcaatcgcaacgtacgttacagatttcagagtcgtgtttg
ttctacaaaattaattagatcattgggtgtttttagatgatccct**ATGGAAACAGGGACGACGAGTTCTTCCTCATC**
AGATGTAAATCCGCAGCTGATTGATCCAGATTCAAGCCTAGAGCGGCCAGCTTACCATCCTCATT
ACGGCGTGGTTATCACCCCCTACCAACTCCAACTCCTCAGGGATCAAATTGCAAGCTATGCAACCA
TCTGTTTGAAGCTGATAGACATGCACAAAGCATTGGTCAATGGTTACCATGGTAGTACCAATGGT
AACACCGAGGTTAACCATGGTAGGGTCCCTTACAACAACATGAGTGATGATCAGATGAGTGAAC
TTGAACGTGAAGGTGAACATGATCAAGGAAGGGTGATTAGCAGGAAGAAAAACTTGGTTAGTG
GTAGTGGTAATGGTAATCTAACCAAAGCAGGTACGACTAGGCACAGATGGACTCCAACTCAGAC
ACAACTCAAGATTTTAGAGGATTTATTTGGGGTTCATGGTATGAATAATACTCCAAATAAGAGGA
GAGTGAGTGAGATTACGGCAGATTTGGCTAAACACGGTCCCATTTCTGAGTCTAATGTCTCCAAC
TGGTTCCAGAATCGTAAGGCCAGGTATAGGCGACTCTTGAGGTCTTGAATTGATCAAATGAGCCA
ATGGACATTCCATAGTTTTTGTGTTTGTTTATACGTTTTTCTCTTTGATGAAAACAACTTTTGTGTCC
TTCTCGAC

- partial mRNA

atggaaacagggacgacgagttcttcctcatcagatgtaaatccgcagctgattgatccagattcaagcctagagcggccagctta
ccatcctcattacggcgtggttatcacccccctaccaactccaactcctcagggatcaaattgcaagctatgcaaccatctgtttgaa
gctgatagacatgcacaaagcattggtcaatggttaccatggtagtaccaatggtaacaccgaggttaaccatggtagggtccctt
acaacaacatgagtgatgatcagatgagtgaacttgaacgtgaaggtgaacatgatcaaggaagggtgattagcaggaagaaa
aacttggttagtggtagtggtaatggtaatctaaccaaagcaggtacgactaggcacagatggactccaactcagacacaactca
agattttagaggatttatttggggttcatggtatgaataatactccaaataagaggagagtgagtgagattacggcagatttggct
aaacacggtcccatttctgagtctaatgtctccaactggttccagaatcgtaaggccaggtataggcgactcttgaggtcttgaatt
gatcaaatgagccaatggacattccatagtttttgtgtttgtttatacgttttttctctttgatgaaaacaacttttgtgtccttctcgac

- predicted protein

METGTTSSSSSDVNPQLIDPDSSLERPAYHPHYGVVITPYQLQLLRDQIASYATICLKLIDMHKALVNGYH
GSTNGNTEVNHGRVPYNNMSDDQMSELEREGEHDQGRVISRKKNLVSGSGNGNLTKAGTTRHRWT
PTQTQLKILEDLFGVHGMNNTPNKRRVSEITADLAKHGPISESNVSNWFQNRKARYRRLLRS

S.kraussiana WOX13C

- genomic locus
- cagctggaagctgtcgcatggctgtacaatcacagtatacgagacgtatacacgacgctggttagctatactggtga
agatttctgcaagaagctgtccattctacgtagcagcctttcgcagtgcttgtccgagggacagggttgcatgaaccg
ggttgtgagggcctgtgatacggtggtaccatcggttgatggtgagcaatcggtttccagagtcgcggtactgctgttc
agttcgtctcggaaggattgcctcatcgttagaagcctggtgaccaaaatggtatggtcgcttgtggaagtggacgttg
gtaatggtgatggtaacgacgtcctggacgctgggttggacgctgtacacaaacatacaggtaacttggttaagcca
gtcgttaaacgtagttaaatgtaaactttggttaaaatgtgtcgtaatgtcgttaatgtagtagttaaacgtcgttaaagta
gtagttaaaagtctttaaactgccgtgttggttgttaagtagttaagcgtcttcgaacttatttaaatgtcgtttttatttagtag
ttaaaagtctttaaactaggtagttaaaccagttaaacgtcattgaacgaatctgaatgttcttcaagcgatagctagag
cagttaagtgtttttaaacatagttaacgttcgttaaaccaatgggttaagcgtcttcaaatgtgtcaaacacgtgtgacg
tagtttaacatcgttaaaactctgttaatccctactaaactacgttaaactcgcaggcattgacagggactccttgatcgt
tgacaccacgtttcgagacgttcattgcatgaaccatgcaacccgtgtttatacgatgatatgcaaaggcagcgacgt
cgagatcaaacctagttcatccatcgaagaagctctctggatttctctcgaggagctacgatcgaagtaagtgtcgat
gattcttccaagagatttttacgttctttagggctgaggctccgcttcttgaaacgtcgggttggggtgtcaatacggccg
aaggcatcgactacttccgtatacagcctctactcccaccgtactcgtctgggtaattgtatgttgtatactagacttttag
gtctcgtcggaaactgcaggaaggaaatcgagctccaaacgaagtccgaaactacggatatatcatgcgacgag
gaaaaacggtatgtttttcgctgatatttttcgatgtgatctgatgtttttggggtatttttttcaggcctgaagctgtggaact
ccagcaagtggctcttctcaagcaggcaagttttgtatcgtgcaatgtataacatcagataacatacgtacattgtatttt
gtgtaatcgatgttctacggttagggttgtgatttacctctttagggtctagggttatctgcctcttttagggtttaggtttaga
ggtgtatgatttagggttaggtctgatgataattggtttctgcagaacgaggagattagcgacactgcgaaggatgga
ATGGAGATGATTAGCTGGTCGAATCAGTCGCCGGATCCACAAGACCTACCGT
CGTCCCCGACGAACCCTTCTCCGGCGGTGACGCAGCCGAGGAAGCCGAGA
CACCGATGGACGCCGAGCCGGAACCACCTGAGCATTCTAGAACGGCTCTTC
AAGCAGGGAACCGGAACTCCAAACAAGCAACGGATCAAGGAGATCGCAAC
CGACTTGGTCCAATACGGCGAGATCTCCGAGGCGAATGTATACAACTGGTTC
CAGAACCGCAAGGCCAAGGAAAAGAAGCTCATGTCGCAGAGCGGCTCGGC
CCACCTCCGACACGACGGAGAGGCCGAGATCGAGGCCGTTGCTCCGAGGG
AAAAACGGCGCCGAATGGACATCGACGAGATCATCAACCCTCGGCCCTCGC
GTTTGAGTCagattggcttcagaaaattgacgtttttgtgatctcgttcatcttcgtgtgttcatttgtattt**AGGAA**
TTGGAGGGGGCGAAGAGTACCGTGAAAACGGAAGCTGACGTTGATCTAGAT
GAgcaggtaccctaccctaatcctaattttcctaacctaacctaaccctaaaacctgatctgggctt**GCAGAAT**
GCTGTGACCGAGGAGGGATCGCGGGATAACATTTGTGCAACCAACTTAGgggt
gcgtacccgttgaacgtctacttcataccattcgtcgttgtacatgcagtggagagaagtaggcatggtagctttcgcgt
ttattagttcgagggacgacggtggtaacccccgtcaagcgggaccactaaccgtgggatttgttc**AGGGGAA**
GGAGCGGCGTAGGAGCTTCTCAGAGACGGACGCCAAGCGTACGAAGACggta
tctatacacttgtacgaaaacatagcaaaatcgtggatttttttca**GGACGAAAACTGTGACGAGGAA**
GAGGTGGACTTACTCTTGAAACTCAAAGACCCAGttcaggttcgtgaacagaaatttaggttt
agggtatagggttaaatatgccgatgttttttt**TTCAGGACTTGGACGAATTGTGCTTGCGAGGT**
GGCTTGCCGATCCCGTTTTACAAGGTGCAATCGACTCCTCACAAATCAAgtagg
tacatggtattctacgttgtgggttttagcttcgcatatgtgattgcag**CCCAGTATTTGTACACTGCTAC**
GGTCCAGATTTGCACGCTGAGGAATGAGCGTTCCGCTGTAGGTACGCCTTCG

**GTGGATTATAATGAAGCAAAGGTGTCTGCCGCCTCTAGAATGCTAGGACGCC
TCTACCTTGAGAGGTCTCGACTATATAGCAATGCATGAGTGATGATTTCAGG
GGCTGATGTTCTATACTAGAGCTAACACGACTATTATTATTTGTTGGG**

- partial mRNA

atggagatgattagctggtcgaatcagtcgccggatccacaagacctaccgtcgtccccgacgaacccttctccggcggtgacgca
gccgaggaagccgagacaccgatggacgccgagccggaaccacctgagcattctagaacggctcttcaagcagggaaccggaa
ctccaaacaagcaacggatcaaggagatcgcaaccgacttggtccaatacggcgagatctccgaggcgaatgtatacaactggtt
ccagaaccgcaaggccaaggaaaagaagctcatgtcgcagagcggctcggcccacctccgacacgacggagaggccgagatc
gaggccgttgctccgagggaaaaacggcgccgaatggacatcgacgagatcatcaaccctcggccctcgcgtttgagtcaggaat
tggagggggcgaagagtaccgtgaaaacggaagctgacgttgatctagatgagcagaatgctgtgaccgaggagggatcgcgg
gataacatttgtgcaaccaacttagaggggaaggagcggcgtaggagcttctcagagacggacgccaagcgtacgaagacgga
cgaaaactgtgacgaggaagaggtggacttactcttgaaactcaaagacccagttcaggacttggacgaattgtgcttgcgaggt
ggcttgccgatcccgttttacaaggtgcaatcgactcctcacaaatcaacccagtatttgtacactgctacggtccagatttgcacg
ctgaggaatgagcgttccgctgtaggtacgccttcggtggattataatgaagcaaaggtgtctgccgcctctagaatgctaggacg
cctctaccttgagaggtctcgactatatagcaatgcatgagtgatgatttcaggggctgatgttctatactagagctaacacgacta
ttattatttgttgggaaaaaaaaaaaa

- predicted protein

MEMISWSNQSPDPQDLPSSPTNPSPAVTQPRKPRHRWTPSRNHLSILERLFKQGTGTPNKQRIKEIAT
DLVQYGEISEANVYNWFQNRKAKEKKLMSQSGSAHLRHDGEAEIEAVAPREKRRRMDIDEIINPRPSRL
SQELEGAKSTVKTEADVDLDEQNAVTEEGSRDNICATNLEGKERRRSFSETDAKRTKTDENCDEEEVDLL
LKLKDPVQDLDELCLRGGLPIPFYKVQSTPHKSTQYLYTATVQICTLRNERSAVGTPSVDYNEAKVSAASR
MLGRLYLERSRLYSNA

S.moellendorffii WOX13A

- partial mRNA

atggatcgacaggagaatcccaggtacagtaagaggctgcgagccaaggcggaggagaaatccccggtgaagcgcgagccgc
caaatgcggatgaaatcctcctccgctcggcgctggatcggccggaataccatccggattttgggatcgtgatgagcgcccagcag
ctggacgaattgcggcgccagatcgccgtctacgccacgatctgccagcagctggtggagatgcacaaggcgtcaatggcgaatc
ccaacggtatggtacttctagctctagaccaccgccgccatcgccgctaccgccgcccgtgaaagccaccactcgccagaggtgg
gcgcccagccaggcccaggtcaagctcctcgagagcctctacgacgttggaatggggacgccacacaagcagcgagtgcgaga
gatcacggcggagctcagccagcttgggccggtgaacgagtccaacgtttacaactggttccagaaccgaaaggccaggacgag
gaggaggaatcggcagcagccgagtgctctgggaggcctggagccacagaactttcctcacagggagctcgaggaggtggattc
ggaggtggacgccatggaaggtggtggtgctcgtgggtctccgggagtgttgaaaaggctcaagccagagggcgctggtccatc
aaccgagcacgctccacactccaacgcaagtctcctgtgacggtttttcgatgcagttcttcggcttgttttttttttttgttgttgctcg
aggacttatataccgaaattgtgcaggttctcggtcgtcctctcgaagtaagacaaaattttgcaaaaaaaaaaaaa

- predicted protein

MDRQENPRYSKRLRAKAEEKSPVKREPPNADEILLRSALDRPEYHPDFGIVMSAQQLDELRRQIAVYATI
CQQLVEMHKASMANPNGTSSFRPPPPSPLPPPVKATTRQRWAPSQAQVKLLESLYDVGMGTPHKQR
VREITAELSQLGPVNESNVYNWFQNRKARTRRRNRQQPSALGGLEPQNFPHRELEEVDSEVDAMEGG
GARGSPGVLKRLKPEGAGPSTEHAPHSNASLL

S.moellendorffii WOX13B

- partial mRNA

atggaatcgatctggacggaggattcagctgccatggctgctgctgctgccgatgccgcgggcgtcgtcgtcgacgatgcgttcca
gatgcctcatttcctgctccctcctcccaatctccctcacaatttcgcgcaaagctgcctcgccaatcccgcgcaggtgatgaccgag
gagcagcttgagacgctgcggcgccagatttcggtctacgccacgatctgccagcagctcgtggagatgcacaaggcaacgatct
cacaccagcacacatacaatggtttgcttctcggccaccaatctcctgccatccaggactcgtctccaatgctcctgggaatccacc
acaagccaacgtcgcggcaaagatggacaccatcgcagaaccagctgaggatcctcgagaggctcttcaagcagggcaatggg
acgccaaaccggcaaaggatcaaggagatcacgagcgagctgagccagcacggccaaatctccgagaccaatgtctacaactg
gttccagaaccggaaggctcgagcaaagaggaagcaacgacacaacaatgcgacccccctccacgaccaccacctcctcgcagc
acaaggacgccgaatcggaagtggagaccgatggagatcactcgccggaagaaaagaggagcaaagtaagctcgtccacgcc
gcagcagcagctccagatggatcaaagcaacaccaccaccgaagcgattggtactcgctacgcggtcgtcatgctcaatggaaa
ggcctggaaagtaaaaccagggagaatcaacgtaaggagtaactttggagacaatgccgtgctgctagatccgagaggtcatgt
ggtggccacgagcgagcaaggcttgactttagatcctctacaacctggtggaagctacacggttgctgtgtgaataaattacaaca
aagaaccataaacaagagcattgatgtttga

- predicted protein

MESIWTEDSAAMAAAAADAAGVVVDDAFQMPHFLLPPPNLPHNFAQSCLANPAQVMTEEQLETLR
RQISVYATICQQLVEMHKATISHQHTYNGLLLGHQSPAIQDSSPMLLGIHHKPTSRQRWTPSQNQLRIL
ERLFKQGNGTPNRQRIKEITSELSQHGQISETNVYNWFQNRKARAKRKQRHNNATPSTTTTSSQHKDA
ESEVETDGDHSPEEKRSKVSSSTPQQQLQMDQSNTTTEAIGTRYAVVMLNGKAWKVKPGRINVRSNF
GDNAVLLDPRGHVVATSEQGLTLDPLQPGGSYTVAV

S.moellendorffii WOX13C

- partial mRNA

aacgagagatttttttgttaccttgttgaggttcgggctgcgagaattccggaagaaacaaggtcccgtttggaggtgaagttgcgg
cggcgatcttggaggtggcgttggcttcgtggtgatggtggtggtggtggtgatggtgatcgagcttggatctcttgcctttggagtc
gacgtcggtgtctacctcggactcgccatcgttttgctgcatctgcttttgcttgcgcttggctcgagcctttcggttgtggaaccagtt
gtggacgttggcctccgtaacatcaccttggcgagcgagatccacggcgatctctttgatccgctgcttgttgatactgtcgccctcc

tcctcgaacagccggacgagcatccggagctgctcctcgttcggtttccatcgaactttgacgacggcgggaggcaattcttgcaa
agcttgctgctgctgctgctggtaatggctttcctccat

- predicted protein
  MEESHYQQQQQQALQELPPAVVKVRWKPNEEQLRMLVRLFEEEGDSINKQRIKEIAVDLARQGDVTE
  ANVHNWFHNRKARAKRKQKQMQQNDGESEVDTDVDSKGKRSKLDHHHHHHHHHHHEANATSKIAA
  ATSPPNGTLFLPEFSQPEPQQGNKKSLV

ERKLÄRUNG I

Ich versichere, daß ich die von mir vorgelegte Dissertation selbständig angefertigt, die benutzen Quellen und Hilfsmittel vollständig angegeben und die stellen del Arbeit – einschließlich Tabellen, Karten und Abbildungen –, die anderen Werken im Wortlaut oder dem Sinn nach Entnommen sind, in jedem Einzelfall als Entlehnung kenntlich gemacht habe; daß diese Dissertation noch keiner anderen Fakultät oder Universität zur Prüfung vorgelegen hat; daß sie – abgesehen von unten angegebenen Teilpublikationen – noch nicht veröffentlicht worden ist sowie, daß ich eine solche Veröffentlichung vor Abschluß des Promotionsverfahrens nicht vornehmen werde.

Die Bestimmungen dieser Promotionsordnung sind mir bekannt. Die von mir vorgelegte Dissertation ist von Pr. Dr. Wolfgang WERR betreut worden.

Ich versichere, daß ich alle Angaben wahrheitsgemäß nach bestem Wissen und Gewissen gemacht habe und verpflichte mich, jedmögliche, die obigen Angaben betreffenden Veränderungen, dem Dekanat unverzüglich mitzuteilen.

....

Datum Unterschrift

UN GRAZIE A... / A THANKS TO...

E finalmente siete arrivati alla fine. E qui giungono i ringraziamenti.

A Wolfgang, per avermi permesso di fare il mio Ph.D nel suo lab, e per i consigli e le strigliate che mi sono beccato.

A Giuseppe, per avermi guidato nei primi passi nel mondo della Scienza, per avermi supportato nella mia candidatura qui a Colonia e, ne sono certo, anche per il mio futuro lavoro a San Diego.

Alla mia Arianna, per essermi stata accanto durante quest'ultimo anno abbondante, quando sono stato intrattabile ed assolutamente antipatico per via del lavoro che non andava.

Ai miei genitori, senza i quali dire che non sarei qui è riduttivo. Grazie.

A Pascal, che sopra tutti si è rivelato un amico prima ancora di un collega. Ed un grazie anche a tutto il gruppo WERR, un grazie immenso, direttamente proporzionale all'aiuto che mi è stato dato.

A Jan, Britta e Anne.

All'impagabile Kristen, senza la quale, ne sono certo, non avreste capito molto di ciò che avete appena letto.

Al Prof. Hülskamp ed alla Prof. Höcker per il tempo che mi stanno già dedicando e che ancora mi dedicheranno.

A tutti voi, grazie.

And finally you got the end. And here thanks come.

To Wolfgang, for giving me the opportunity to perform my Ph.D in his lab, and for all the advices and all the scoldings he gave me.

To Giuseppe, for guiding me, first, in the Science world and for supporting my application here in Cologne and, I am pretty sure, also for my next position in San Diego.

To my Arianna, for be just beside me during the last year, whenever I was intractable or totally unpleasant.

To my parents, without whom I wouldn't be here, and this is anyway reductive. Thanks.

To pascal, who overall turned out to be a friend, not just a colleague. And a thanks also to all AG WERR members, an immense thanks, directly proportional to the help you gave me.

To Jan, Britta and Anne.

To the priceless Kristen, without whom, I am sure of it, you would have not understood very much of what you have just read.

To Prof. Hülskamp and Prof. Höcker for the time they have already spent for me and for the time they are going to spend soon.

For all of you, grazie.